SEISMIC ANALYSIS OF CONCRETE GRAVITY DAMS WITH KEYED CONTRACTION JOINTS

BY

AHMED MOHAMED EL-NADY, B. Sc., M. Sc.

A Thesis

Submitted to the School of Graduate Studies

in Partial Fulfilment of the Requirements

for the Degree of

Doctor of Philosophy

McMaster University

1992

SEISMIC ANALYSIS OF CONCRETE GRAVITY DAMS WITH KEYED CONTRACTION JOINTS

TO MY PARENTS

DOCTOR OF PHILOSOPHY (1992)
(Civil Engineering and Engineering Mechanics)

McMaster University
Hamilton, Ontario

TITLE: Seismic Analysis of Concrete Gravity Dams With Keyed Contraction Joints

AUTHOR: Ahmed Mohamed El-Nady, B.Sc. Cairo University
M.Sc. Cairo University

SUPERVISOR: Professor T. S. Aziz
Professor A. Ghobarah

NUMBER OF PAGES: 193

ABSTRACT

Most of the design of concrete gravity dams is based on a two dimensional analysis which is suitable for monoliths with smooth, unkeyed, contraction joints. However, when keyed contraction joints are used, it is expected that the dam monoliths will interact in a manner that may affect the overall response of the system. The objective of this study is to investigate the seismic behaviour of concrete gravity dams, built with keyed contraction joints, including the effect of monoliths interaction. The scope of research work included: 1) development of a simplified procedure to investigate the effect of monoliths interaction on the seismic behaviour of the structure, 2) after this was proved to be important, a detailed and comprehensive procedure was developed and 3) investigation of the parameters which affect the response of the structure and significantly influence monoliths interaction.

In the simplified procedure, each monolith of the dam is modeled using beam elements which has the advantages of keeping the number of degrees of freedom to a minimum and being available in most of structural engineering computer codes. The approximate added mass technique is used to simulate the hydrodynamic effects when the dam and reservoir are subjected to an earthquake ground motion. The importance of including monoliths interaction is illustrated by analyzing different cross-sections of concrete gravity dams.

In the proposed detailed analysis of gravity dams, a substructuring technique is employed to model the structure. The dam is divided into a number of substructures equal to the number of monoliths. Each monolith is then reduced to a few degrees of

freedom on the upstream face and Ritz vectors are used to represent internal degrees of freedom. The analysis is carried out in the frequency domain to include the frequency-dependent terms which appear when including reservoir-dam-foundation interactions. The results obtained are compared to typical three-dimensional analysis and a good agreement is obtained. It is noted that the importance of monoliths interaction is dependent on two factors; 1) the type of contraction joints used in construction and 2) the longitudinal profile of the dam.

The effect of monoliths interaction is to increase the natural frequencies of the structure and as a result leads to a change in its overall response. It is concluded that in many cases the effect of monoliths interaction is important and should be included in the analysis. The geometry and material properties of contraction joints have a significant effect on the overall response of the dam. Depending on the crack width, the shear behaviour of the joints varies widely. The longitudinal profile of the dam was also found to have a substantial effect on monoliths interaction. Important variations in the response of the dam, from that calculated using typical two-dimensional analysis, is obtained for some cases. This is usually the case for short dams with rigid monoliths at the sides or for dams built in steep canyons.

ACKNOWLEDGEMENTS

I would like to express my sincere gratitude to Dr. A. Ghobarah and Dr. T. S. Aziz for their guidance, advice and interest during the course of this study.

Special thanks are due to Dr. J. Wilson and Dr. M. Dokainish, members of my supervisory committee, for their valuable comments and suggestions.

I would like to thank my parents for their continuous support, help, patience and inspiration.

TABLE OF CONTENTS

		Page
ABSTRACT		iii
ACKNOWLEDGEMENTS		v
TABLE OF CONTENTS		vi
LIST OF FIGURES		ix
LIST OF TABLES		xii
CHAPTER 1	INTRODUCTION	
	1.1 General	1
	1.2 Cases of Dam failure	2
	1.3 Experimental Performance Data	3
	1.4 Existing Dam Design	4
	1.5 Dynamic Response	5
	1.5.1 Design Basis Earthquake	6
	1.5.2 Reservoir Modelling	7
	1.5.3 Foundation Modelling	11
	1.5.4 Dam Modelling	12
	1.6 Objectives and Scope	15
CHAPTER 2	SIMPLIFIED PROCEDURE	
	2.1 General	18
	2.2 Background on Monoliths Interaction	19
	2.3 Analysis Procedure	22
	2.3.1 Dam Domain	23
	2.3.1.1 Monoliths Modelling	24
	2.3.1.2 Joint Modelling	25
	2.3.2 Fluid Domain	28

	2.4	System Considered	31
	2.5	Response Results	32
	2.6	Summary	37
CHAPTER 3	MONOLITHS INTERACTION		
	3.1	General	56
	3.2	Limitations of the Simplified Procedure	56
	3.3	Substructure Methods	57
	3.4	Monoliths Interaction	61
		3.4.1 Formulation of Each Substructure	65
		3.4.2 Formulation of the Connecting Elements Stiffness	66
	3.5	Strain Energy in the Model	70
	3.6	Testing of the Procedure	74
	3.7	Response Analysis	76
		3.7.1 Effect of Dam Cross-Section	77
		3.7.2 Monoliths Interaction Effects	77
		3.7.3 Effect of Dam Height	78
	3.8	Summary	79
CHAPTER 4	DAM - RESERVOIR - FOUNDATION SYSTEM		
	4.1	General	94
	4.2	Soil - Structure Interaction	94
	4.3	Reservoir - Structure Interaction	99
	4.4	Response of the System	104
	4.5	Summary	107

CHAPTER 5 TYPES OF CONTRACTION JOINTS

5.1 General 126

5.2 Types of Contraction Joints 127
5.2.1 Smooth Joints 127
5.2.2 Keyed Joints 128
5.2.3 Reinforced Joints 128

5.3 Force Transfer at Contraction Joints 128
5.3.1 Cohesion 130
5.3.2 Friction 130
5.3.3 Aggregate Interlocking 131

5.4 Shear Strength and Stiffness of Joints 132

5.5 Joint effect on the Overall Behaviour 136

5.6 Summary 137

CHAPTER 6 EFFECT OF THE LONGITUDINAL PROFILE ON THE RESPONSE OF CONCRETE GRAVITY DAMS

6.1 General 149

6.2 Canyon Cross-Section 150
6.2.1 (h/H) Ratio 151
6.2.2 (L/H) Ratio 153

6.3 End Conditions 154

6.4 Overflow Monoliths 156

6.5 Frequency Content of the Ground Motion 157

6.6 Summary 159

CHAPTER 7 CONCLUSIONS AND RECOMMENDATIONS

7.1 General 183

7.2 Conclusions 184

7.3 Recommendations 186

REFERENCES 188

LIST OF FIGURES

FIGURE		PAGE
1.1	Typical Cross-Section of a Concrete Gravity Dam	17
2.1	Dam section Used by Rashed and Iwan (1984)	41
2.2	Geometry of Piedra del Aguila dam in Argentina	42
2.3	Modelling of the Longitudinal Profile of Concrete Gravity Dams	43
2.4	Cross-section of the Model Structure	43
2.5	Crest Displacement Time History of the Dam Structure	44
2.6	Longitudinal Deflection Profile of a Concrete Gravity Dam	45
2.7	Stiffness of the Connecting Links	45
2.8	Geometry and Dimensions of an Idealized Dam Structure	46
2.9	Modelling of the Dam Structure	46
2.10	Crest Displacement Profile of The Model Structure $H_1/H_2 = 0.25$	47
2.11	Crest Displacement Profile of the Model Structure $H_1/H_2 = 0.50$	47
2.12	Cross-section of the Model Structure	48
2.13	Longitudinal Profile of the Model Structure	49
2.14	Crest Displacement Time History without Hydrodynamic Forces	50
2.15	Crest Displacement Time History with Hydrodynamic Forces	50
2.16	Envelope of Horizontal Displacement of the Critical Monolith Excluding Hydrodynamic Forces	51
2.17	Envelope of Horizontal Displacement of the Critical Monolith Including Hydrodynamic Forces	51
2.18	Maximum Principal Tensile Stress Distribution in the Model Structure	52
2.19	Earthquake Ground Motion Records	53
2.20	Envelope of Horizontal Displacement of the Critical Monolith for High A/V Ratio Input Ground Motion	54
2.21	Envelope of Horizontal Displacement of the Critical Monolith for Low A/V Ratio Input Ground Motion	55
3.1	Typical Longitudinal Profile of Concrete Gravity dams	83
3.2	Modelling of Gravity Dams to Include Monolith Interaction	84
3.3	Model for Connecting Elements	85
3.4	Elevation of The Model Structure	86
3.5	Cross sections of The Model Structure	86
3.6	Mode Shapes of the Structure Case A	87
3.7	Time History of the Crest Displacement Cases A and D	87
3.8	Geometry of Cases I and II	88
3.9	Envelope of Horizontal Displacements for Critical Monolith	89
3.10	Time History of the Top Displacement H=100 m Taft Record	89
3.11a	Envelope of Horizontal Displacements for Critical Monolith	90

3.11b	Time History of the Top Displacement H = 100 m, Parkfield Record	90
3.12a	Envelope of Horizontal Displacements for Critical Monolith	91
3.12b	Time History of the Top Displacement H = 100, Long Beach Record	91
3.13a	Envelope of Horizontal Displacements for Critical Monolith	92
3.13b	Time History of the Top Displacement H = 140 m	92
3.14a	Envelope of Horizontal Displacements for Critical Monolith	93
3.14b	Time History of the Top Displacement H = 60 m	
4.1	Dam-Reservoir-Foundation Interaction	113
4.2	Geometry of the Model Structure	114
4.3	Envelope of Horizontal Displacement of the Critical Monolith	115
4.4	Crest Displacement Time History of the Critical Monolith	116
4.5	Envelope of Horizontal Displacement of the Critical Monolith	117
4.6	Crest Displacement along the Dam Longitudinal Axis	118
4.7	Crest Displacement Time History of the Critical Monolith	119
4.8	Envelope of Horizontal Displacement of the Critical Monolith	120
4.9	Crest Displacement Time History of the Critical Monolith of Rectangular Section (Uniform Profile)	121
4.10	Crest Displacement Time History of the Critical Monolith of Rectangular Section(Non-uniform Profile)	121
4.11	Envelope of Horizontal Displacement of the Critical Monolith of Rectangular Section (Uniform Profile)	122
4.12	Crest Displacement Time History of the Critical Monolith of Rectangular Section (Non-uniform Profile)	122
4.13	Envelope of Horizontal Displacement of the Critical Monolith of Rectangular Section (Uniform Profile)	123
4.14	Envelope of Horizontal Displacement of the Critical Monolith of Rectangular Section (Non-uniform Profile)	123
4.15	Crest Displacement Time History of the Critical Monolith of Triangular Section (Uniform Profile)	124
4.16	Crest Displacement Time History of the Critical Monolith of Triangular Section (Non-uniform Profile)	124
4.17	Envelope of Horizontal Displacement of the Critical Monolith of Triangular Section (Uniform Profile)	125
4.18	Envelope of Horizontal Displacement of the Critical Monolith of Triangular Section (Non-uniform Profile)	125
5.1	Classification of Contraction Joints	141
5.2	Different Types of Contraction Joints	141
5.3	Upper and Lower Bounds of Shear Strength	142
5.4	Shear Transfer Mechanism in Cracked Joints	143
5.5	Typical Mean Shear Stress-Shear slip relationships for Aggregate Interlock Mechanism (Park and Paulay, 1975)	144
5.6	Shear Transfer Mechanism in Uncracked Joints	145
5.7	Crest Displacement of the Model Structure with Different Joint Stiffness	146
5.8	Displacement Profile of the Critical Monolith with Different Joint Stiffness	147

5.9	Maximum Stresses within the Model Structure with Different Joint Stiffness	148
6.1	Factors Affecting Response of Gravity Dams Including Monoliths Interaction	165
6.2	Examples of Longitudinal Profiles of Concrete Gravity Dams	166
6.3	Longitudinal Profile Modelling of Gravity Dams	167
6.4	Cross-Section of Structure Cases A and B	167
6.5	Envelope of Maximum Displacement for Structure A with Different h/H ratios	168
6.6	Crest Displacement Time Histories for Structure A with Different h/H ratios	168
6.7	Envelope of Maximum Displacement for Structure B with Different h/H ratios	169
6.8	Crest Displacement Time Histories for Structure B with Different h/H ratios	169
6.9	Crest Displacement Time Histories for Structure A with Different L/H ratios	170
6.10	Envelope of Maximum Displacements for Structure A with Different L/H ratios	170
6.11	Crest Displacement Time Histories for Structure B with Different L/H Ratios	171
6.12	Envelope of Maximum Displacement for Structure B with Different L/H ratios	171
6.13	Envelope of Maximum Displacement for Structure A with Fixed End Conditions and Variable h/H	172
6.14	Envelope of Maximum Displacement for Structure B with Fixed End Conditions and Variable h/H	172
6.15	Envelope of Maximum Displacement for Structure A with Fixed End Conditions and Variable L/H	173
6.16	Envelope of Maximum Displacement for Structure B with Fixed End Conditions and Variable L/H	173
6.17	Cross-section of Overflow and Nonoverflow Monoliths	174
6.18	Envelope of Maximum Displacement for Structure B with Overflow Monoliths	175
6.19	Crest Displacement Time History of Structure B with Overflow Monoliths	175
6.20	Time History Records of the Selected Earthquakes	176
6.21	Response Spectrum for the Exciting Ground Motions 10 % Damping	179
6.22	Maximum Displacements of the Critical Monolith of the Structure High A/V ratio	180
6.23	Maximum Displacements of the Critical Monolith of the Structure Intermediate A/V ratio	181
6.24	Maximum Displacements of the Critical Monolith of the Structure Low A/V ratio	182

LIST OF TABLES

TABLE		PAGE
1.1	Concrete Gravity Dams Subjected to Significant Seismic Events	16
2.1	Frequencies of Free Vibration (rad/s) of Rectangular Section	38
2.2	Frequencies of Free vibration (rad/s) of Conventional Dam Section	38
2.3	Natural Frequencies (Rad/s) of The Idealized Dam	39
2.4	Natural Frequencies (Rad/s) of The Model Structure	39
2.5	Earthquake Ground Motion Records	40
3.1	Configuration of the Different Cases of the Idealized Structure	80
3.2	Comparison of Natural frequencies (Rad/sec) for Cases A & C	80
3.3	Natural Frequencies (Rad/s) for Case C with Different Number of Ritz Vectors	81
3.4	Natural Frequencies (Rad/s) of Different Dam Profile Cases	81
3.5	Natural Frequencies (Rad/s) of the Dam (Cases I and II)	82
3.6	Natural Frequencies (Rad/s) of the Dam with Different Ritz Vectors (Case I)	82
3.7	Natural Frequencies (Rad/s) of the Dam with Different Ritz Vectors (Case II)	82
4.1	Cases Studied with Dam-Reservoir-Foundation Interactions	109
4.2	Material Properties used in the Analysis	110
4.3	Natural Frequencies of Rectangular Dam Section with Uniform and Nonuniform Longitudinal Profiles (rad/s)	111
4.4	Natural Frequencies of Triangular Dam Section with Uniform and Nonuniform Longitudinal Profiles (rad/s)	111
4.5	Natural Frequencies (rad/s) of the Structure with Rectangular Section	112
4.6	Natural Frequencies (rad/s) of the Structure with Triangular Section	112
5.1	Natural Frequencies of the Structure with Rectangular Section (Uniform Profile)	139
5.2	Natural Frequencies of the Structure with Rectangular Section (Nonuniform Profile)	139
5.3	Natural Frequencies of the Structure with Triangular Section (Nonuniform Profile)	140
6.1	Natural Frequencies of Dam of Rectangular Section with Different h/H (rad/s)	161
6.2	Natural Frequencies of Dam of Triangular Section with Different h/H (rad/s)	161
6.3	Natural Frequencies of Dam of Rectangular Section with Different L/H (rad/s)	161
6.4	Natural Frequencies of Dam of Triangular Section with Different L/H (rad/s)	162
6.5	Natural Frequencies of Dam of Rectangular Section with Fixed End Conditions (rad/s)	162
6.6	Natural Frequencies of Dam of Triangular Section with Fixed End Conditions (rad/s)	163

6.7	Natural Frequencies of Dam with Overflow Monoliths (rad/s)	163
6.8	Description and Data for Earthquake Records Used in the Analysis	164

CHAPTER 1

INTRODUCTION

1.1 GENERAL

Dams are constructed to impound reservoirs. They are designed to resist lateral loads resulting from the difference in water levels between the upstream and downstream sides of the structure. According to its material, dams are classified as earthdams, rockfill dams or concrete dams. Concrete dams are subdivided according to their structural system of load resistance to gravity, arch and buttress dams. Selecting the type of dam for a particular application depends on many factors such as location, site geology and conditions, and proposed dam height. Concrete gravity dams are triangular in shape and made of massive plain concrete monoliths separated by vertical construction joints. In resisting lateral pressure, the monolith depends on its own weight. As a result, the width/height ratio is a very important parameter in the dam stability against the sliding force and overturning moment resulting from water pressure. In practice, width/height ratios of 0.6 - 0.8 are usually used in the design of gravity dams. The upstream face of the dam is normally vertical or has a slight slope. Internal stresses are not the governing parameter under normal operating conditions but they become the major one during earthquakes. The main objective of the seismic design of a dam is to ensure that there is no failure or collapse in the case of a severe ground motion.

1.2 CASES OF DAM FAILURE

A dam failure with full reservoir represents a catastrophic disaster and would endanger many lives. For this reason, dam safety issues are the subject of attention from researchers, designers and government regulatory authorities. A recent study presented data in terms of annual probability of numbers of fatalities resulting from several man made disasters. It was concluded that deaths are considerably more likely to result from dam failures than from nuclear power plant disasters. There has been gravity dam failures due to different reasons but there have been no reported collapse because of earthquakes (Hansen and Roehm, 1979). About 100 concrete dams have been shaken by earthquakes that could be felt at the dam sites. About a dozen of these dams experienced peak ground accelerations of 0.2 g or greater (Bureau, 1990). Relatively few dams have been significantly damaged by earthquakes compared to the large number of dams in operation worldwide. Table (1-1) gives a list of concrete gravity dams which were subjected to significant seismic events. A well studied case of a gravity dam subjected to severe ground motion is the Koyna Dam in India (Chopra and Chakrabarti, 1972). The reservoir behind this 300 foot high dam started filling in 1962, and in 1963 a number of small magnitude earthquakes occurred in the vicinity of the dam. As the depth of the water in the reservoir increased in the following years, the frequency of occurrence and the magnitudes of these local shocks increased. In 1967, a damaging M 6.5 earthquake occurred within 3 km of the dam. The strong shaking caused horizontal cracks at about 2/3 the height with slight traces of water leakage visible on the downstream face of the dam (Okamoto, 1984).

1.3 EXPERIMENTAL PERFORMANCE DATA

Experimental work on the dynamic behaviour of concrete gravity dams are very few in the literature due to the difficulties inherent in building and testing a model. Two types of tests were conducted; 1) field tests on existing dams using vibrators on the top of the dam to excite the structure at different frequencies (Zhu et al, 1984), 2) constructing small models in which the dimensions and properties have to be carefully scaled to represent the actual performance (Niwa and Clough, 1980). The former type is usually used to determine the vibration characteristics of the dam. However, this approach cannot be used to evaluate the performance of the dam under moderate to strong ground motions. In addition, the measurements of the dam response during actual earthquakes are scarce (Chopra, 1987). Although many dams are instrumented, not many have yielded actual response records during severe or damaging earthquakes. On the other hand, shake table testing of dam models remains a difficult task. It is very difficult to model the material of the dam, foundation and reservoir in one small model as well as the scaling of the exciting ground motion. It is doubtful that reliable response results obtained from such an analysis, using separate monolith, will represent the actual response of the structure. Niwa and Clough (1980) carried out shake table tests on one monolith of Koyna dam. In their tests, cracks were observed through the monolith which indicated that the equivalent static method originally used in the design of the dam does not produce adequate seismic design. No tests were carried out on dams consisting of a number of monoliths connected by contraction joints.

Another series of shake table tests were performed on three models of concrete gravity dams in order to simulate earthquake shaking (Donlon and Hall, 1991). The models represented small scale separate monoliths of gravity dams neglecting the existence of contraction joints. No failures occurred even though the levels of shaking employed were unrealistically high. The good performance was due to the development of crack profiles which had favourable orientations to resist sliding failures in each case. However, it was concluded that the development of an unfavourable crack profile, which can not be ruled out, and the possibility of water intrusion into open cracks which was not included in the experiments, could lead to failure under significantly lower levels of excitation than those employed. It was observed that the added masses for a prototype gravity dam during an earthquake may be less than that predicted by a two dimensional mathematical model assuming that the monoliths are not vibrating in phase. The results of the three tests were different with the variation of the construction technique of the model which indicate that much improvement in the modelling and testing technique are required before the results can be applied in practice.

1.4 EXISTING DAM DESIGN

Most of the existing concrete gravity dams were designed on the basis of stresses calculated using the static approach. The critical case of loading for the seismic analysis of dams is considered to have a full reservoir upstream and no water at the downstream side. Although this is not necessarily the case when the earthquake occurs, it is typically assumed to represent the worst loading on the dam. The effect of ground motions on the dam is taken into consideration as an equivalent lateral static load acting at the centre of gravity of the structure. The horizontal load is taken as a percentage of the weight of the structure. Depending on the location of the dam and the experience of the designer, this percentage varies from 5 to 25% (U.S. Bureau of Reclamation, 1976 and 1987). The hydrodynamic effects were modeled by equivalent lateral forces using Westergaard's formula (1933). The traditional design criteria requires that an ample factor of safety be provided against overturning, sliding and overstressing under all loading conditions. Tensile stresses were often not permitted. In representing the effects of the horizontal ground motion, normal to the axis of the dam, by lateral static forces, neither the dynamic response characteristics of the dam-water-foundation rock system nor the characteristics of earthquake ground motion are recognized. Furthermore, the response of existing dams during earthquakes does not agree with the predicted behaviour postulated by the equivalent static method of analysis as demonstrated by the damage to Koyna Dam during the 1967 earthquake.

1.5 DYNAMIC RESPONSE

The dynamic approach includes methods of analysis which determine the response based on the dynamic characteristics of the structural system and the dynamic nature of the earthquake loading. Realistic analyses of the seismic response of dams were not possible until the development of the finite element method, recent advances in dynamic analysis procedures, and the availability of large capacity high speed computers. Thus, much of the necessary research did not start until the mid -1960 's (Chopra 1987). Extensive research has been devoted to evaluating the significance of hydrodynamic and foundation interaction effects in the seismic response of concrete gravity dams. The dynamic analysis procedure for gravity dams typically includes; a) the selection of a representative ground motion for the dam site and the establishment of the design earthquake, b) modelling the dam-reservoir-foundation system, as shown in figure (1-1), and c) evaluating the dynamic response of the system. Due to the complexity involved in the three dimensional finite element analysis of gravity dams, it is very difficult and time consuming to model and analyze the three domains of the system; reservoir, foundation and dam simultaneously.

1.5.1 Design Basis Earthquake

The first step in the design of gravity dams is to estimate the magnitude and epicentral distances of probable earthquakes to which the structure may be subjected and to determine the resulting rock motions at the site. Methods of predicting a design earthquake which represent an operating basis event are normally outlined in the applicable design codes. Three aspects should be considered: 1) historical records to obtain frequency of occurrence versus magnitude, 2) useful life of the structure, and 3) a statistical approach to determine probable occurrence of earthquakes of different magnitudes during the life of the structure. Most earthquakes are the result of crustal movements of the earth along faults. Geologic examinations of the area are necessary to locate all faults, determine how recently activity has occurred , and estimate the probable length of the fault. Records of seismological activity in the area are also studied to determine the magnitude and location of recorded earthquakes that may affect the site.

Based on these geological and historical data, hypothetical earthquakes, usually having magnitudes greater than the historical events, are estimated for all active faults in the area. These earthquakes are considered to be the most severe associated with the faults and are assumed to occur at the points of those faults closest to the site (Bureau of Reclamation Report, 1977). The subject of reservoir induced seismicity has recently received the attention of geologists. However, the prediction and the incorporation of these earthquakes into the dam design is lacking. An example of reservoir induced earthquakes is the case of the High Dam, Egypt, which was subjected to few earthquakes after the reservoir was filled. In the literature, little attention has been paid to the effect of different earthquake characteristics on the response of gravity dams. Two earthquake parameters are believed to have the major effect on linear analysis of structures: earthquake magnitude and peak ground acceleration. However, the investigation of El-Nady et al (1990) showed that the response of the structure varies significantly with the variation in the frequency content of the earthquake.

1.5.2 Reservoir Modelling

The response of the water in the reservoir during seismic ground motions is evaluated using the governing differential equation of the fluid as well as the boundary conditions. Choosing the proper model of the reservoir depends on its boundary conditions. For uniform cross-section and infinitely long reservoirs, a continuum approach may be considered appropriate (Chopra et al, 1980). In cases of irregularity in any of the boundary conditions, such as nonuniform section or limited length reservoir, a finite element descritization must be used (Hall and Chopra, 1980).

One of the assumptions used in the continuum approach is that the upstream face of the dam is vertical. This assumption is considered reasonable for actual concrete gravity dams because their upstream face is typically vertical or very close to vertical for most of the height. For those structures with upstream faces close to vertical, it was shown that the effect is minor (Aviles and Sanchez-Sesma, 1989). Successful analyses have been performed by the method of substructures in which the fluid effects are included in the equations of motion of the dam by the addition of hydrodynamic forces which act on the upstream face of the dam (Chopra, 1967, 1968 and 1970). These hydrodynamic terms are computed from solutions to the wave equation over the fluid domain substructure subjected to appropriate boundary conditions. Utilizing such an analysis procedure, it was shown that the dam-water interaction and water compressibility have a significant influence on the dynamic behaviour of concrete gravity dams under earthquake ground motions. Although studies conducted as early as 1968 concluded that water compressibility effects may be significant in the response of concrete gravity dams (Chopra 1968 and 1970), there continued to be much interest in research to neglect water compressibility in earthquake analysis of concrete gravity dams. The reason is that such an assumption leads to significant simplification of the analysis. The key parameter that determines the significance of water compressibility in the earthquake response of gravity dams is the ratio of the fundamental frequency of free vibration of the impounded water to the fundamental frequency of the dam alone. It has been demonstrated that the effects of water compressibility becomes insignificant in the response of gravity dams if this frequency ratio is greater than 2. In most cases, water compressibility should be included which requires carrying out the analysis in the frequency domain. Because of hydrodynamic effects, the vertical component of ground motion is more important in the response of gravity dams than in other classes of structures (Chakrabarti and Chopra, 1973 and 1974). A simplified procedure was developed by (Chopra, 1978) in which the maximum response due to the fundamental mode of vibration was represented by equivalent lateral forces, which were computed directly from the earthquake design spectrum without a response time history analysis. The hydrodynamic forces on the upstream face of the dam are represented by added masses in which the water compressibility is neglected. Recently, this simplified analysis of the fundamental mode response has been extended to include the effects of dam - foundation rock interaction and of reservoir bottom materials (Fenves and Chopra, 1985 and 1987).

For reservoirs with nonuniform cross-section or with limited length, the finite element or the boundary element approximations must be used. The boundary element method was succesfully used to model the reservoir (Humar and Jablonski, 1987 and 1988). The available methods use a finite element idealization of the structure with displacements as the response quantity, but they differ in the formulation for the fluid. Zienkiewicz et al (1983) used hydrodynamic pressure as the unknown variable in a finite element discretization of the fluid domain. However, the unsymmetrical equations of motion of the coupled fluid - structure system require special time integration methods for transient analysis. Another approach is to represent the fluid response in terms of a potential function for displacement or velocity (Newton, 1981). Again the coupled equations of motion are unsymmetric, but the irrotationality condition on fluid motion is automatically satisfied. A third major formulation uses displacements of the fluid as the response quantity. This method was used earlier by Chopra and substantial contributions have been made by Hamdi et al (1978), Bathe and Hahn (1979), Olson and Bathe (1983) and Wilson and Khalrati (1983). The major advantages of the displacement formulation are that the fluid elements can be coupled to the structure elements using standard finite element assembly procedures, and the equations of motion are symmetric. The disadvantage of the displacement formulation, compared to scalar formulations, is the large number of displacement components, particularly for three dimensional fluid domains.

Another major approach for computing the response of fluids involves a combination of the formulations described above. Liu and Chang (1985) developed a mixed solution procedure for the transient analysis in which the pressure is approximated in a different manner than the fluid velocity. The transient analysis procedure explicitly solves for the pressure, which is then used in an implicit solution for the velocity. In another mixed approach, Olson and Bathe (1985), used pressure and velocity potential as the unknown functions for the fluid to overcome shortcomings in the displacement formulation for certain classes of fluid-structure systems. Although the choice of these scalar functions reduces the number of unknowns and results in symmetric equations of motion, special interface elements must be developed to couple the fluid and structure domains. In a different application, Taylor and Zienkiewicz (1984) presented a mixed formulation for viscous fluid flow. The work combined independent approximation of the velocity, pressure, and stress, and it demonstrated an improved representation of nonlinear material models. A numerical procedure for computing the dynamic response of coupled fluid structure systems was developed and used to evaluate the effects of nonlinear behaviour of the structure and fluid (Loli and Fenves, 1988). The procedure included cavitation of the fluid, which was modeled as a bilinear compressible material, in addition to nonlinear models of the structure. A mixed displacement pressure formulation for the fluid is used, in which the pressure is approximated independently of the fluid displacement. Response results show that cavitation and nonlinear structural behaviour can interact to affect the response of the coupled system. However, cavitation appears to have a small effect on the earthquake response of concrete gravity dams. Cavitation alters the maximum deformation and stress only in extreme earthquake intensities and for very high structures. Zienkiewicz et al (1983) demonstrated that neglecting cavitation effects would not seriously reduce safety consideration for most dams. The major drawback of some studies on modelling the reservoir is that they complicated the modelling so much that it was necessary as compensation, to use oversimplified assumptions of the dam (Tsai et al, 1990). The purpose of modelling reservoirs is to calculate the hydrodynamic pressure which consequently is used in the design of the dam.

1.5.3 Foundation Modelling

The foundation rock or soil region may be idealized as either a continuum, a viscoelastic halfspace for example, (Chopra et al, 1980) or as a finite element system

(Vaish and Chopra, 1974 and Gutierrez and Chopra, 1978). The former is used for uniform soils extending for large depths while the finite element analysis is used for sites which have different formations. Using the visco-elastic half space, whenever possible, reduces the number of degrees of freedom of the structure. In this case, the substructure method is used to include the dam-foundation interaction. The effect of the reservoir-foundation interaction is also included in the substructure method. An example of the modelling of the alluvium and sediments invariably present at the bottom of actual reservoirs was suggested (Fenves and Chopra, 1984). The results obtained showed the importance of including these interactions on the overall response of the structure. Time domain analyses using nonlinear contact elements located at the dam - foundation interface were applied to determine the dynamic sliding and uplifting response of gravity dam monoliths considering various elastic foundation properties (Leger and Katsouli, 1989). The numerical results have shown that the non-linear behaviour of the dam foundation interface reduces the seismic response of the system, indicating the possibility of more rational and economical designs.

1.5.4 Dam Modelling

Finite Element approximation with displacement degrees of freedom are normally used to model the dam structure. Assuming that unkeyed contraction joints between monoliths will fail during earthquakes, each monolith is assumed to vibrate independently. Plane stress and plane strain two dimensional elements are used to model the dam. The analyses described before assumed a linear elastic behaviour of the dam.

Although linear analysis is convenient and simple, it is not suitable for some purposes such as the determination of the collapse load and damage of dams subjected to severe seismic excitation. However, shaking table tests of small scale models also show concrete cracking and demonstrate the occurrence of water cavitation as well (Niwa and Clough, 1980). Neglecting the hydrodynamic effects, the damage to Koyna dam was studied using a smeared (Pal, 1976 and Bicanic and Zienkiewicz, 1983) and discrete (Skrikerud and Bachmann, 1986) crack approaches. In the Smeared Crack Approach (SCA), the effects of cracking are distributed over a finite element, so the exact location of a crack can not be known, while in the Discrete Crack Approach (DCA), cracks are generated between the elements. The DCA requires a substantial computational effort to modify the mesh after each step. For this reason, SCA was often used. The concrete constitutive models used in the literature were simplified and the difference in behaviour between massive and structural concrete was neglected. Mlakar (1987) studied the earthquake response of three dams of different heights using the smeared crack method with added masses to represent the hydrodynamic effects. A finite element procedure to model the nonlinear earthquake response of concrete gravity dam system was presented (El-Aidi and Hall, 1989). The nonlinear behaviour is represented by smearing techniques and include tensile cracking with subsequent opening, closing and sliding, as well as water cavitation in the reservoir. To achieve frequency independence, the foundation stiffness and damping functions are taken to be constants as evaluated at a frequency equal to the fundamental frequency of the dam-reservoir-foundation system.

The analyses of concrete gravity dams discussed above are based on a two dimensional analysis which is suitable for smooth, unkeyed contraction joints. However, when keyed contraction joints are used, it is expected that monoliths will interact in a manner that may affect the overall response of the system. A simplified three dimensional analysis of the dam that neglects the contraction joints by assuming monolithic structure, was presented by Rashed and Iwan (1984). It was concluded that a reduction of up to 80% of the response could be obtained depending on the length/height ratio of the dam. Although many approximations have been considered in this study, it still shows the importance of the third dimension of the structure. It was demonstrated that a new method of solution based on a Ritz transformation of a reduced system of generalized coordinates using load dependent vectors is able to maintain the high expected accuracy of modern computer analysis. The approach significantly reduces the execution time over eigen solution procedures (Leger and Katsouli, 1989). A three dimensional modelling of 160 ft gravity dam was carried out for different ratios of length (L) to height (H) ratios (Haroun and Abdel Hafez, 1991). It was concluded that the effect of the dam-reservoir interaction is more pronounced near the fundamental frequency than at higher frequencies and that the relative difference in the frequencies for dams with large L/H ratios is larger than that for dams with smaller ratios. The seismic analysis of Piedra del Aguila dam in Argentina was performed by Stuardi and Prato (1990). The results obtained, which will be discussed in chapter 2, are significantly different than those obtained by Rashed and Iwan (1984). It was concluded that the effect of monoliths interaction on the response of gravity dams built with keyed contraction joints is not yet well established. As a traditional three dimensional analysis, based on the theory of elasticity, is complex and practically not feasible, new engineering solutions are required.

1.6 OBJECTIVES AND SCOPE

The objective of this study is to analyze concrete gravity dams with keyed contraction joints including the effect of monoliths interaction. As a typical two dimensional analysis cannot be used for such purpose, a new engineering procedure is developed. Using this procedure, the response of gravity dams is evaluated and compared with those analyses without monoliths interaction. Also, the parameters which affect the degree of monoliths interactions are investigated. In chapter 2, a simplified procedure is suggested for the analysis of gravity dams with keyed contraction joints. Simplicity as well as the ability to use most of the available structural analysis codes are the main factors considered when introducing the procedure. However, due to its simplicity, the procedure is intended for the preliminary design of gravity dams. In chapter 3, a more refined approach is proposed. The method of analysis uses a substructuring technique as well as a reduction technique to model the structure. The new procedure is verified and compared to traditional three dimensional analysis. Chapter 4 describes the reservoir - dam interaction and foundation - dam interaction and their effect on the overall analysis. The properties of different types of contraction joints are described in chapter 5. The shear strength of each joint as well as its shear stiffness are determined and included in the analysis of the dam. The effect of the longitudinal profile of the dam on its response is presented in chapter 6. Three parameters are included; canyon cross-section, end conditions of the dam and overflow monoliths. Chapter 7 summarizes the conclusions and recommendations for future work.

Table (1-1) Concrete Gravity Dams Subjected to Significant Seismic Events (Bureau, 1990)

Name and Year Completed	Country	Height (m)	Length (m)	Earthquake Date	Distance to fault (km)	E.Q. magnitude	Remarks
Lower Crystal Springs, 1890	USA	47	183	April 18, 1906	.4	8.3	no damage
Hoover, 1936	USA	220	379	Many starting 1936	8	5.0	no damage
Blackbrook, 1900	England	30.5	147	Feb. 11, 1957	6.4	Grade 8 on English Scale of 10	Cracks in downstream masonry face
Koyna, 1963	India	103	835	Dec. 11, 1967	3	6.5	Cracks in both faces

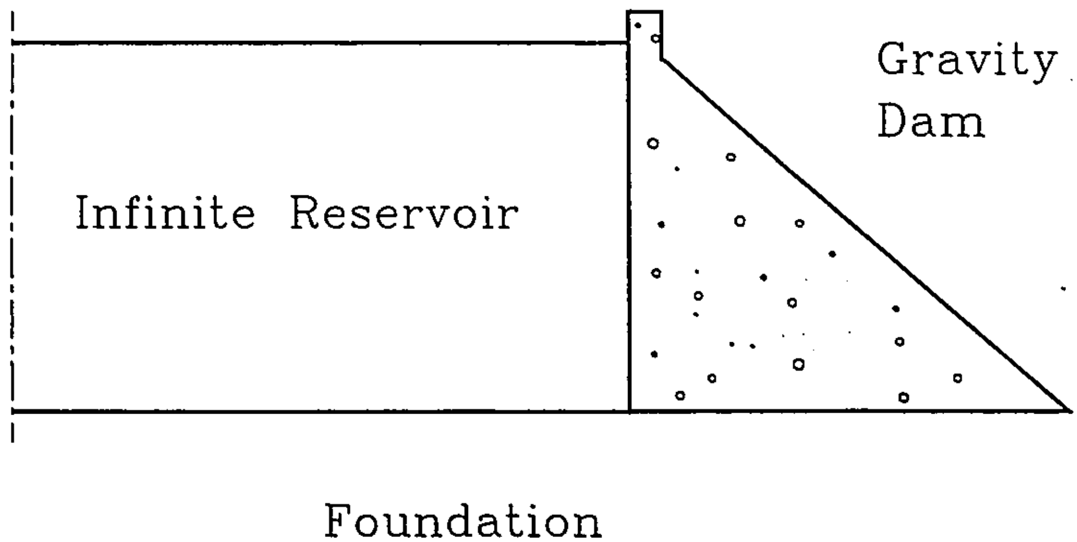

Figure (1-1) Typical Cross-Section of a Concrete Gravity Dam

CHAPTER 2

SIMPLIFIED PROCEDURE

2.1 GENERAL

The majority of previous studies on gravity dams used a two dimensional plane stress or plane strain model to represent the structure. The two dimensional analysis is based on the assumption that the geometry and material properties of the structure as well as the seismic motion do not vary along the dam's longitudinal axis. It is also assumed that the joints between the dam monoliths do not transfer shear forces. A two dimensional analysis is considered acceptable when unkeyed contraction joints are used in construction on the basis that monoliths will vibrate independently under strong shaking (Okamoto, 1984 and Chopra, 1987).

Initially, unkeyed contraction joints, or smooth joints, were commonly used in dam construction until it was discovered that this type of joints is suspectable to water leakage. Although water stop plates and several other remedies were attempted, the results were unsatisfactory. As a result, concrete shear keys were introduced in the design of most of the recent concrete gravity dams. The monoliths are expected to interact during earthquakes as long as the shear keys are capable of transmitting shear forces. In this case, it becomes important to include the effect of the third dimension along the dam's longitudinal axis. In this chapter, the three dimensional analysis presented by various authors are discussed. A simplified procedure to investigate monoliths interaction is presented. The effect of monoliths interaction is included in the analysis of different dam structures to investigate its design implications.

2.2 BACKGROUND ON MONOLITHS INTERACTION

The exact analytical evaluation of the dynamic behaviour of concrete gravity dam-reservoir-foundation system including monoliths interaction, is extremely difficult. A three dimensional finite element treatment of the system involves a very large number of degrees of freedom which is not practical to conduct. For this reason, simplified models were used in two studies related to the effect of monoliths interaction by Rashed and Iwan (1984) and Stuardi and Prato (1990).

Rashed and Iwan (1984) simplified the analysis by making the following assumptions:

1) The dam is founded in a rectangular canyon, has a rectangular cross-section uniform along its length and rests on a rigid foundation as shown in figure (2-1).
2) The concrete material of the dam is homogeneous, isotropic and linearly elastic.
3) The out of plane deformations of the dam is modeled by thick plate theory which neglects bending effects.
4) The reservoir is of constant depth and has parallel sides extending to infinity in a direction normal to the dam's face.

In their analysis, an approximate solution was obtained through the use of the assumed modes method. The dam displacement was expressed as a linear combination of a number of admissible functions, satisfying the essential boundary conditions of the dam.

The results obtained in this study showed that the change in the length / height ratio significantly affects the frequency domain response of the dam, both in magnitude and location of resonant peaks. This in turn would affect the dam's response to earthquake ground motion. Variations in the response of the structure to transverse ground motion, perpendicular to the axis of the dam, with the change in the length / height ratio were found to be within the range of 20 to 80% of the two dimensional response. It was concluded that the two dimensional solution, currently used in the seismic analysis of gravity dams, could greatly overestimate the earthquake response of a dam whose length is less than four to five times its height. In such cases, a three dimensional analysis should be used. However, some of the assumptions used by Rashed and Iwan oversimplify the model and are not necessarily applicable or practical such as the use of rectangular cross-section for the dam monolith. They also assumed a rectangular cross-section for the canyon which is not necessarily true as it may have different shapes. The use of assumed admissible functions to express the response of the structure is an example of oversimplifying the analysis. As a result, a more accurate and representative method of analysis to evaluate the effect of monoliths interactions is needed.

The seismic analysis of Piedra del Aguila dam in Argentina was performed using a simplified 3-D analysis, with the purpose of evaluating the influence of the valley cross section on the seismic response of typical dam monoliths (Stuardi and Prato, 1990). The concrete gravity dam, which consists of 42 monoliths of conventional triangular cross section, has a crest length of 820 m and maximum height of 173 m as shown in figure (2-2). The contraction joints were kept open to allow relative displacements between blocks, except in the lower central region of the valley. The dam monoliths are 20 m wide. The fluid domain was solved using finite element mesh as an infinite prismatic channel, while each monolith of the dam was represented by its first two modes of vibration. The results obtained were compared with those from a two dimensional plane stress model for the highest and intermediate monoliths. Results showed a significant increase in seismic response of the highest blocks when compared with the plane model, while very little influence is observed for the intermediate blocks. In spite of the three dimensional nature of their analysis, monoliths interaction has not been included assuming that the dam is built with smooth contraction joints. As a result, the slight increase in the response of the critical monolith, is mainly due to the change in the hydrodynamic forces acting on the upstream face of the dam. This procedure has its limitations as it is only applicable to dams with open contraction joints. The assumed mode shapes are different than those obtained when using keyed joints.

The results and conclusions presented in the two studies appear to contradict each other. While Rashed and Iwan excepted a reduction of the dam response due to the inclusion of the third dimensional effect, Stuardi and Prato suggested the opposite, at least for the critical monolith. The increase or decrease in the response is due to several reasons among which are the increase in the frequency of free vibration and the characteristics of the ground motion input. The objective of this chapter is to investigate the importance of monoliths interaction, as a form of three dimensional behaviour, on the overall response of the structure. A simplified model is developed and its results are compared to predictions of the more accurate three dimensional procedure in a few specific simple examples. The effect of monoliths interaction is evaluated for different valley cross sections.

2.3 ANALYSIS PROCEDURE

The equations of motion for each monolith can be written in the general form:

$$[M]\{\ddot{r}\}+[C]\{\dot{r}\}+[K]\{r\}=[M][I]\{\ddot{u}_g\}+[R] \tag{2-1}$$

Where,

[M], [C] and [K] are the mass, damping and stiffness matrices of the dam, respectively.

{r} is the nodal displacements vector.

[I] is the influence matrix for the ground motion components.

{ $\ddot{u}_g$ } is the ground acceleration vector

[R] is the matrix of interaction forces which may be written in terms of the three components:

$$[R] = [R_r] + [R_f] + [R_m] \tag{2-2}$$

where,

$[R_r]$ represents the forces resulting from the reservoir - dam interaction

$[R_f]$ represents the forces at the foundation - dam interface

$[R_m]$ represents forces due to monoliths interaction

For simplicity the foundation - dam interaction is neglected in this preliminary investigation by assuming the dam to be built on rigid foundation. Although previous research emphasized the importance of this interaction for dams with flexible foundation, it is not included in the present investigation to maintain the simplicity of the procedure. In the following sections the modelling of each domain is discussed in details.

2.3.1 Dam Domain

Gravity dams consist of a number of monoliths separated by contraction joints. To include the effect of monoliths interaction, the structure is divided into two components; monoliths and contraction joints, as shown in figure (2-3). The monoliths are modeled using beam elements while the contraction joints are modelled using one dimensional shear links. The following assumptions were adopted in developing the model:

1- No longitudinal forces along the dam's axis are allowed to transfer across the contraction joints. This is based on the fact that in most contraction joints the grouting is usually cracked or in some cases no grouting is used. This assumption reduces the forces transferred through contraction joints to shear forces only.

2- The contribution of the longitudinal ground motion component acting in the direction of the dam axis is assumed to be small and is not included in the analysis. This assumption is based on the results presented by Rashed and Iwan (1984) which showed that the contribution of this component is less than 8% of the horizontal transverse component acting normal to the dam's axis.

3- The contraction joints used in this study are keyed joints with large stiffness. It is assumed that they can resist the shear forces without slip. This is regarded as upper bound for the behaviour of the contraction joints with the lower bound being to completely neglect their shear strength resulting in a two dimensional analysis. This assumption which is compatible with the simplified nature of this study has been used to show the maximum effect of monoliths interaction. More investigation on the shear behaviour of contraction joints will be presented in chapter 5.

2.3.1.1 Monoliths Modelling

Each monolith of the dam is modeled using beam elements which has the two advantages of keeping the number of degrees of freedom to a minimum and being available in most of structural engineering computer codes. The properties of the elements were varied along the height as the dimensions of the monolith change. The dimensions at the mid height of each beam element are used to evaluate the section properties. The use of tapered beam elements is expected to slightly improve the accuracy but on the other hand will exclude the use of many available programs. As the depth to span ratio of the monolith is high, shear deformations are included in the analysis. To evaluate the accuracy of replacing typical finite element modelling of monoliths with beam elements, rectangular and the conventional triangular dam cross sections with different width/height ratios shown in figure (2-4) were analyzed. The frequencies of free vibration of the structure obtained using beam elements and 3-D

Finite Element (F.E.) codes are compared in tables (2-1) and (2-2). The difference in the frequency results for the fundamental mode of vibration is in the order of 5 %. It is noted that the triangular section has a lower accuracy at higher modes than the rectangular sections. The structure was subjected to the horizontal component of the taft ground motion. The time history of the top displacements using beam and the finite element models are compared when using triangular section with width/height ratio= 1.0 as shown in figure (2-5a). When a rectangular section with width / height ratio= 0.7 is used, the comparison is shown in figure (2-5b). The two response plot comparisons in figures (2-5a and b) show very close agreement between the analysis using beam elements and finite elements. The two graphs almost coincide except for small differences at the peaks. It is concluded that using beam elements to model the dam gives reasonable results in comparison to the finite element approach. As the accuracy of the beam model decreases for higher modes and because modelling of fluid effect is based on the fundamental mode of the dam, the proposed model in this study is restricted to the first mode only. The error resulting from this restriction is small as gravity dams are short period structures and their response is mainly in the fundamental mode.

2.3.1.2 Joint Modelling

Contraction joints between monoliths are assumed to have large shear stiffness. By using beam elements to model the monoliths, the length of the monolith in the longitudinal direction of the dam is represented by a single point, as shown in figure (2-3). As a result, the longitudinal profile of the transverse displacement of the dam will be constant along the dam length which does not represent the expected displacement profile as shown in figure (2-6). Including the torsional degrees of freedom for beam elements will not remedy the situation as each monolith will be allowed to rotate but they still have to fulfil the condition of equal displacements at the same level because of the rigid joints assumption. The displacement profile shown in figure (2-6) as a broken line is considered to be a better approximate representation of the deflection. This deflection profile can be obtained by introducing some flexibility in the connecting links. A practical procedure is proposed for the evaluation of this flexibility. The difference in deflection between two points at the same level, in the monolith shown in figure (2-7), will result from different forces on the two edges (F_1 and F_2). If both F_1 and F_2 are equal, no variation in the deflection profile across the monolith will be encountered and the load is totally resisted in the vertical direction. This corresponds to the case of typical two dimensional analysis. When the two forces are different, part of the load is carried in the horizontal direction and the rest in the vertical direction. The result is a torsional moment on the section which causes a difference between the displacements of ends A and B. As relative values of forces and displacements are more important at this stage, the monolith with two different shear forces at its end joints F_1 and F_2 is replaced by an equivalent system as shown in figure (2-7). The length of the monolith in plan is represented by a cantilever. The force F acting at the free end represents the difference between F1 and F2. The horizontal stiffness of this cantilever including shear deformations is given by the formula,

$$k = \frac{1}{\frac{L^3}{3EI} + \frac{L}{GA_r}} \tag{2-3}$$

where, E is modulus of elasticity of concrete

G is the shear modulus of concrete

L is length of the monolith

I is the moment of inertia of the monolith about the lateral axis

A_r is the shear area of the monolith

The first term on the right hand side represents bending deformations within the monolith and the second term represents shear deformations.

To verify the accuracy of the proposed approach, a simplified concrete gravity dam with rectangular cross-section, as the one used by Rashed and Iwan (1984), is analyzed. The idealized dam structure, shown in figure (2-8), is assumed to consist of 12 monoliths of different heights. The linear analysis of gravity dam response to seismic ground motion was performed using the finite element code SAP IV assuming 5% damping ratio. Different cases of the ratio H_1/H_2 were considered in order to evaluate the effect of sudden change in span topography on the accuracy of the results. The simplified three dimensional model of this structure is shown in figure (2-9).

The natural frequencies of the structure with different H_1/H_2 ratios evaluated by the proposed new model as well as the traditional three dimensional finite element analysis, are summarized in table (2-3). It is noted that high accuracy is obtained for the case of $H_1/H_2 = 0.0$ which represents a uniform foundation profile under the structure.

In this case, no shear forces are transmitted through the contraction joints as the response of each monolith to the ground motion is the same. However, increasing the ratio H_1/H_2 leads to a decrease in the accuracy of the natural frequencies especially for higher modes.

To verify the new approach's predictions, the displacements at different points of the crest are also compared under the horizontal component of the Taft Ground motion. The maximum displacement profile for the dam crest evaluated by the proposed model as well as the three dimensional procedure for the case $H_1/H_2 = 0.25$, are shown in figure (2-10). Good accuracy is achieved when using the new procedure as compared to the three dimensional finite element analysis. Similar results for the case $H_1/H_2 = 0.5$ are shown in figure (2-11). Good agreement between the two approaches is also observed. The results start diverging somewhat as the ratio H_1/H_2 increases. For practical purposes, the observed accuracy is considered acceptable for a ratio $H_1/H_2 < 0.5$

2.3.2 Fluid Domain

Several methods are available for including the hydrodynamic effects in the dynamic response analysis of concrete gravity dams. The equivalent static approach, developed by Westergaard (1933) is the simplest of these methods. However, this approach underestimates the hydrodynamic forces on the dam as it neglects the water compressibility and dam flexibility. Another method is to model the fluid using a continuum approach or a finite element approach (Chopra, 1967). A continuum approach is mostly effective for infinitely long uniform reservoirs with constant cross-section while the finite element approach is suitable for nonuniform reservoirs. A combined approach is sometimes used in the case of reservoirs with limited nonuniformity close to the structure. For the purpose of this study, the approximate added mass technique is used to simulate the hydrodynamic effects considering the horizontal component of an earthquake. This approximation was suggested by Chopra (1978). In this method the effect of the fluid interaction is assumed to be the same as added masses on the upstream face of the dam. The approach was successfully applied by several researchers studying various aspects of the seismic response of gravity dams (Malkar, 1987 and El-Nady et al, 1990). The main advantages of this method are the saving in computation time and effort and the fact that no special programming is required. The dynamic analysis procedure uses a displacement finite element formulation for the dam with added masses to approximate the hydrodynamic effects. Only the fundamental mode of vibration of the dam was included in calculating the added masses. The equations of motion of the system including hydrodynamic effects are written in the form:

$$[M^*]\{\ddot{r}\}+[C]\{\dot{r}\}+[K]\{r\}=-[M^*][I]\{\ddot{u}_g\} \tag{2-4}$$

$$[M^*]=[M]+[M_a] \tag{2-5}$$

where,

$[M_a]$ is the added mass matrix, at the upstream face of the dam, representing the hydrodynamic effects which is estimated by the formula proposed by Chopra (1978):

$$m_a(y)=\frac{P(y,\omega_s)}{\psi(y)} \tag{2-6}$$

where, ω_s is the fundamental natural circular frequency of dam with full reservoir and y represents the vertical spatial coordinates. ψ is the shape of the fundamental mode of vibration of the dam without water and P is the hydrodynamic pressure, in excess of the static pressure, as a function of the elevation on the upstream face of the dam and the fundamental frequency of the system, as given by the formula:

$$P(y,\omega_s)=\frac{2w}{gH}\sum_{n=1}^{\infty}\frac{I_n}{\sqrt{\lambda_n^{\,2}-\frac{\omega_s^{\,2}}{c^2}}}\cos\lambda_n y \tag{2-7}$$

where,

$$I_n=\int_0^H \psi(y)\cos\lambda_n y\,dy \tag{2-8}$$

$$\lambda_n=[(2n-1)\pi]/2H \tag{2-9}$$

where,

w is the unit weight of water

c is the velocity of sound in water

H is the water depth

g is the gravity acceleration

Because the dam - reservoir interaction lowers the fundamental natural vibration frequency of the dam, the damping ratio for the equivalent system ξ_s is less than the damping ratio ξ for the dam alone (Chopra, 1978). The damping ratio for the equivalent system is modified according to the following formula:

$$\xi_s = \frac{\omega_s}{\omega}\xi \tag{2-10}$$

where $\hat{\omega}$ is the fundamental natural frequency of the dam alone.

2.4 SYSTEM CONSIDERED

The critical cross section of the concrete gravity dam structure was analyzed using the proposed procedure to study the effect of monoliths interaction on the response of the structure during earthquake ground motions. A cross section having the same dimensions as the Pine Flat dam is selected as it has been extensively studied using a typical two dimensional analysis. The dam is 122.0 m high with base width equal to 95.6 m (at the critical section) and crest length of 550 m. The geometry and dimensions of the selected dam cross-section are shown in figure (2-12). For the purposes of the present study, the longitudinal profile of the model structure is assumed to have the geometry and shape of a typical valley as shown in figure (2-13a). For simplicity, the foundation under the dam is assumed horizontal and the upstream face of the structure is assumed vertical. The concrete in the dam is assumed to be homogenous, isotropic and linear elastic, with the following properties: unit weight of 24.3 kN/m^3, shear modulus of 14.74 x 10^6 kPa and Poisson's ratio of 0.17 which corresponds to a modulus of elasticity of 34.45 x 10^6 kPa.

Stiffness proportional damping is assumed to be 5 % of the critical damping at the fundamental vibration frequency of the dam alone. The water has a unit weight of 10 kN/m^3 and the velocity of wave propagation is 1440 m/s. Only the critical case of full reservoir has been considered in this study.

The dam was divided into seven monoliths, three of which have critical height. The final model for the structure consists of 7 cantilever beams connected in the horizontal direction as shown in figure (2-13 b). The properties of the connecting beams at various levels are different and are evaluated by equation (2-3). The horizontal input ground motion is assumed constant at the base of the dam and is considered to be the same at different foundation levels.

The planar finite element model for the typical two dimensional analysis consists of 100 - four node, isoparametric, quadrilateral, plane stress elements of unit thickness. To include the hydrodynamic effects, horizontal concentrated masses were added to the nodes at the upstream face of the dam using equation (2-6). The earthquake ground motion record used in this study is the S69E component of the (1952) Taft earthquake recorded at the Lincoln School Tunnel. This record is considered to be an intermediate frequency earthquake with an estimated dominant circular frequency content of $\omega = 12.5$ rad/s (Naumoski, 1988). This record was selected because it has been frequently used in dam analysis.

2.5 RESPONSE RESULTS

A comparison between the natural frequencies of the structure using the simplified procedure and a typical two dimensional analysis, is shown in table (2-4). The results of typical three dimensional analysis of the structure is also included in the table to check the accuracy of the simplified model. The fundamental frequency obtained using the three dimensional and simplified procedures are almost identical for the first mode while there are differences in higher modes. It is noted that the three dimensional analysis of concrete gravity dams gives higher natural frequencies for the first four modes than the typical two dimensional analysis for the critical section. This results from the fact that most dams built across valleys have a typical cross-section with maximum depth at the middle and decreasing gradually towards the sides. The critical section is restrained by neighbouring shorter and stiffer monoliths.

The time history of the crest displacement of the model structure, in case of empty reservoir, evaluated using the simplified procedure and the typical 2-D analysis are shown in figure (2-14). The dam response evaluated using the two dimensional analysis is overestimated. The percentage of overestimation can be as high as 65 % . The decrease in response by using the simplified procedure as compared to the typical 2-D analysis is associated with the contribution of the longitudinal dimension to the load carrying system. The maximum displacement occurs at different times in each analytical procedure. The dam response evaluated by the simplified and the two dimensional procedures is shown in figure (2-15) when the hydrodynamic effects are included. Similar pattern of behaviour was observed. In this case, the percentage difference resulting from neglecting monoliths interaction, reaches approximately the same value of 65% obtained without hydrodynamic forces. The displacement profile along the height of the critical monolith evaluated by the two procedures without hydrodynamic forces are shown in figure (2-16). The same relationship including the reservoir - dam interaction is shown in figure (2-17). In both cases, when the effect of interaction in the longitudinal direction is neglected, the dam's response was overestimated by the two dimensional analysis.

The accuracy of stresses calculated directly from the beam model decreases dramatically when the height / span ratio of the monolith increases. However, good accuracy can still be obtained by calculating stresses by a simple indirect procedure. The shear forces calculated using the previous analysis can be reapplied as a time history record, to the two dimensional plane stress model. These forces are applied at the centreline of the dam cross-section and the response of the structure during the ground motion input is evaluated using the typical two dimensional model except for the addition of the shear forces which represent adjacent monoliths interaction. The maximum principal tensile stresses in the critical monolith, as evaluated by the two procedures without hydrodynamic effects are shown in figure (2-18 a and b). The decrease in the calculated stresses when using the proposed procedure is quite noticeable. A reduction of up to 28 % may result.

Earthquake records are classified according to their peak horizontal ground acceleration (in g)/ peak horizontal ground velocity (in m/sec), A/V ratio, into three categories: high, intermediate and low. The A/V ratio is considered to be an indication of the frequency content in the record. The earthquake ground motion record used in this study is considered to be in the intermediate range. To investigate the effect of the frequency content of the input ground motion on the response results, a representative record of each category is applied to the model structure. The two records representing high and low frequency contents are the horizontal components of; the Long Beach earthquake recorded at the subway terminal, L.A. 1933 and Parkfield earthquake recorded at the temblor No. 2, 1966. The three ground motions were recorded in California and the soil condition at the station sites are rock, which is normally the case for gravity dams. Details of the records are shown in table (2-5) and the first 8 seconds of each record is shown in figure (2-19). The envelope of the horizontal displacement for the critical monolith was evaluated for the two records, representing high and low frequency contents, and the results are presented in figures (2-20) and (2-21), respectively. It is noted that the response of the dam decreases when including monolith interaction. Although these results give indication that in most cases the response decreases, it is expected that there may be a few exceptional cases. In the case of low frequency content earthquake applied to the structure without hydrodynamics, as shown in figure (2-21 a), the response is almost the same when calculated using 2-D analysis or 3-D analysis. This may happen when the shifted frequencies of the structure are close to the dominant frequencies in the earthquake record and as a result resonance may occur. The increase in the fundamental frequency due to the longitudinal interactive effect move the dam frequency beyond the normal range for recorded earthquake ground motions.

The dam cross sections used in this study were chosen to be similar to the previous studies; rectangular sections as used by Rashed and Iwan (1984) and triangular sections as used by Staurdi and Prato (1990). For both types of cross-section, the conclusions reached in this work support those noted by Rashed and Iwan (1984). Stuardi and Prato have concluded that the canyon cross section will most likely cause an increase in the response of the critical monolith. This appears to contradict the conclusions of this study which was mainly concerned with structural effects. It is worth noting that the type of contraction joints used are different. Stuardi and Prato applied their procedure to dams with open joints which means that the interaction forces among the monoliths are not created. The effect of the canyon cross section on the structure resulted from the variation of the hydrodynamic forces which are different from those obtained assuming typical two dimensional analysis. The effect of the monolith interaction investigated in this study is quite different from the effect of the increased hydrodynamic forces due to three dimensional effects of canyon configuration as was considered by Stuardi and Prato. For dams built with keyed contraction joints, it is expected that a reduction in the response of the critical monolith may take place, depending on the longitudinal profile of the dam. In the present analysis, the effect of canyon configuration on hydrodynamic forces is ignored.

2.6 SUMMARY

A simplified procedure for the analysis of concrete gravity dams is developed to investigate the effect of monoliths interaction. Simplicity as well as accuracy were the main motivations in developing the procedure. Beam elements are used to model monoliths and connecting joints. The effect of monoliths interaction is demonstrated to be important and should be included in the analysis of gravity dams constructed with keyed contraction joints specially for irregular canyon cross sections. Including monoliths interaction causes a shift in the natural frequencies of the structure to higher values leading to a stiffer structure. This is expected to cause a reduction or increase in the response of the structure depending on whether the dominant frequency of the exciting ground motion matches the shifted frequencies of the structure. In general, the response is expected to differ from that obtained from a typical two dimensional analysis. Limited analysis of typical concrete gravity dams indicate that the increased fundamental frequency is high enough to fall beyond the dominant frequency in earthquake ground motion records.

The model suggested in this study is recommended for preliminary evaluation of the importance of monoliths interaction for gravity dams. However, for detailed analysis of gravity dams including monoliths interaction, a more refined model which overcomes the drawbacks of the simplified one is suggested in chapter 3.

Table (2-1) Frequencies of Free Vibration (rad/s) of Rectangular Section

Mode No.	B=.4 H		B=.7 H		B= H	
	Beam	F.E.	Beam	F.E.	Beam	F.E.
1	13.96	14.07	21.17	21.14	25.64	25.7
2	59.07	59.90	59.07	60.51	59.07	60.52
3	62.43	60.47	76.40	67.45	83.66	67.33
4	132.2	127.1	149.6	132.4	156.1	96.69
5	175.4	176.8	175.4	134.4	175.4	118.2

Table (2-2) Frequencies of Free vibration (rad/s) of Conventional Dam Section

Mode No.	B=.4 H		B=.7 H		B= H	
	Beam	F.E.	Beam	F.E.	Beam	F.E.
1	19.48	19.14	28.44	28.26	32.53	33.43
2	39.05	45.40	57.47	62.83	66.37	70.34
3	63.33	83.39	84.67	84.08	80.24	81.38
4	87.97	89.22	84.99	107.8	95.32	115.7
5	107.4	136.2	133.4	160.8	141.5	162.0

Table (2-3) Natural Frequencies (Rad/s) of The Idealized Dam

Mode No.	$H_1/H_2=0.0$		$H_1/H_2=0.25$		$H_1/H_2=0.5$	
	Simplified procedure	3-D Analysis	Simplified Procedure	3-D Analysis	Simplified Procedure	3-D Analysis
1	120.9	121.1	105.8	102.8	95.2	92.5
2	169.6	171.0	156.8	161.5	150.7	157.2
3	268.8	264.5	256.0	255.4	244.0	242.3
4	367.3	304.9	297.5	298.8	249.1	280.9
5	369.2	374.9	315.2	319.6	269.5	295.3

Table (2-4) Natural Frequencies (Rad/s) of The Model Structure

Mode No.	With Hydrodynamic		Without Hydrodynamic		
	Simplified Procedure	2-D at Critical Section	3-D	Simplified Procedure	2-D at Critical Section
1	21.52	16.65	30.53	30.58	24.53
2	35.58	27.68	41.25	59.29	55.08
3	45.88	37.55	47.04	63.41	66.99
4	49.83	52.03	55.03	87.37	92.68
5	61.21	65.69	59.28	87.99	135.90

Table (2-5) Earthquake Ground Motion Records

No.	Event	Date	Magnitude	Station & Comp.	Max. Acc. in (g)	Max. Vel. in (m/s)	A/V
1	Parkfield	1966	5.6	Temblor N65W	.269	.145	1.86
2	Kern county	1952	7.6	Taft S69E	.179	.177	1.01
3	Long beach	1933	6.3	L.A. Subway N51W	.097	.237	0.41

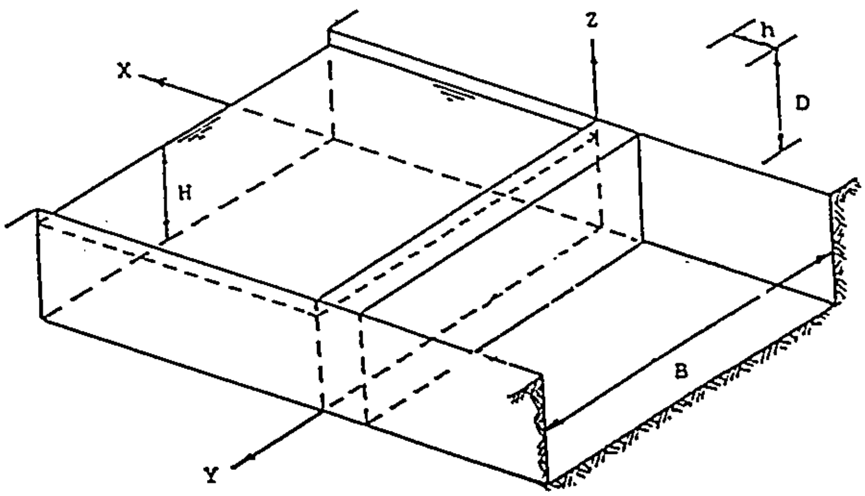

Figure (2-1) Dam section Used by Rashed and Iwan (1984)

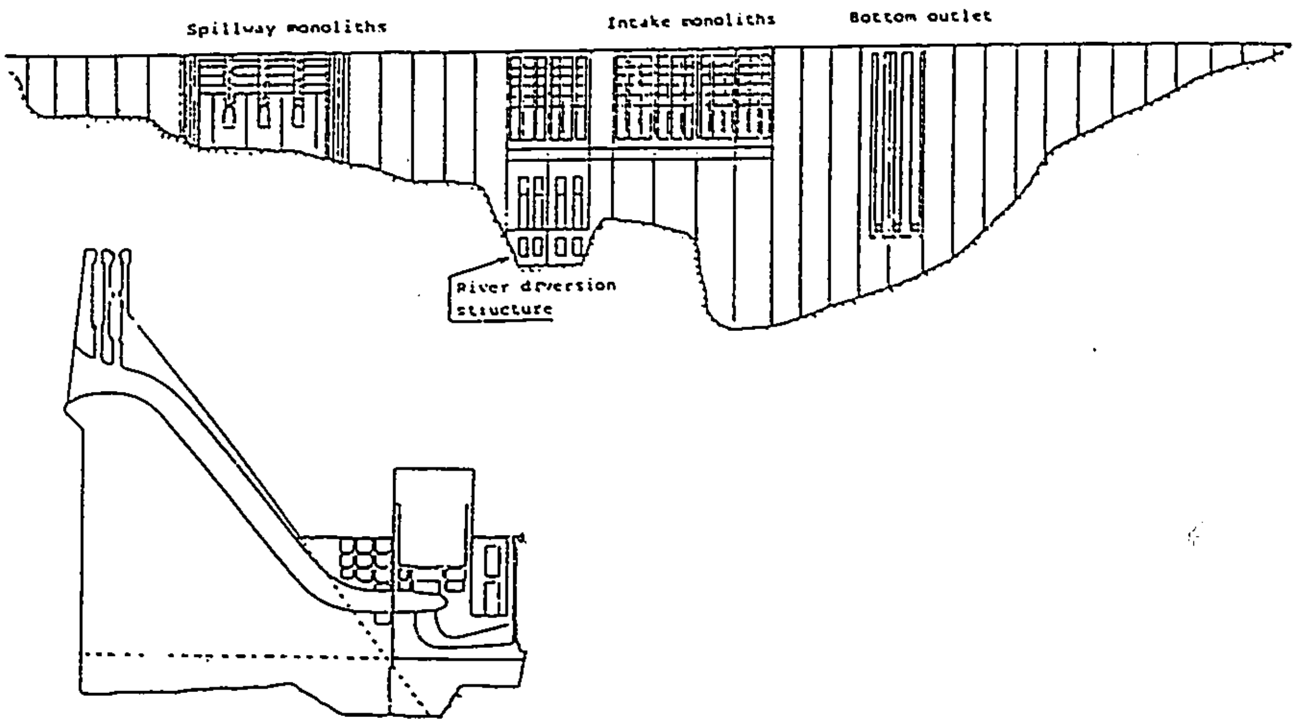

Figure (2-2) Geometry of Piedra del Aguila dam in Argentina
(Stuardi and Prato, 1990)

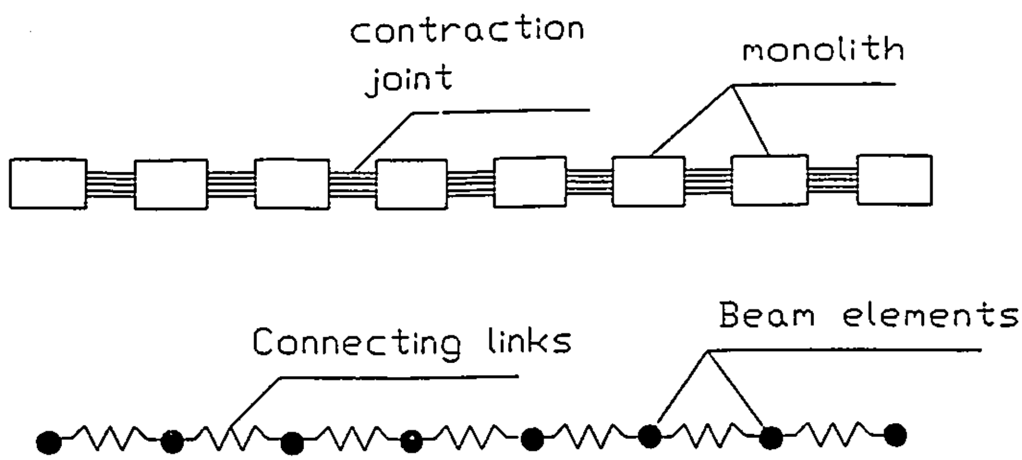

Figure (2-3) Modelling of the Longitudinal Profile of Concrete Gravity Dams

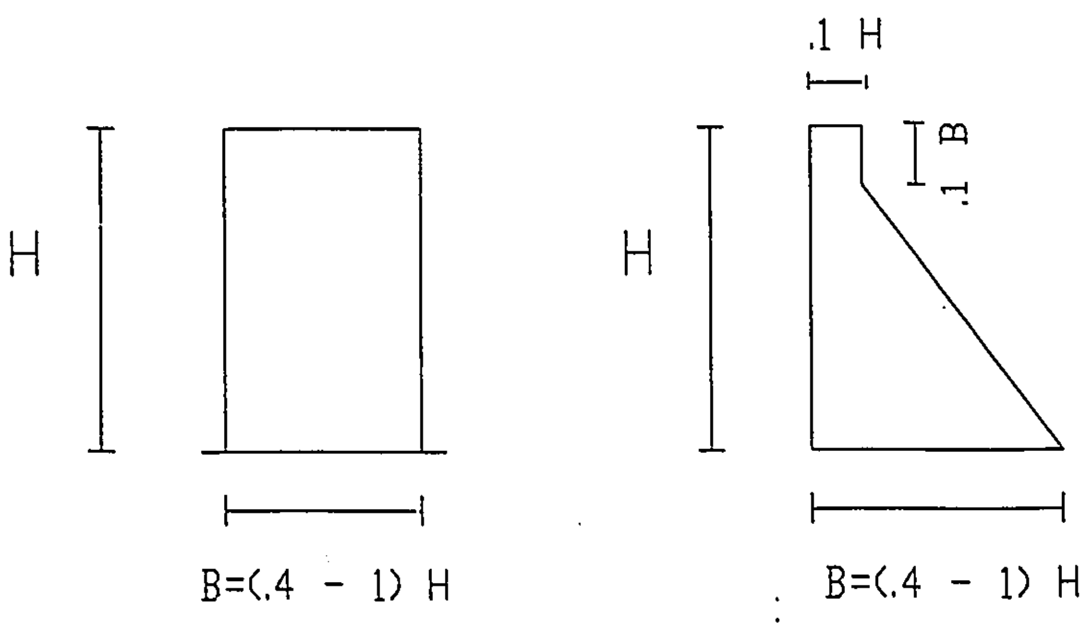

Figure (2-4) Cross-section of the Model Structure

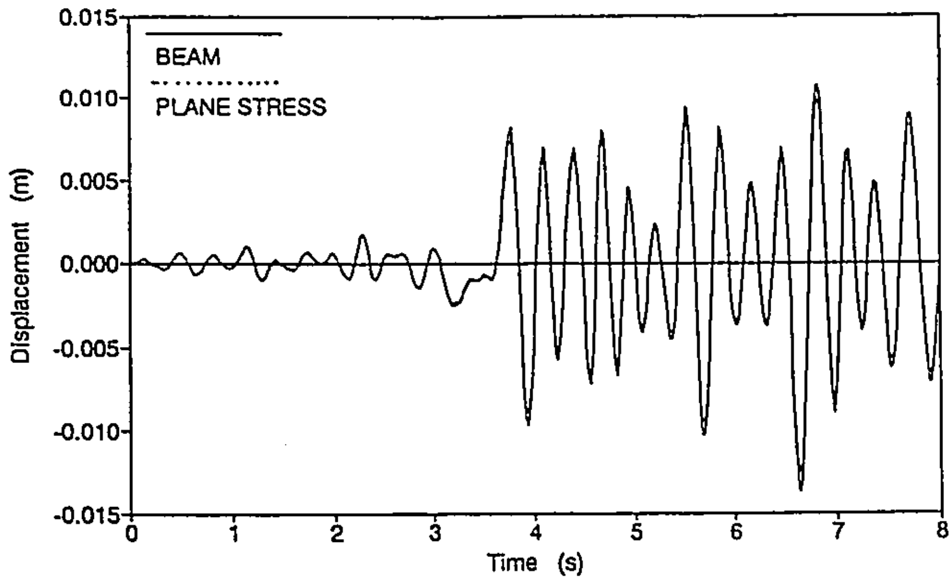

a) Triangular Section; B=100 m

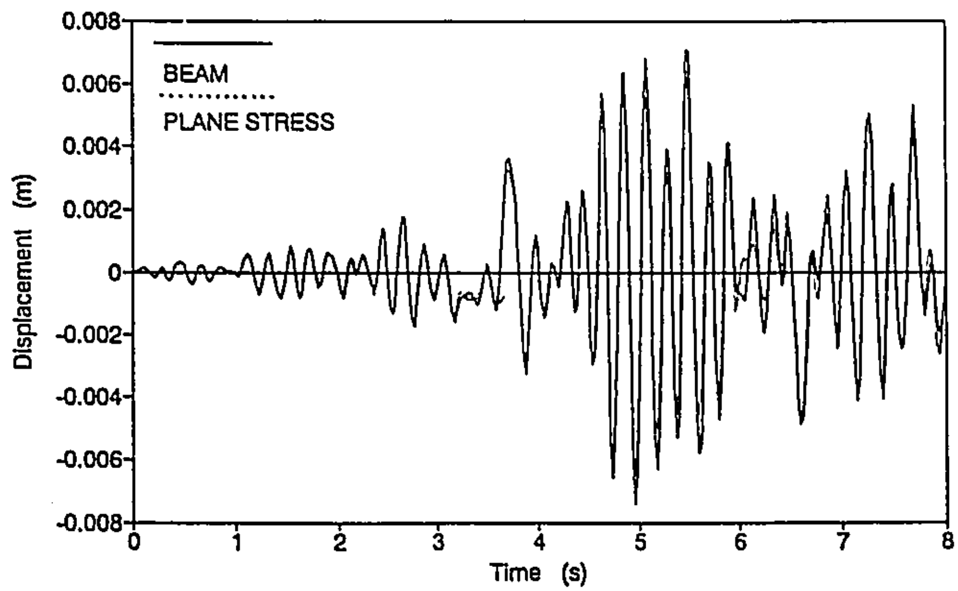

b) Rectangular Section; B=70 m

Figure (2-5) Crest Displacement Time History of the Dam Structure

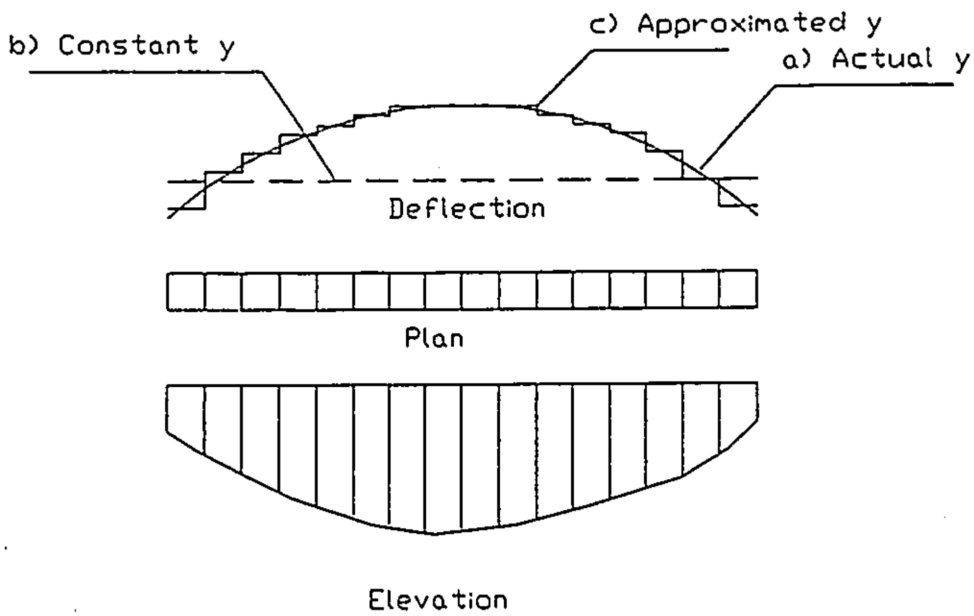

Figure (2-6) Longitudinal Deflection Profile of a Concrete Gravity Dam

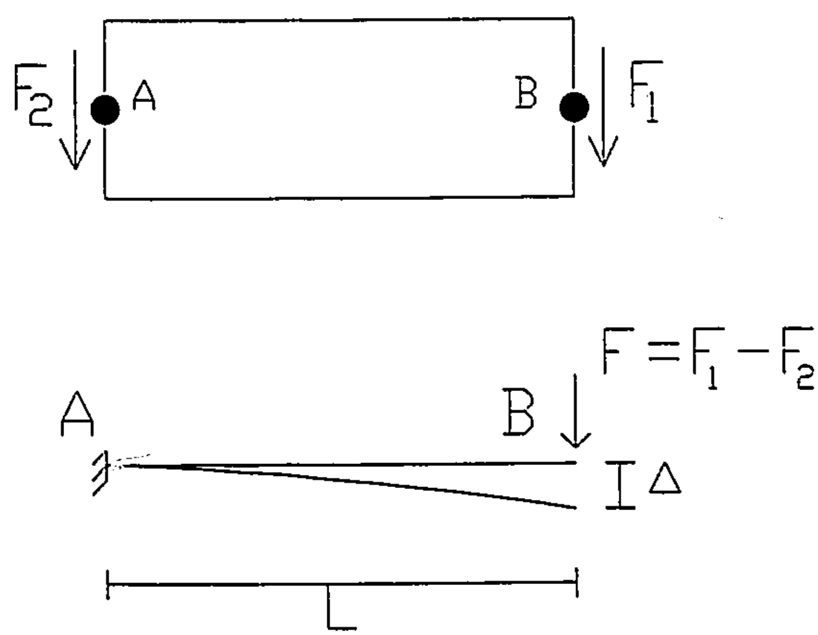

Figure (2-7) Stiffness of the Connecting Links

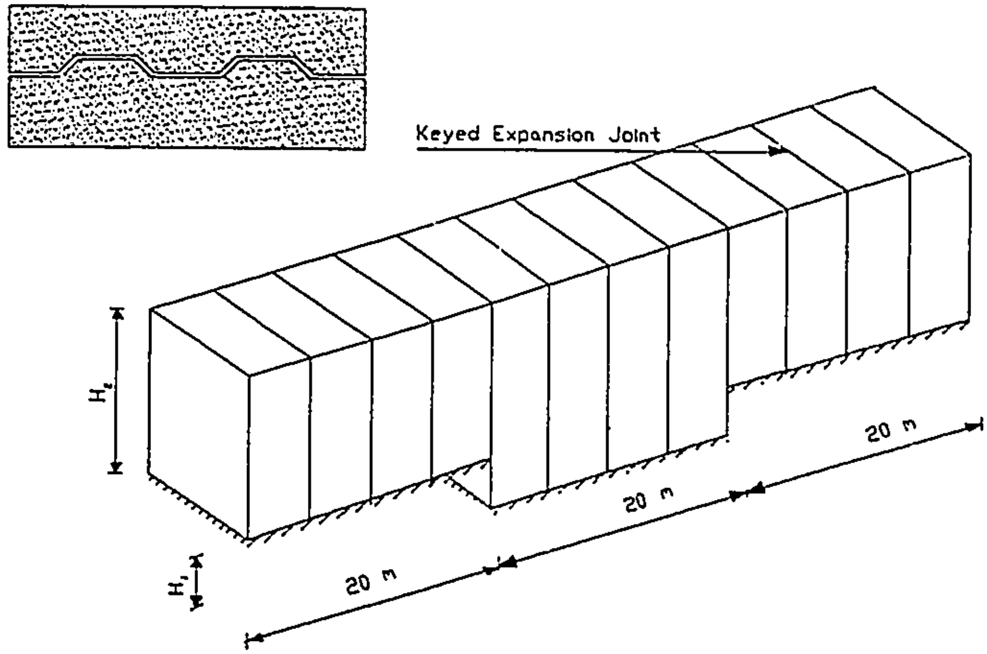

Figure (2-8) Geometry and Dimensions of an Idealized Dam Structure

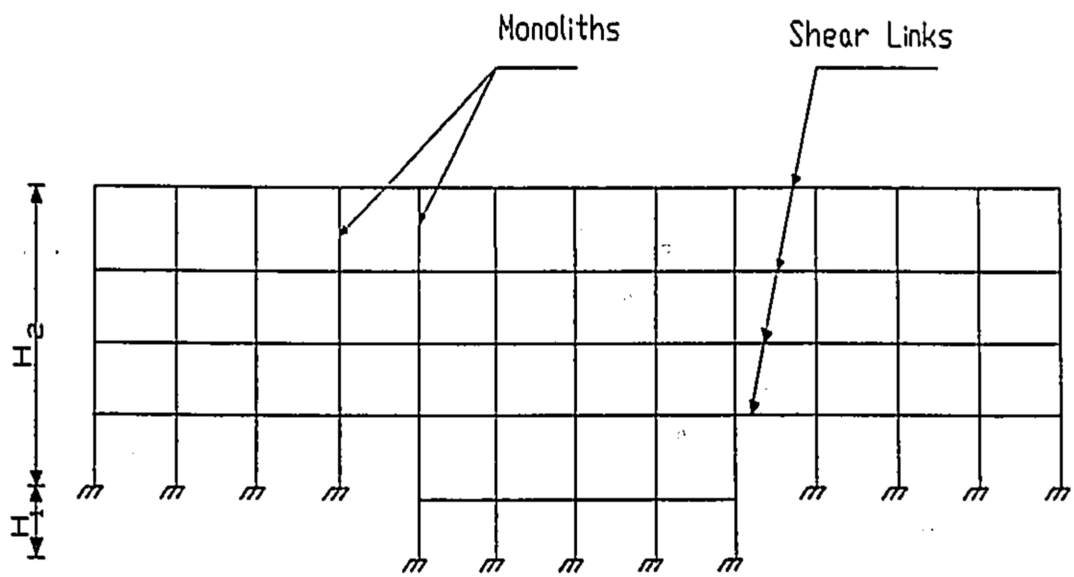

Figure (2-9) Modelling of the Dam Structure

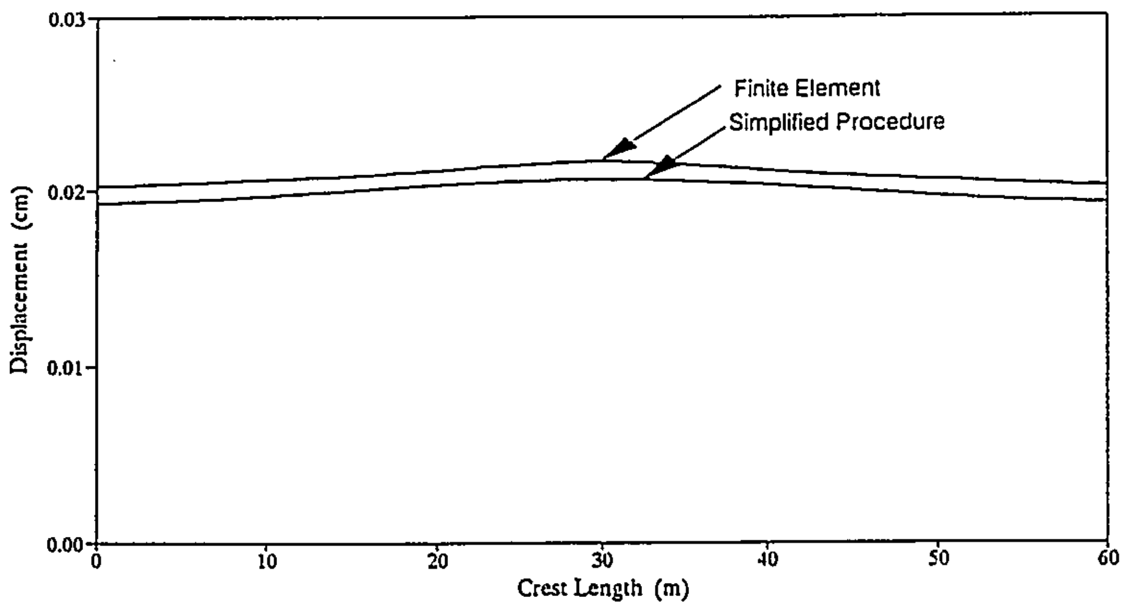

Figure (2-10) Crest Displacement Profile of The Model Structure
$H_1/H_2 = 0.25$

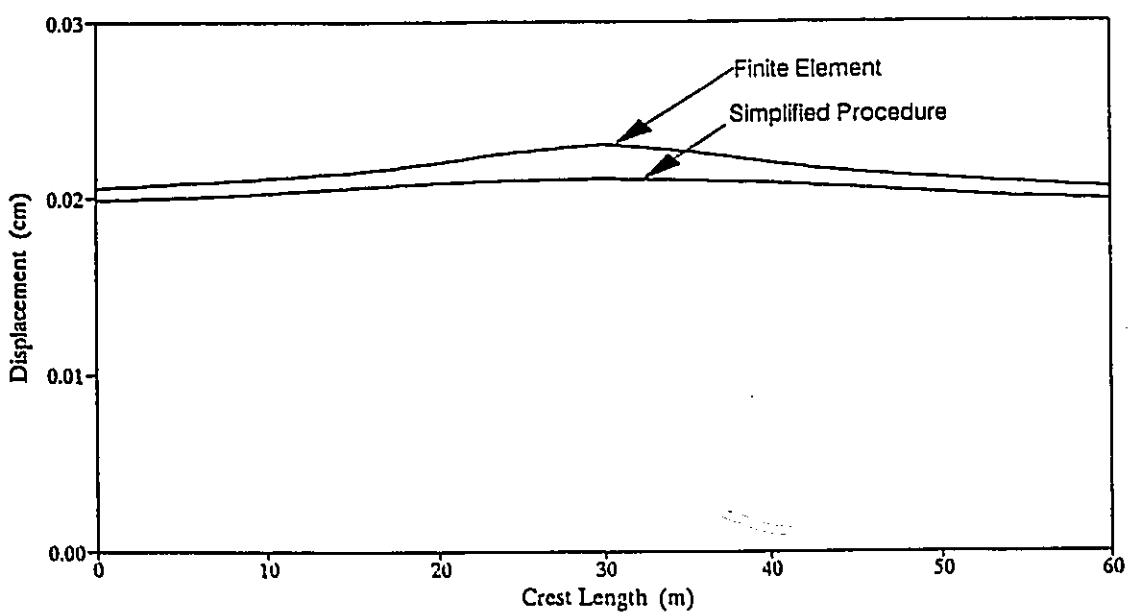

Figure (2-11) Crest Displacement Profile of the Model Structure
$H_1/H_2 = 0.5$

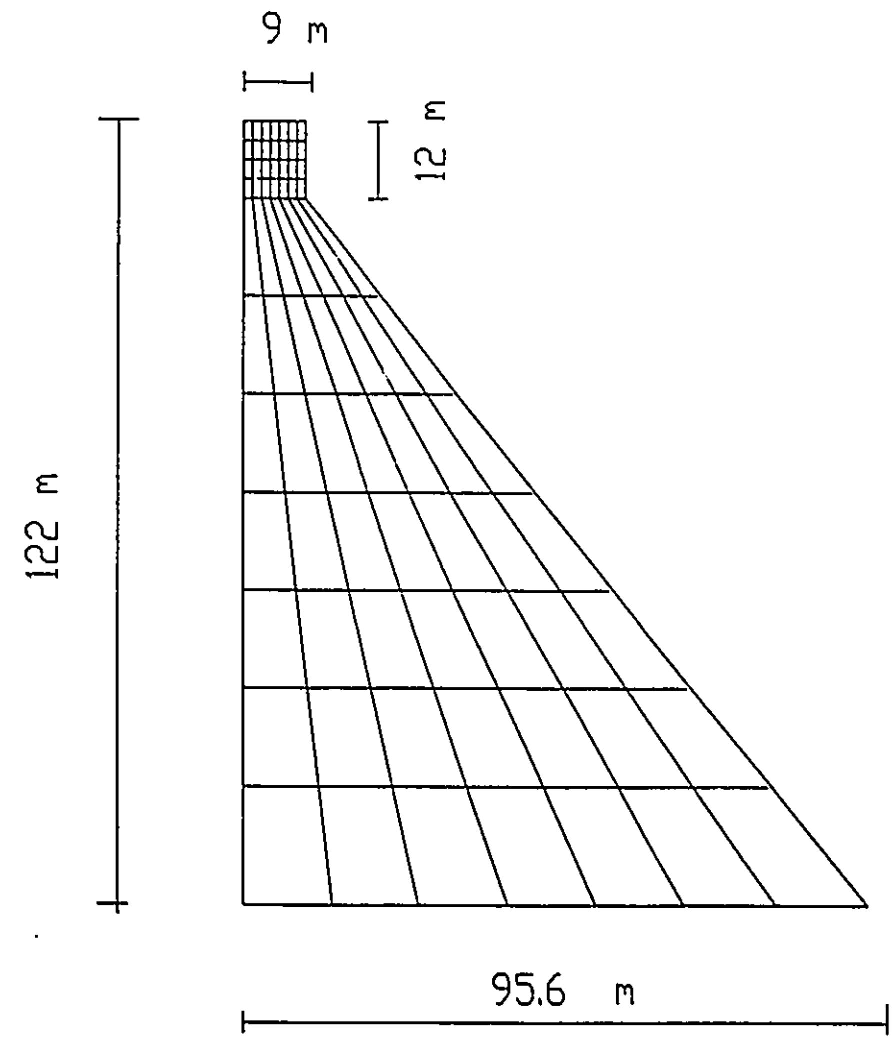

Figure (2-12) Cross-section of the Model Structure

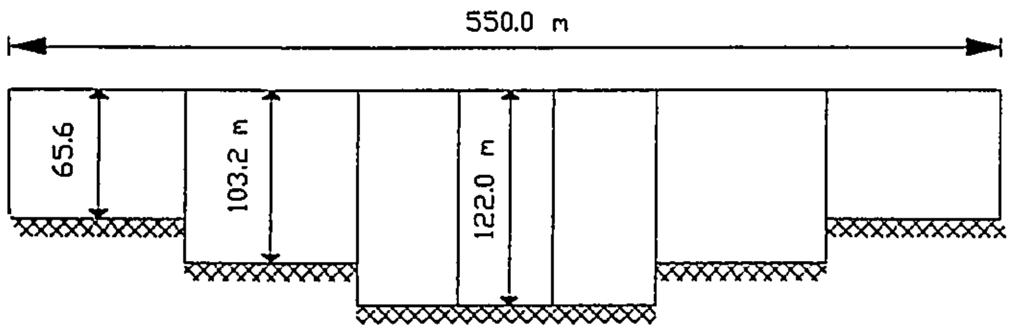

a) Elevation

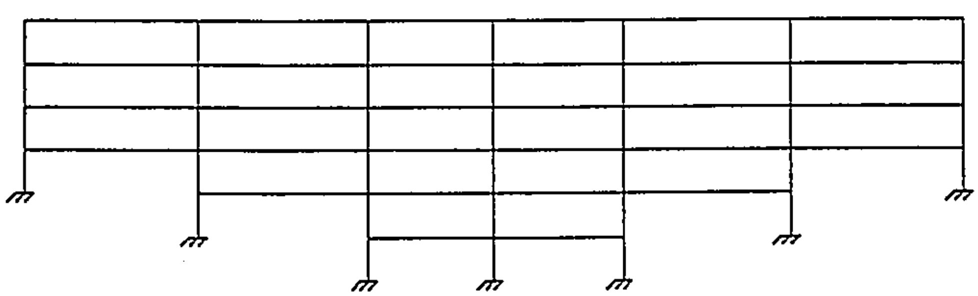

b) Structural Model

Figure (2-13) Longitudinal Profile of the Model Structure

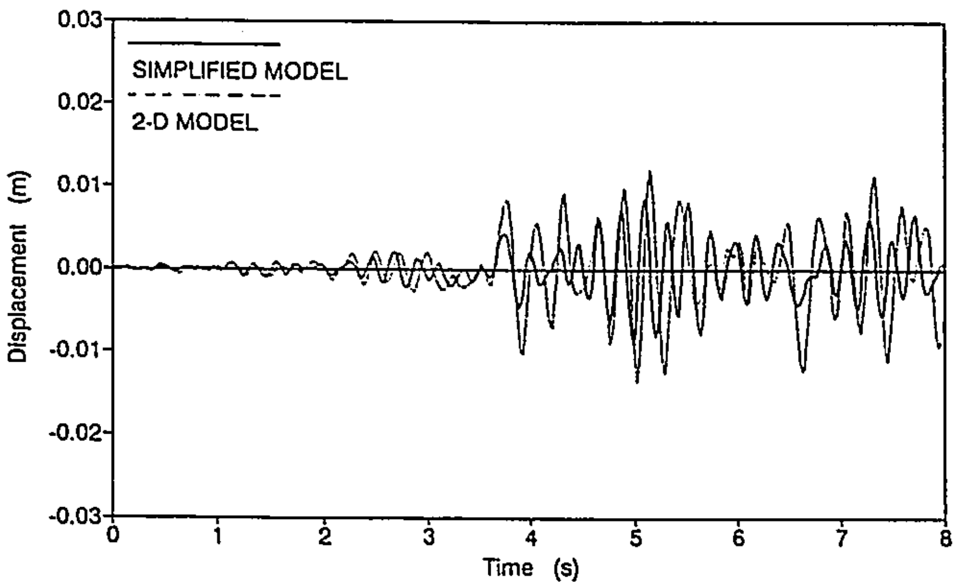

Figure (2-14) Crest Displacement Time History without Hydrodynamic Forces

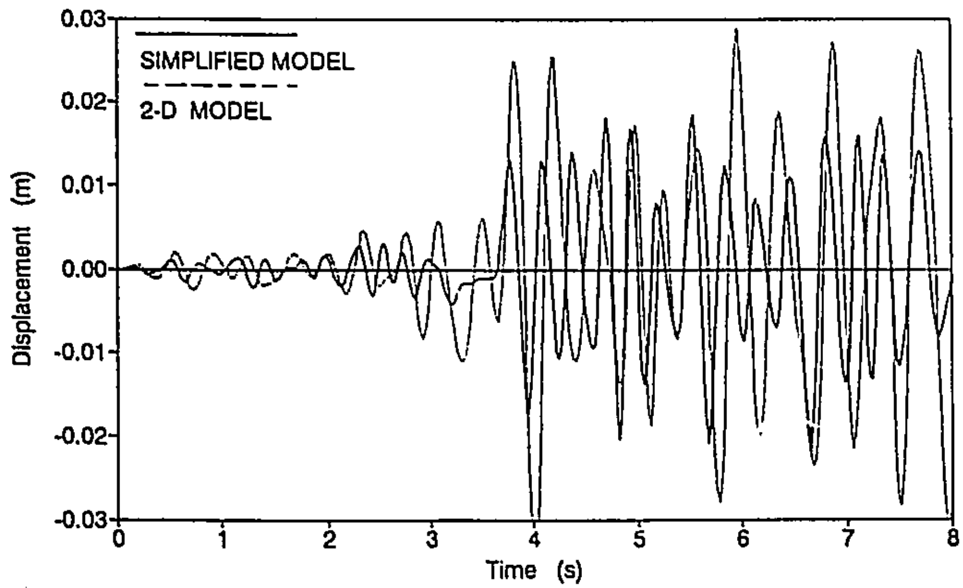

Figure (2-15) Crest Displacement Time History with Hydrodynamic Forces

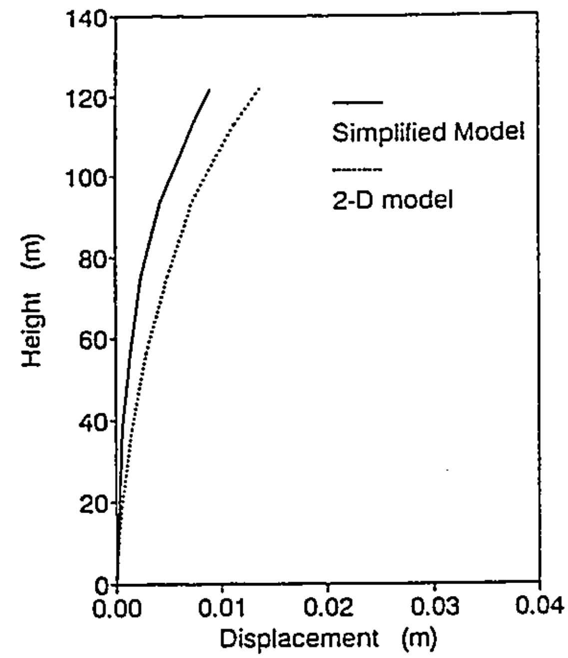

Figure (2-16) Envelope of Horizontal Displacement of the Critical Monolith Excluding Hydrodynamic Forces

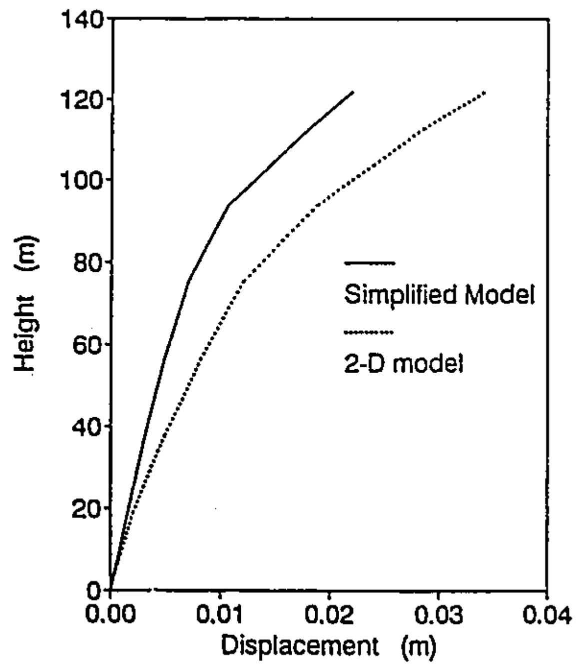

Figure (2-17) Envelope of Horizontal Displacement of the Critical Monolith Including Hydrodynamic Forces

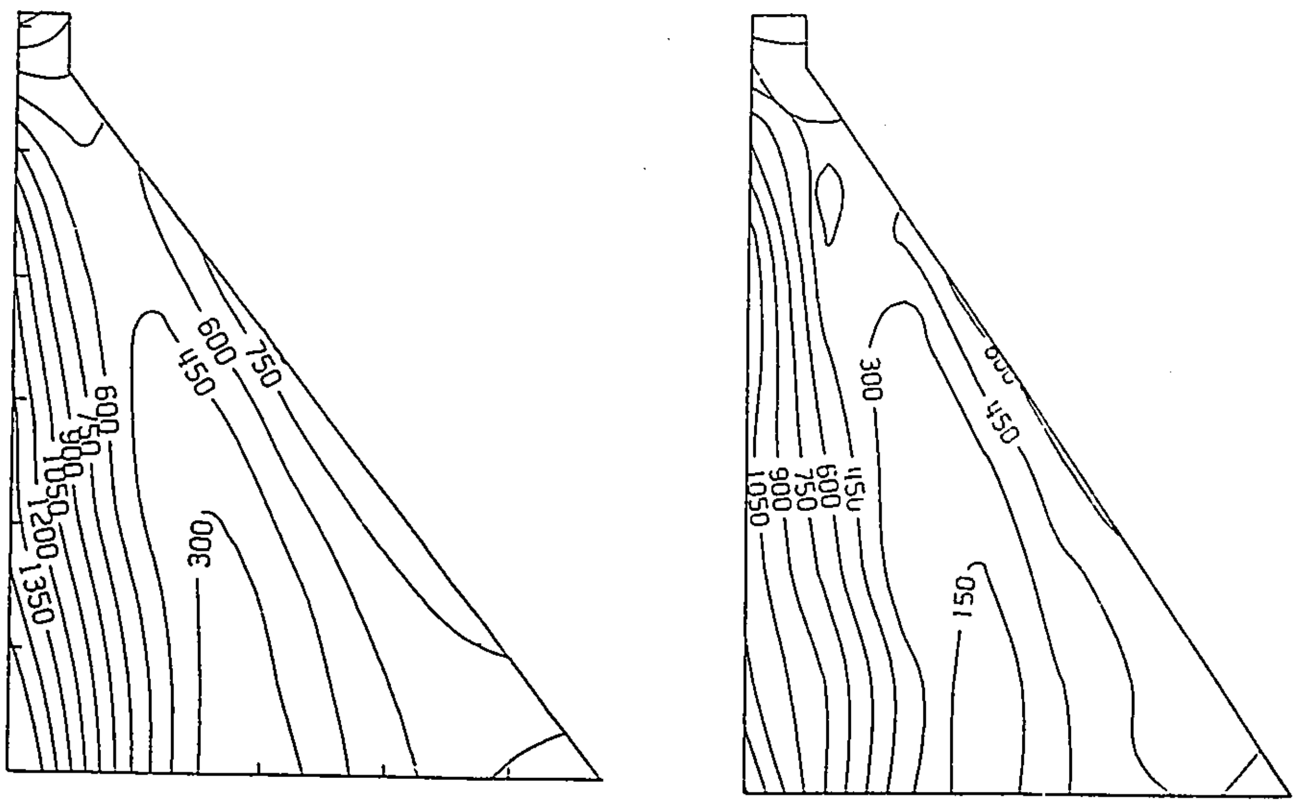

a) 2-D Analysis

b) Simplified Procedure

Figure (2-18) Maximum Principal Tensile Stress Distribution in the Model Structure (kPa)

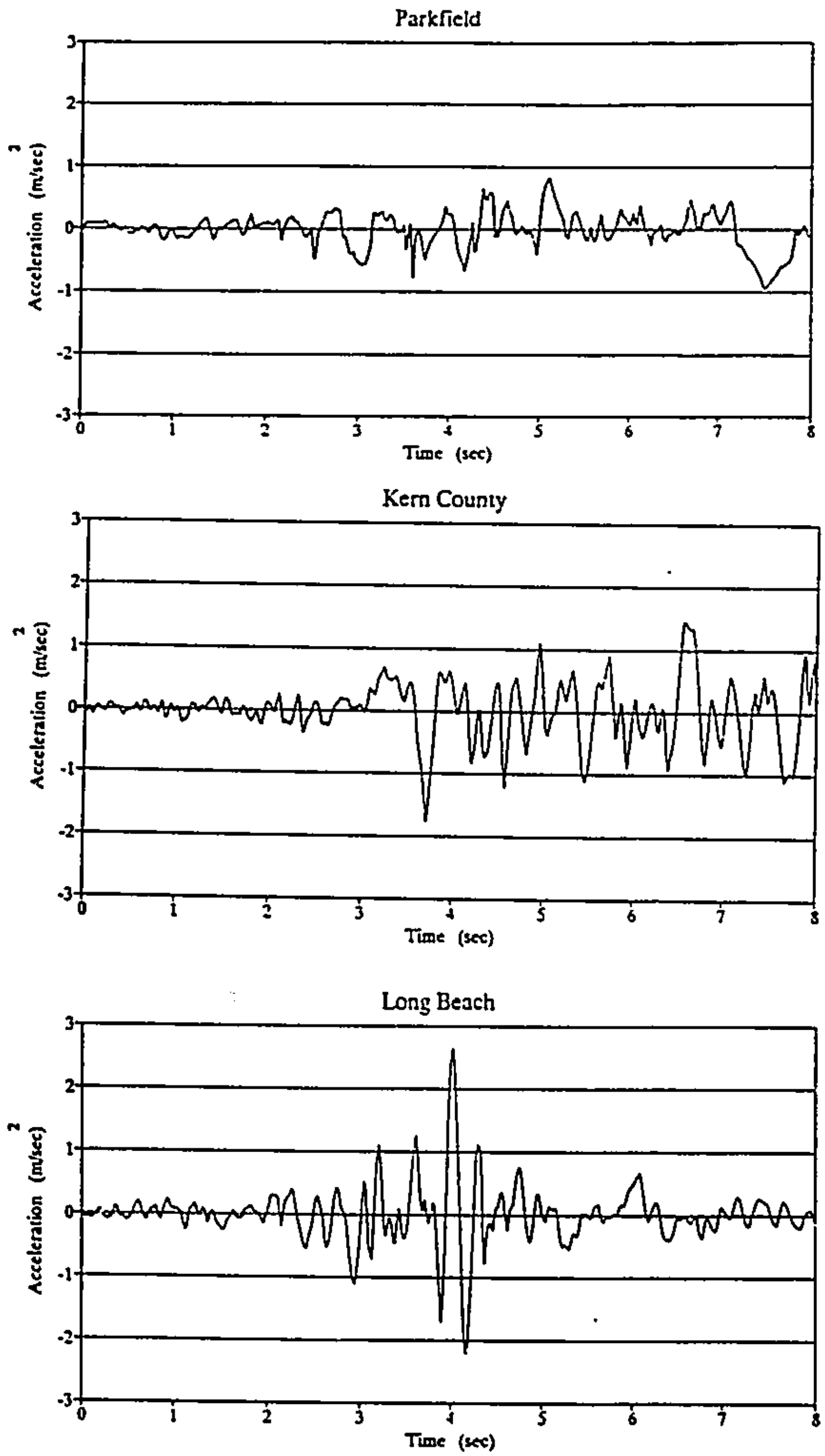

Figure (2-19) Earthquake Ground Motion Records

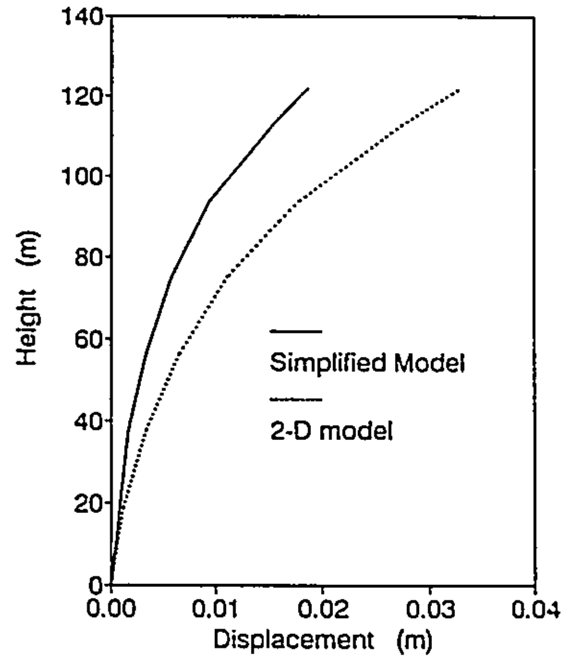

a) Without Hydrodynamic Forces

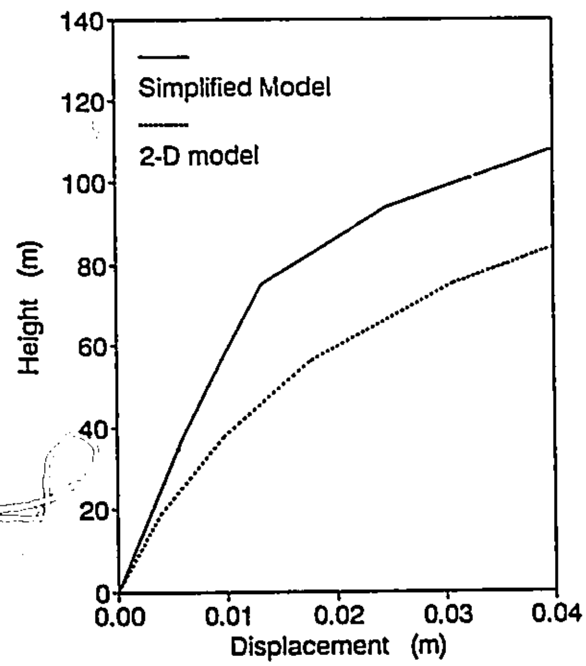

b) With Hydrodynamic Forces

Figure (2-20) Envelope of Horizontal Displacement of the Critical Monolith for High A/V Ratio Input Ground Motion

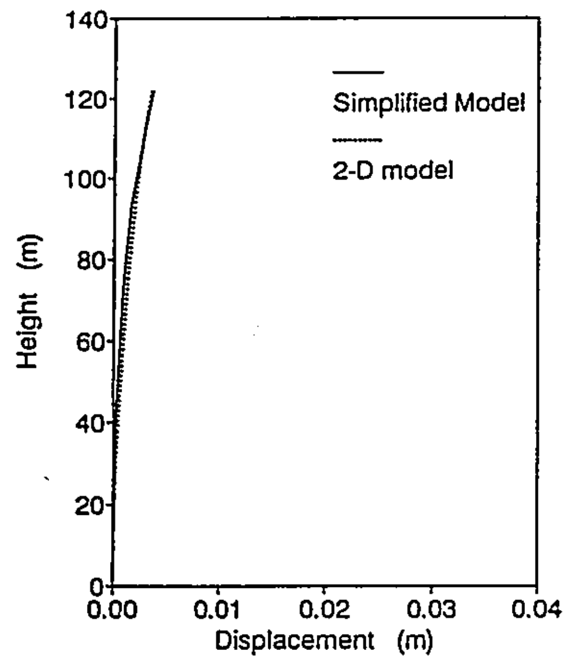

a) Without Hydrodynamic Forces

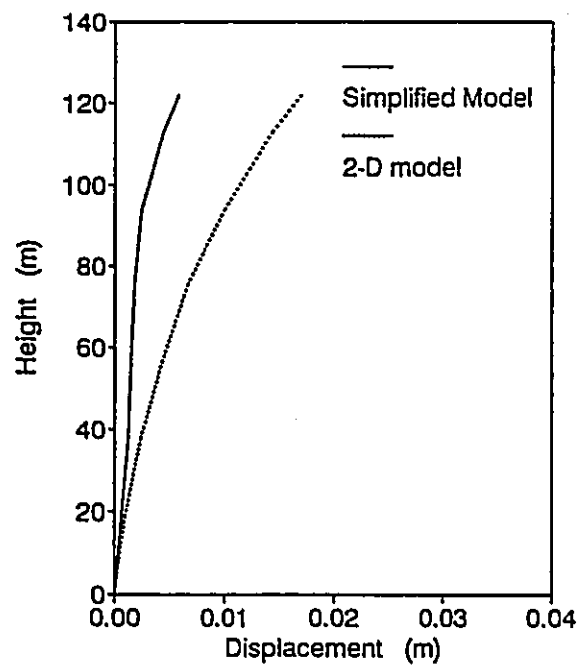

b) With Hydrodynamic Forces

Figure (2-21) Envelope of Horizontal Displacement of the Critical Monolith for Low A/V Ratio Input Ground Motion

CHAPTER 3

MONOLITHS INTERACTION

3.1 GENERAL

In most of previous research on gravity dams, a two dimensional planar model was used to represent the structure. This model has its limitations such as in the case when keyed contraction joints between the monoliths are used in the construction of gravity dams with variable longitudinal profile. In this case, monoliths interaction affects the overall response of the structure. In chapter 2, a simplified procedure was developed to investigate the importance of monoliths interaction. Because of it's simplicity, the procedure is adequate for the preliminary stage of design of gravity dams. However, for detailed analysis, a refined procedure is described in this chapter. The new model is validated by comparing its results to typical three dimensional analysis. Gravity dams with different geometry were analyzed using the new procedure to study the effect of monoliths interaction on the overall response of the structure.

3.2 LIMITATIONS OF THE SIMPLIFIED PROCEDURE

the simplified procedure suggested in chapter 2 has the following limitations:

1- The accuracy of the fundamental mode of vibration appears to be in adequate range. However, it decreases for higher modes especially for typical triangular sections of gravity dams.

2- The added masses used to represent the hydrodynamic effects are calculated using the solution based on the fundamental mode of the dam.

As a result of 1 and 2, the procedure is limited to the fundamental mode of vibration of the structure.

3- The procedure is carried out in the time domain which limits the accuracy of the frequency dependent parameters that appear when including dam-reservoir-foundation interaction.

4- The foundation is assumed rigid. The accuracy of the results decreases as the foundation flexibility increases.

5- The calculation of stress distribution within the dam is carried out in an indirect fashion.

As a result of these limitations, it is suggested that the procedure be used for the preliminary design stage. For detailed analysis, a more refined procedure is described. The approach developed in this chapter to include monoliths interaction is based on less restrictive assumptions which is expected to give more appropriate modelling of the dam response. The procedure uses substructure as well as reduction techniques to include the effect of the adjacent monoliths on the critical one.

3.3 SUBSTRUCTURE METHODS

The objective of most dynamic substructure methods is to evaluate, approximately mode shapes and frequencies to be used subsequently in a dynamic response analysis. In the substructuring approach, the system is divided into two or more subsystems. In the case of gravity dams, each monolith is considered to be a substructure. The main concept in analysis by substructuring is that the response of the total system is obtained from the complex frequency response functions of the individual substructures. Advantages of the substructure method are not very apparent for small systems. However, for a large system, since the problem is reduced to the solution of two or more smaller systems, there may be considerable saving of computational effort and computer storage. Representation of displacements of the substructure in terms of the normal modes of vibration is not essential for the method. However, if the substructure has many degrees of freedom and the dynamic response is contained essentially in only the first few modes of vibration, the modal transformation will lead to considerable savings in computational effort. Such is the case in determining the response of gravity dams to earthquake ground motion. The method of substructure analysis also offers special advantages for systems in which a part of the structure is discretized but the other part is treated as a continuum which is infinite in one or more dimensions (Chopra, 1973). For example, the dam-water system or the dam-foundation system, where the water or the foundation may be idealized as a continuum by solving a boundary value problem, and at the same time it is essential to represent the other substructure as a finite element system because of its geometrical complexity. These substructuring techniques produce practical solutions to complex problems; however, it is difficult to ensure the accuracy of the results since there is no assurance that all significant modes are accounted for.

For large structural systems the Guyan (1965) reduction method has also been used to reduce the size of the eigenvalue problem to be solved. In this chapter, a numerical algorithm for solution of gravity dams by substructuring is presented. It is shown that the previously presented dynamic substructure methods and Gayun reduction are special applications of the well - known Ritz method for the reduction of the number of dynamic degrees of freedom. In addition, the use of special Ritz vectors, which are derived using the spatial distribution of dynamic loads, will assure that important response modes are not missed. The efficiency of this technique has been demonstrated by solving several problems in one, two and three dimensional structural systems.It was shown that the exact free vibration mode shapes are not the best basis for a mode superposition dynamic analysis of structures subjected to certain types of loading. It has been demonstrated that dynamic analyses based on a unique set of Ritz vectors yield more accurate results than the use of the same number of exact mode shapes. The reason is that they are generated by taking into account the spatial distribution of the dynamic loading, whereas the direct use of the exact mode shapes neglects this very important information. Since the Ritz vectors are automatically generated with a fraction of the numerical effort required for the calculation of the exact eigenvectors, they become more suitable candidates for the reduction of large systems (Bayo and Wilson, 1984). The participation of a particular eigenvector in the final solution will depend on the properties of the dynamic loading. It is well known that a mode shape with a natural frequency near the dominant frequencies of the loading will participate significantly in the solution. However, of equal importance is the spatial distribution of loading. Eigenvectors which are orthogonal to the loading are not excited even if their frequency is contained in the loading. Also, in the case of concentrated loads, a large number of eigenvectors may be required to capture the static load effects.

The analysis using the exact eigenvectors has the following drawbacks when compared to Ritz vectors:

1- The solution of the exact eigenvalue problem for large systems is time consuming and costly.

2- The number of eigenvectors required to obtain an accurate dynamic solution is not known until after the eigenvalue problem is solved.

3- There is no indication that the use of exact eigenvectors gives better results than any other set of orthogonal vectors.

On the other hand, one of the drawbacks of using any other set of orthogonal vectors is that the transformed stiffness and damping matrices are not diagonal.

Substructure methods of dynamic analysis have been developed to reduce the number of degrees of freedom of the system, to analyze complex structures with different domains and to design different portions of the structure individually. Two categories of substructure methods are available in the literature. The first category is based on the elimination of the internal degrees of freedom, slaves, in the dynamic stiffness relations. The second category is based on defining the substructure by partial modes. Among the first category, the method of Guyan (1965) has been widely used and is referred to as eigenvalue economization. To achieve reasonably accurate results, the masters must be chosen with care, or some of the lowest frequencies in the eigen spectrum may be lost. The second category can be further classified as fixed interface methods, free interface methods or both depending upon whether the mode shapes used to define the substructure co-ordinates are obtained with the master degrees of freedom fixed, free or a combination. It was noted that the fixed interface methods produce better accuracy.

A substructure method of the first category was used by Chopra since 1967 to model the dam system using three substructures: dam, soil and reservoir. Only the degrees of freedom on the interaction faces of the dam were retained for both soil and reservoir. This analysis was carried out differently for each substructure depending on its type.

3.4 MONOLITHS INTERACTION

The traditional procedure to include monoliths interaction is to use three dimensional analysis of the complete system. However, a major drawback of this approach is the large number of degrees of freedom used and the large amount of input and output data involved in the analysis. These aspects made a three dimensional analysis very difficult and impractical impossible to conduct for the complete dam-reservoir-foundation system.

In the procedure described below, a substructuring condensation technique is employed. The dam structure is divided into a number of substructures equal to the number of monoliths. Each monolith is then reduced to a few degrees of freedom, as will be described, then the stiffness, mass and load vectors are added to form the global system matrices.

The dynamic analysis of a complete concrete gravity dam structure as shown in figure(3-1), including all substructure degrees of freedom, is given by

$$[M]\{\ddot{r}\} + [C]\{\dot{r}\} + [K]\{r\} = -[M]\{\ddot{a}_g(t)\} + \{F_c(t)\} \tag{3-1}$$

where,

[M], [K] and [C] are the mass, stiffness and damping matrices of the structure

$\{F_c\ (t)\}$ is the vector of the interaction forces between different monoliths

is the horizontal ground acceleration

r , r and r are the displacement, velocity and acceleration vectors

The displacement degrees of freedom r, can be divided into the displacements within the substructures, r_i, and the global displacements, r_g, at the boundaries of the substructures (or other degrees of freedom to be retained at a higher substructure level). The mass, damping and stiffness of the dam structure can be expressed in the following submatrix form:

$$[M] = \begin{bmatrix} m_1 & 0 & . & . & m_{1g} \\ 0 & m_2 & . & . & m_{2g} \\ . & . & . & . & . \\ . & . & . & . & . \\ m_{1g}^T & m_{2g}^T & . & . & m_g \end{bmatrix} \tag{3-2}$$

$$[C]=\begin{bmatrix} c_1 & 0 & . & . & c_{1g} \\ 0 & c_2 & . & . & c_{2g} \\ . & . & . & . & . \\ . & . & . & . & . \\ c_{1g}^T & c_{2g}^T & . & . & c_g \end{bmatrix} \tag{3-3}$$

$$[K]=\begin{bmatrix} k_1 & 0 & . & . & k_{1g} \\ 0 & k_2 & . & . & k_{2g} \\ . & . & . & . & . \\ . & . & . & . & . \\ k_{1g}^T & k_{2g}^T & . & . & k_g \end{bmatrix} \tag{3-4}$$

and the dynamic equilibrium equation of a typical substructure of the dam can be expressed in the following form:

$$\begin{bmatrix} m_i & m_{ig} \\ m_{ig}^T & m_g^{(i)} \end{bmatrix} \begin{Bmatrix} \ddot{r}_i \\ \ddot{r}_g \end{Bmatrix} + \begin{bmatrix} c_i & c_{ig} \\ c_{ig}^T & c_g^{(i)} \end{bmatrix} \begin{Bmatrix} \dot{r}_i \\ \dot{r}_g \end{Bmatrix} + \begin{bmatrix} k_i & k_{ig} \\ k_{ig}^T & k_g^{(i)} \end{bmatrix} \begin{Bmatrix} r_i \\ r_g \end{Bmatrix} = \begin{Bmatrix} f_i \\ f_g^{(i)} \end{Bmatrix} \tag{3-5}$$

where,

r_i refers to internal or slave degrees of freedom

r_g refers to boundary or master degrees of freedom

The local Ritz vectors for any substructure are calculated by the basic algorithm given by Wilson and Bayo (1986) with the matrices $[m_i]$ and $[k_i]$ as the structural properties and $\{f_i\}$ is the interaction forces. Additional substructure displacement, r_i, due to global displacement, r_g, are assumed to satisfy the following condensation equation

$$K_i r_i + K_{ig} r_g = 0 \tag{3-6}$$

the transformation matrix is written as:

$$T = -K_i^{-1} K_{ig} \tag{3-7}$$

and as a result:

$$\begin{bmatrix} r_1 \\ r_2 \\ . \\ . \\ r_g \end{bmatrix} = \begin{bmatrix} x_1 & 0 & . & . & T_1 \\ 0 & x_2 & . & . & T_2 \\ . & . & . & . & . \\ . & . & . & . & . \\ . & . & . & . & I \end{bmatrix} \begin{bmatrix} Y_1 \\ Y_2 \\ . \\ . \\ r_g \end{bmatrix} \tag{3-8}$$

where, Y_i is a Ritz vector to represent internal degrees of freedom for the i substructure and T_i is the transformation matrix for the i substructure. The total response of the complete system of substructures is now approximated by the following generalized and physical coordinates:

$$\begin{bmatrix} r_i \\ r_g \end{bmatrix} = \begin{bmatrix} x & T \\ 0 & I \end{bmatrix} \begin{bmatrix} Y \\ r_g \end{bmatrix} \tag{3-9}$$

by applying this transformation to the system, a reduced form of the structural matrices are obtained in the form M^*, C^* and K^*. This transformation is exact if all possible substructure Ritz vectors are used. If no substructure vectors are retained, the resulting equations are identical to those produced by the Guyan reduction technique. The formulation of each substructure as well as the formulation of the connecting links are described in details in the following paragraphs.

3.4.1 Formulation of each Substructure

Each monolith is modeled using a finite element mesh with 4 node plane stress elements. The Degrees of Freedom (DOF) of each monolith are divided to master and slave DOF. The master DOF are those on the boundary with other substructures and the slave DOF are the internal ones. Assuming harmonic ground excitation and considering that damping of the structure is hysteretic, the equations of motion can be written in the following form:

$$-\omega^2 \begin{bmatrix} m_i & 0 \\ 0 & m_g \end{bmatrix} + (1+i\eta) \begin{bmatrix} k_i & k_{ig} \\ k_{gi} & k_{gg} \end{bmatrix} - \begin{Bmatrix} f_i \\ f_g \end{Bmatrix} \qquad (3\text{-}10)$$

where, the subscript i refers to internal nodes and g refers to global nodes

η is hysteretic damping ratio

f is the vector of forces on each substructure

ω is the frequency of the exciting motion

This reduction technique dramatically reduces the number of DOF of each substructure and consequently the overall number of DOF for the system. In general as gravity dams are short period structures, their response can be accurately represented by a few generalized coordinates which further reduces the number of DOF. In this transformation, the physical DOF (displacements) of the original structure are transformed to both physical and generalized DOF, represented by displacements at the boundary and Ritz vectors for internal nodes. As the analysis is mainly concerned with the critical monolith, all its DOF are considered as master DOF and no reduction is carried out at this stage. This simplifies the process of obtaining critical stresses and displacements. The reduced mass and stiffness matrices of each substructure are then added to form the global matrices. Figure(3-2) shows the suggested model to include the monoliths interaction.

3.4.2 Formulation of the Connecting Elements Stiffness

The approach taken is to divide the dam system into substructures with nodes on the boundary and Ritz vectors representing the internal nodes. Following the formation of the structural matrices for each substructure, the global matrices are formulated. In a typical analysis, individual structural matrices of each substructure are added directly to form the global ones. However, in the proposed analysis, one of the approximations used was to assume two dimensional plane stress elements to model each monolith. As a result, it is implicitly assumed that nodes at the same level will have the same displacement. To overcome these approximations and to achieve better accuracy, the nodes at the boundaries of each substructure are connected by two-node connecting elements. The connecting elements between these monoliths should be able to model two major effects 1) The longitudinal profile of the dam as a result of distributing the load three dimensionally, 2) The shear slip within the joints. Figure (3-3) shows the proposed connecting element consisting of two components; beam element and a shear spring. Three nodes are used in connecting the two elements. Nodes 1 and 2 have two degrees of freedom each; displacement and rotation. Node 3 has only displacement degree of freedom. For the purpose of representing the relative lateral displacement between two adjacent nodes on the boundaries of two substructures, the model shown in figure (3-3) is used. The two springs shown replace both the beam element as well as the spring representing the contraction joints. To develop the equivalent stiffness of both springs, a unit force was applied to the nodes 1 and 3. The total displacement of the connecting element can be written as the superposition of local displacement in each spring.

$$\Delta = \Delta_1 + \Delta_2 \tag{3-11}$$

where,

Δ is the total displacement

Δ_1, Δ_2 are the local displacements of the beam and the joint respectively

Equation (3-11) can be written in the form:

$$\frac{1}{K_e} = \frac{1}{K_b} + \frac{1}{K_j} \tag{3-12}$$

where,

K_e is the equivalent stiffness of the connecting link.

K_j is the stiffness of the spring representing the joint.

K_b is the stiffness of the beam element.

The connecting element stiffness matrix can be written in the form:

$$K=\begin{bmatrix} k_e & -k_e \\ -k_e & k_e \end{bmatrix} \tag{3-13}$$

There is an element which connects each 2 opposite nodes at the boundary of each substructure. Rotation DOF have been retained in the degrees of freedom on the boundary nodes in order to satisfy compatibility and continuity of displacements. The stiffness of each connecting element includes two effects; longitudinal flexibility and joint flexibility. The stiffness of the equivalent spring and the stiffness of the two component springs are described in more details in the next section.

a) Longitudinal Flexibility

By modelling each monolith assuming a plane stress condition, the change in lateral displacements within each monolith have been eliminated. This leads to a constant lateral displacement of all the nodes at the same level along the dam which is not realistic. To compensate for this, boundary nodes on each substructure were connected by links which are capable of producing the lateral longitudinal profile of the dam. Beam elements have been used to connect the monoliths. For this purpose, rotational degrees of freedom were added to ensure compatibility and continuity at each node. As the depth of each beam is relatively large compared to its span, the effect of shear deformations have been included in the analysis. Based on the assumption that shear keys are only capable of transmitting lateral shear forces, i.e. no forces are developed in the case of relative vertical displacements between the monoliths, only the horizontal degrees of freedom are used for the connecting link. Axial and bending deformations are neglected across the construction joints assuming that cracks which usually exist at the joint reduce these deformations. The stiffness matrix of the element is given in the form:

$$K=\frac{EI}{1+2\nu}\begin{bmatrix} \frac{12}{L^3} & \frac{-12}{L^3} & \frac{6}{L^2} & \frac{6}{L^2} \\ \frac{-12}{L^3} & \frac{12}{L^3} & \frac{-6}{L^2} & \frac{-6}{L^2} \\ \frac{6}{L^2} & \frac{-6}{L^2} & \frac{4}{L}(1+\nu/2) & \frac{2}{L}(1-\nu) \\ \frac{6}{L^2} & \frac{-6}{L^2} & \frac{2}{L}(1-\nu) & \frac{4}{L}(1+\nu/2) \end{bmatrix} \tag{3-14}$$

where,

L and I are the length and inertia of the element respectively. E and υ are the modulus of elasticity and Poisson's ratio respectively.

b) Joint Elements

Joint elements consist of two nodes connected by a massless spring with stiffness K_j. The element has two degrees of freedom; horizontal displacement and rotation at each node. The strain vector for a joint element is defined by the relative horizontal displacement of the two joints as measured at the element centre.

$$\epsilon = \Delta r_o \tag{3-15}$$

where Δr_o is the shear strain which is related to displacements by

$$\Delta r_o = \begin{bmatrix} 1 & -1 \end{bmatrix} \begin{bmatrix} r_1 \\ r_2 \end{bmatrix} \tag{3-16}$$

The local joint - element stiffness relating force vector, F, to displacement vector, r, is

$$K_j = \begin{bmatrix} k_j & -k_j \\ -k_j & k_j \end{bmatrix} \tag{3-17}$$

K_j is the stiffness matrix of the contraction joints connecting the monoliths. The evaluation of K_j will be discussed in details in chapter 5. The local stiffness matrix must be rotated to find the term by term contribution to the structural stiffness matrix with respect to global x-y coordinates.

3.5 STRAIN ENERGY IN THE MODEL

The strain energy stored in the suggested model is calculated and compared to that stored in typical three dimensional brick elements. The strain energy density (U_o), which represent the area under the stress-strain diagram, is given by the following formula:

$$U_o = \int \sigma \, d\epsilon \tag{3-18}$$

where σ and ϵ are the stress and strain respectively. The total strain energy (U) is obtained by integrating the strain energy density over the volume of the body,

$$U = \iint_v \sigma \, d\epsilon \, dv \tag{3-19}$$

For linear analysis, the stress-strain relationship is represented by a straight line and the strain energy formula reduces to:

$$U = \frac{1}{2} \int_v \sigma \, \epsilon \, dv \tag{3-20}$$

where σ and ϵ are related by

$$\sigma = \underset{\sim}{D} \, \epsilon \tag{3-21}$$

For a three dimensional isotropic brick element ϵ and D are given by:

$$\epsilon^T = \left[\frac{\partial u}{\partial x} \quad \frac{\partial v}{\partial y} \quad \frac{\partial w}{\partial z} \quad \frac{\partial u}{\partial y} + \frac{\partial v}{\partial x} \quad \frac{\partial v}{\partial z} + \frac{\partial w}{\partial y} \quad \frac{\partial u}{\partial z} + \frac{\partial w}{\partial x} \right] \tag{3-22}$$

$$D = \frac{E}{2(1+\nu)(1-2\nu)} \begin{bmatrix} 1-\nu & \nu & \nu & 0 & 0 & 0 \\ \nu & 1-\nu & \nu & 0 & 0 & 0 \\ \nu & \nu & 1-\nu & 0 & 0 & 0 \\ 0 & 0 & 0 & \frac{1-2\nu}{2} & 0 & 0 \\ 0 & 0 & 0 & 0 & \frac{1-2\nu}{2} & 0 \\ 0 & 0 & 0 & 0 & 0 & \frac{1-2\nu}{2} \end{bmatrix} \tag{3-23}$$

where,

D is the rigidity matrix of the material

x, y and z are the local coordinates

u, v and w are the displacements in the x, y and z respectively

The strain energy (U_E) stored in the structure modeled by three dimensional brick elements is

$$U_E = \frac{1}{2} \int_v \varepsilon^T_{1x6}\, D_{6x6}\, \varepsilon_{6x1}\, dv \tag{3-24}$$

For the model used in this study, the strain energy (U_A) is given by two parts:

$$U_A = U_1 + U_2 \tag{3-25}$$

where U_1 and U_2 are the strain energy stored in the elements representing the monolith and the connecting links respectively. U_1 and U_2 will be calculated using two dimensional elements in the xy and xz planes respectively. The joint flexibility is neglected when calculating U_2. ϵ and D in the xy plane is given by:

$$\epsilon_1^T = \left[\frac{\partial u}{\partial x} \quad \frac{\partial v}{\partial y} \quad \frac{\partial u}{\partial y}+\frac{\partial v}{\partial x}\right] \tag{3-26}$$

$$D = \frac{E}{2(1-\nu^2)}\begin{bmatrix} 1 & \nu & 0 \\ \nu & 1 & 0 \\ 0 & 0 & \frac{1-\nu}{2} \end{bmatrix} \tag{3-27}$$

$$U_1 = \int_a \epsilon_{1x3}^T \, D_{3x3} \, \epsilon_{3x1} \, da \tag{3-28}$$

and in the xz plane is given by:

$$\epsilon_2^T = \left[\frac{\partial u}{\partial x} \quad \frac{\partial w}{\partial z} \quad \frac{\partial u}{\partial z}+\frac{\partial w}{\partial x}\right] \tag{3-29}$$

$$U_2 = \int_s \epsilon_{1x3}^T \, D_{3x3} \, \epsilon_{3x1} \, ds \tag{3-30}$$

evaluating the three integrals and comparing the results for the case of rectangular section, the following relationship can be introduced:

$$U_E = U_1 + U_2 + V \tag{3-31}$$

where V includes different terms which can be classified in two categories: 1) terms which represent the axial deformations in the z direction which is neglected as a result of the assumption of the inability of the contraction joint to transfer the shear forces. 2) terms of higher order which have very small effect on the overall strain energy and can be neglected. The accuracy of the results of the suggested model compared to that of the three dimensional analysis is found to be inversely related to V. For the case of rectangular section and uniform profile, V was found to be less than 8% of U_E.

3.6 TESTING OF THE ANALYSIS PROCEDURE

The proposed analysis approach will be tested by comparing its results with two dimensional and three dimensional finite element analyses. An idealized structure with rectangular cross-section is used to test the proposed procedure and is shown in elevation in figure (3-4). The structure has a maximum height of (H) of 100 m at the middle and decreases gradually to reach a minimum height h at the ends which will be assigned different values. The crest length (L) of the structure is 400 m and the width of the dam cross-section (B) is 60 m. The cross sections of the dam structure at the critical height as well as at the ends are shown in figure (3-5). Five cases of the structure with different values of end heights are used in this study, as shown in table (3-1). The only difference between the five cases is the height of the two ends of the structure.

The concrete in the dam is assumed to be homogenous, isotropic and linear elastic. The concrete material is assumed to have the following properties: unit weight = 24.3 kN/m^3, shear modulus = 14.74 x 10^6 kPa and Poisson's ratio = 0.17, which corresponds to a modulus of elasticity = 34.45 x 10^6 kPa . Stiffness proportional damping is assumed to be 5 % of the critical damping. The results are compared with a typical three dimensional analysis using 8 node brick elements in the program SAP IV. The results of two dimensional analysis as suggested by Chopra and Fenves (1984) are also used for comparison.

The earthquake ground motion record used in this study is the S69E component of the (1952) Taft earthquake as described in chapter 2. The results obtained from the analysis of the model structure shown in figure (3-4) were used to serve two purposes; to test the new procedure by comparing its results to that obtained using typical two and three dimensional analysis and to study the effect of monoliths interaction on the overall response. Both cases A and C are used for the purpose of testing the new procedure. The natural frequencies of the model structure calculated by the new procedure, a typical three dimensional analysis as well as typical two dimensional analysis are listed in table (3-2). For case A, which represents a structure with uniform profile, the fundamental natural frequency of the structure evaluated using the three procedures is almost the same. Higher frequencies are different in the case of two dimensional analysis. This variation is due to the fact that some modes are longitudinal modes which can not be represented using two dimensional models. Figures (3-6) a and b show the first five modes of the structure case A. Figure (3-6a) shows the longitudinal variation of the crest displacement and figure (3-6b) shows the vertical profile at the centre line of the structure.

The results obtained for case C, as an example of nonuniform profile, shows the high accuracy of the new procedure in evaluating the natural frequencies of the structure. Table (3-3) shows the natural frequencies for case C evaluated by the proposed procedure with different number of Ritz vectors to model the internal degrees of freedom for each monolith. It is noted that the change in natural frequencies is insignificant when using different number of Ritz vectors. This can be explained by the fact that concrete gravity dams are short period structures and its response can be represented by a few Ritz vectors. For the rest of the analysis in this study 4 Ritz vectors were used to represent the internal degrees of freedom for each substructure.

3.7 RESPONSE ANALYSIS

The natural frequencies of the structure for the five cases evaluated by the new procedure as well as the frequencies of the critical monolith using typical two dimensional analysis are shown in table (3-4). The change in the longitudinal profile of the structure affects its natural frequencies. As the longitudinal slope of the structure base becomes steeper the structure is stiffer in resisting lateral loads and the natural frequencies increase. Figure (3-7) shows time history of the top displacement at the critical monolith for cases A and D. It is noted that the response of the structure decreases as the longitudinal slope becomes steeper. It is concluded from these results that typical two dimensional analysis may significantly overestimates the response of the critical monolith of the dam depending on its longitudinal profile and the use of keyed contraction joints.

3.7.1 Effect of Dam Cross-section:

The results presented in the previous sections are based on a rectangular cross-section for the dam as used by Rashed and Iwan (1984). However, most of the existing concrete gravity dams have triangular cross sections. To validate the refined procedure suggested in this chapter, the comparison is extended to the triangular section shown in figure(3-8). The cross section has a height H=100 m and base width equal to 0.8 of the height, 80 m. Two cases for the longitudinal profile are considered; a) uniform longitudinal profile with constant height, case I and b) variable longitudinal profile with the height decreases from 100 m at the critical cross-section to 50 m at the end monoliths, case II. Results of the three dimensional analysis as well as the proposed refined analysis are presented in table (3-5). Good agreement between the natural frequencies evaluated using the two procedures is noted. Tables (3-6) and (3-7) show the natural frequencies for the dam evaluated using the refined analysis using different number of Ritz vectors to represent the internal degrees of freedom for the structure cases I and II respectively. Four Ritz vectors were sufficient for predicting the response of the structure accurately.

3.7.2 Monoliths Interaction Effects:

To test the significance of including monoliths interaction on the overall response of the structure, a few comparisons are presented. figure (3-9) shows the envelope of the horizontal displacement for structure cases I and II using the proposed as well as two dimensional analyses. It is noted that two dimensional analysis gives reasonable results for case I, uniform longitudinal profile, but the results diverge as the dam profile becomes nonuniform, case II. Figure (3-10) shows time history of the crest displacement at the critical monolith for cases I and II. Including monoliths interaction for case II shifted the natural frequency of the structure resulting in a different response. To eliminate the effect of the frequency content in the exciting ground motion, two more earthquake records are applied to the structure to represent high and low frequency contents. Figure (3-11) a and b show the results obtained for cases I and II during the horizontal component of the Parkfield record, high A/V ratio. Figure (3-12) a and b show the results obtained for the two cases of the structure during the horizontal component of the Long Beach record, low A/V ratio. In both figures, the reduction in the response of the structure when the longitudinal profile becomes nonuniform can be observed. The effect of the A/V ratio on the overall response will be discussed in more details in chapter 6.

3.7.3 Effect of Dam Height

The height of the structure considered in both cases I and II was changed while the length of the dam was kept the same to emphasize the effect of the length / height ratio on the monoliths interaction. Two values for H, 140 m and 60 m, were used in addition to the case of H=100 m. The response of the structure is presented in figures (3-13) and (3-14). The conclusions obtained before for the case of H= 100 m are applicable to these figures. It is also noted that the reduction in the response, due to including monoliths interaction, for the case H= 140 m is higher than the previous cases. This confirms the effect of the ratio of the length to the height of the dam as was reported earlier by Rashed and Iwan (1984). Decreasing the length / height ratio of the dam is expected to increase the reduction in the response when including monoliths interaction. As many factors affect the amount of reduction in the response of the structure, these parameters will be discussed in details in chapter 6.

3.8 SUMMARY

A refined analysis procedure for including monoliths interaction is presented in this chapter. The effect of monoliths interaction is included by modelling each monolith as a separate substructure. The internal degrees of freedom of each monolith is then reduced to a few generalized coordinates. The monoliths are connected to one another through keyed contraction joints which are assumed to transfer shear forces but not axial forces. The results obtained from the proposed analysis are compared to finite element three dimensional analysis and good agreement was obtained. In most of the cases, including the effect of monoliths interaction reduces the overall response of the structure. However, the percentage of reduction depends on many factors which will be discussed in details in chapter 6. In the following chapter the effect of hydrodynamics as well as the soil - structure interactions will be included in the analysis.

Table (3-1) Configuration of the Different Cases of the Idealized Structure

CASE	B (m)	L (m)	H (m)	h (m)
A	60	400	100	100
B	60	400	100	80
C	60	400	100	60
D	60	400	100	40
E	60	400	100	20

Table (3-2) Comparison of Natural frequencies (Rad/s) for Cases A & C

MODE	TYPICAL	CASE A		CASE C	
	2-D	TYPICAL 3-D	NEW MODEL	TYPICAL 3-D	NEW MODEL
1	19.07	19.00	19.08	24.00	24.86
2	60.57	20.95	21.12	32.59	33.24
3	65.95	26.35	25.49	38.91	38.29
4	133.37	34.64	29.73	44.38	43.64
5	154.15	34.94	32.57	46.29	46.28

Table (3-3) Natural Frequencies (Rad/s) for Case C with Different Number of Ritz Vectors

MODE	2 RITZ	4 RITZ	12 RITZ
1	24.86	24.76	24.76
2	33.24	32.79	32.79
3	38.29	37.64	37.63
4	43.64	42.35	42.33
5	46.28	45.13	45.11

Table (3-4) Natural Frequencies (Rad/s) of Different Dam Profile Cases

MODE	A	B	C	D	E	2-D
1	19.00	21.89	24.86	25.52	26.69	19.07
2	20.95	26.27	33.24	38.35	43.06	60.57
3	26.35	30.94	38.29	48.21	50.16	65.95
4	34.64	39.09	43.64	48.88	57.17	133.4
5	34.94	39.42	46.28	59.22	70.36	154.1

Table (3-5) Natural Frequencies (Rad/s) of the Dam
Cases I and II

Mode	Structure I		Structure II	
	Refined	Typical 3-D	Refined	Typical 3-D
1	28.79	28.53	33.18	33.71
2	29.82	29.2	41.26	39.08
3	32.51	31.49	45.17	43.46
4	36.15	35.27	48.98	47.04
5	39.93	40.38	51.39	50.21

Table (3-6) Natural Frequencies (Rad/s) of the Dam
with Different Ritz Vectors (Case I)

Mode	4-Ritz	8-Ritz	10-Ritz
1	28.79	28.75	28.75
2	29.82	29.77	29.77
3	32.51	32.47	32.47
4	36.15	36.08	36.08
5	39.93	39.86	39.86

Table (3-7) Natural Frequencies (Rad/s) of the Dam
with Different Ritz Vectors (Case II)

Mode	4-Ritz	8-Ritz	10-Ritz
1	33.18	33.16	33.16
2	41.26	41.21	41.19
3	45.17	45.13	45.11
4	48.98	48.91	48.91
5	51.39	51.34	51.33

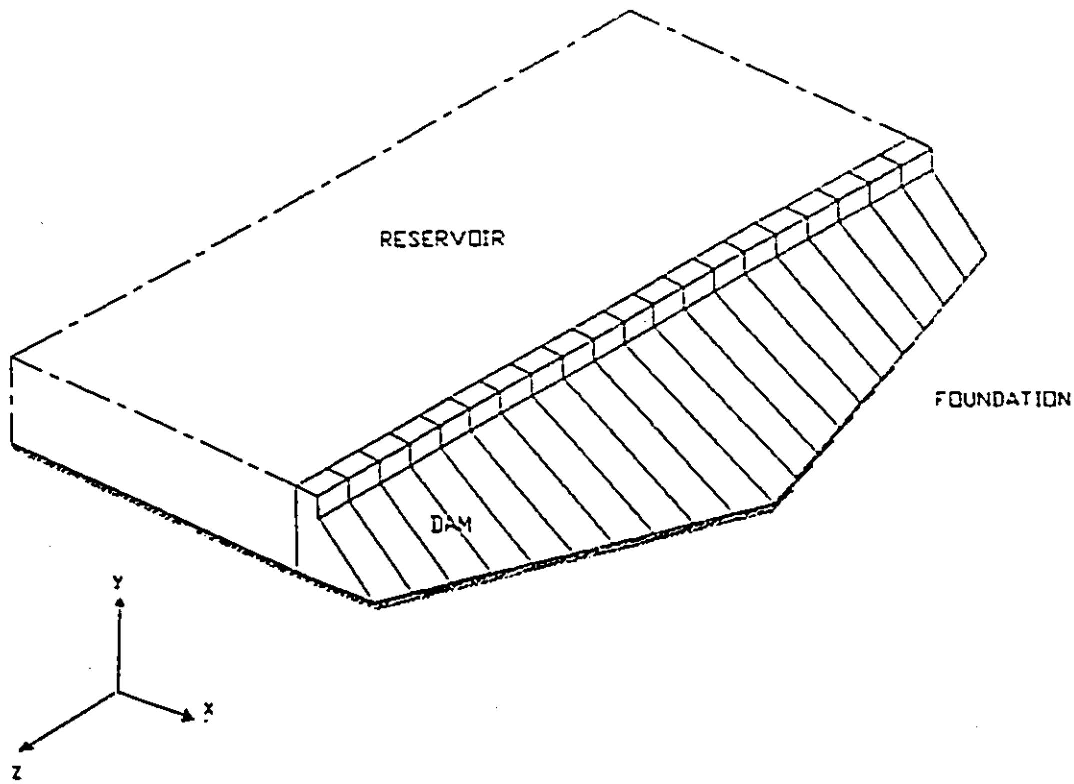

Fig. (3-1) Typical Longitudinal Profile of Concrete Gravity dams

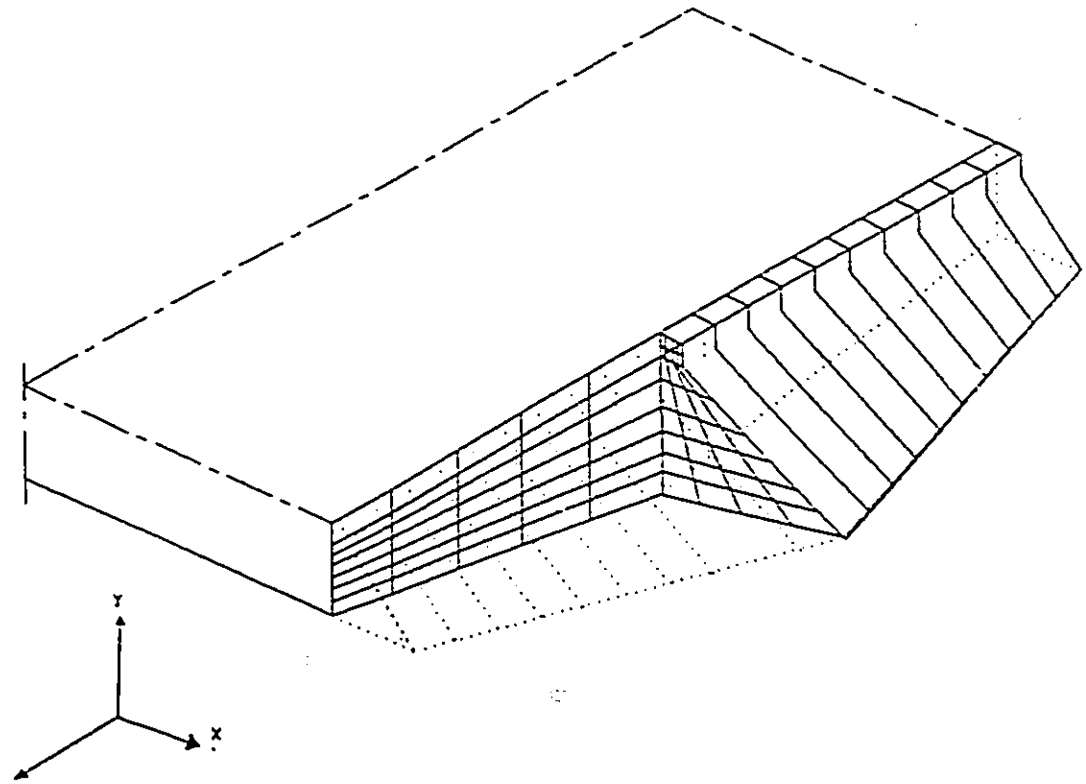

Fig. (3-2) Modelling of Gravity Dams to Include Monolith Interaction

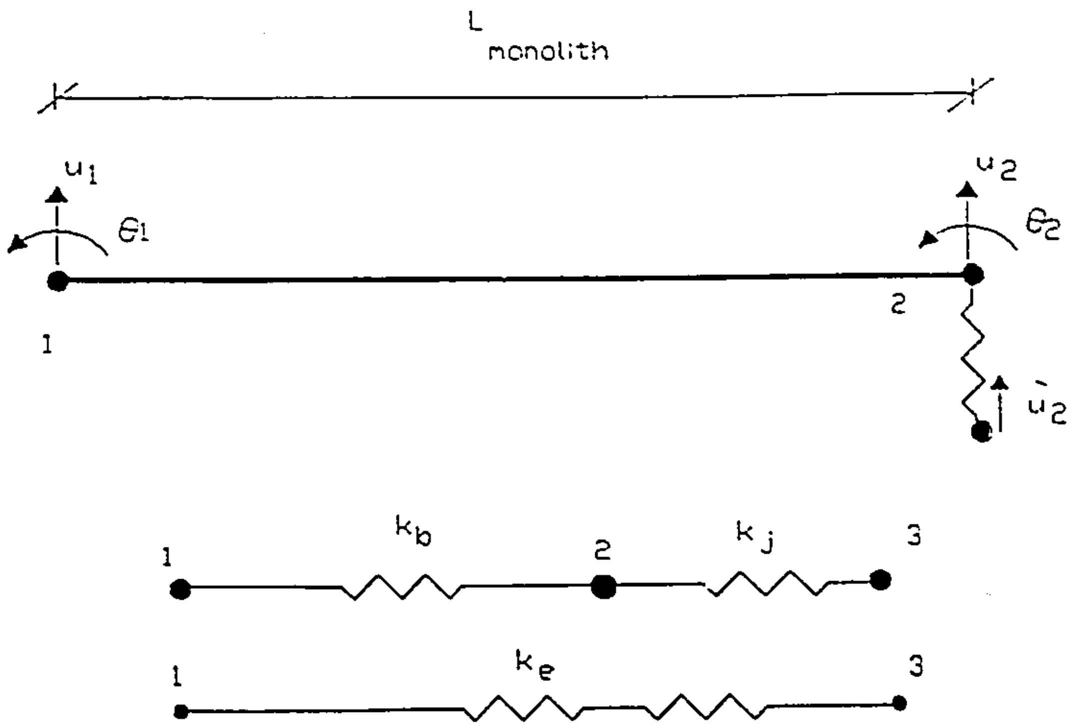

Figure (3-3) Model for Connecting Elements

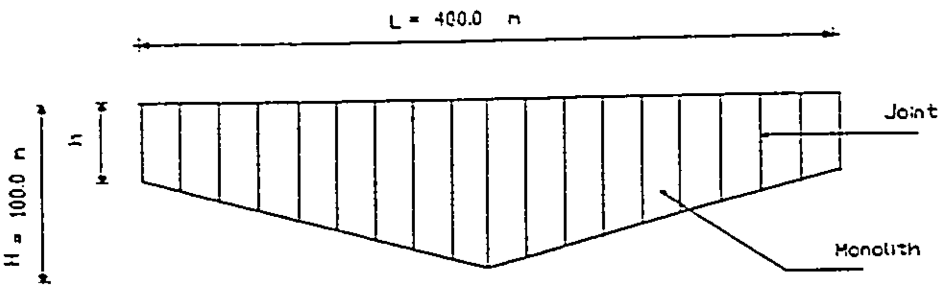

Fig. (3-4) Elevation of The Model Structure

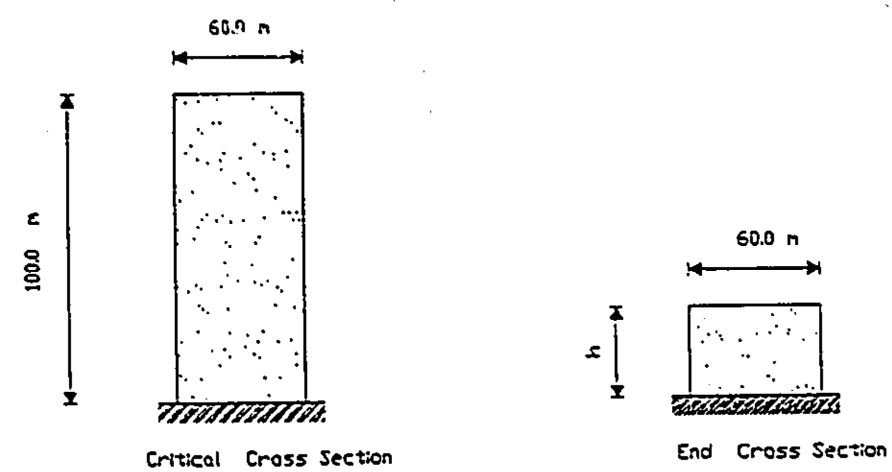

Fig. (3-5) Cross sections of The Model Structure

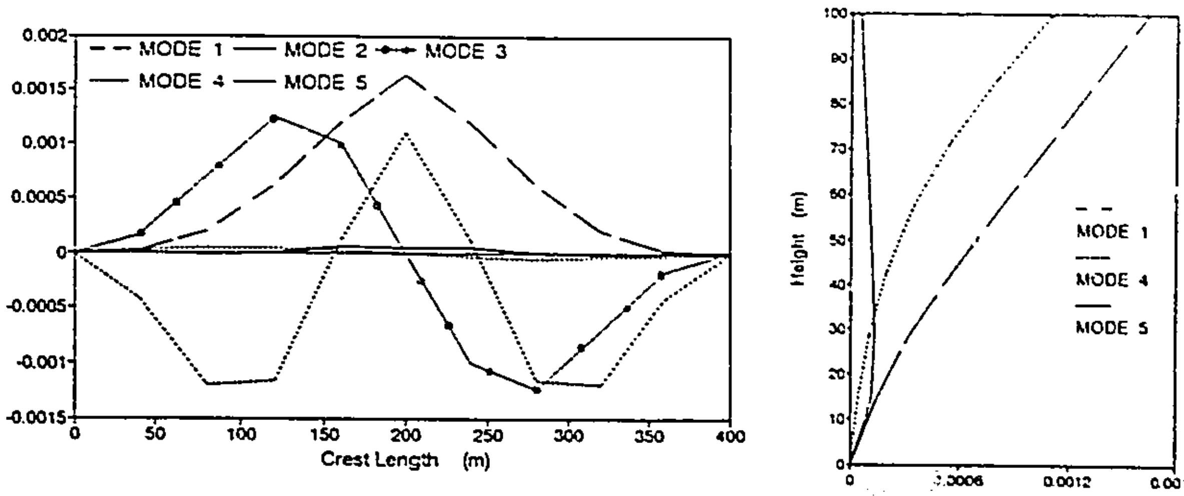

a) Longitudinal Profile

b) Vertical Profile at the Middle

Figure (3-6) Mode Shapes of the Structure Case A

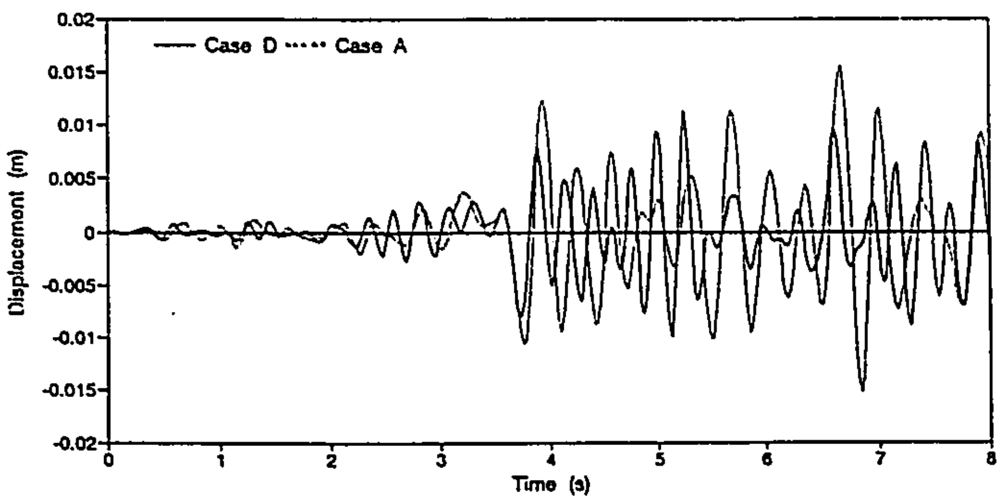

Figure (3-7) Time History of the Crest Displacement Cases A and D

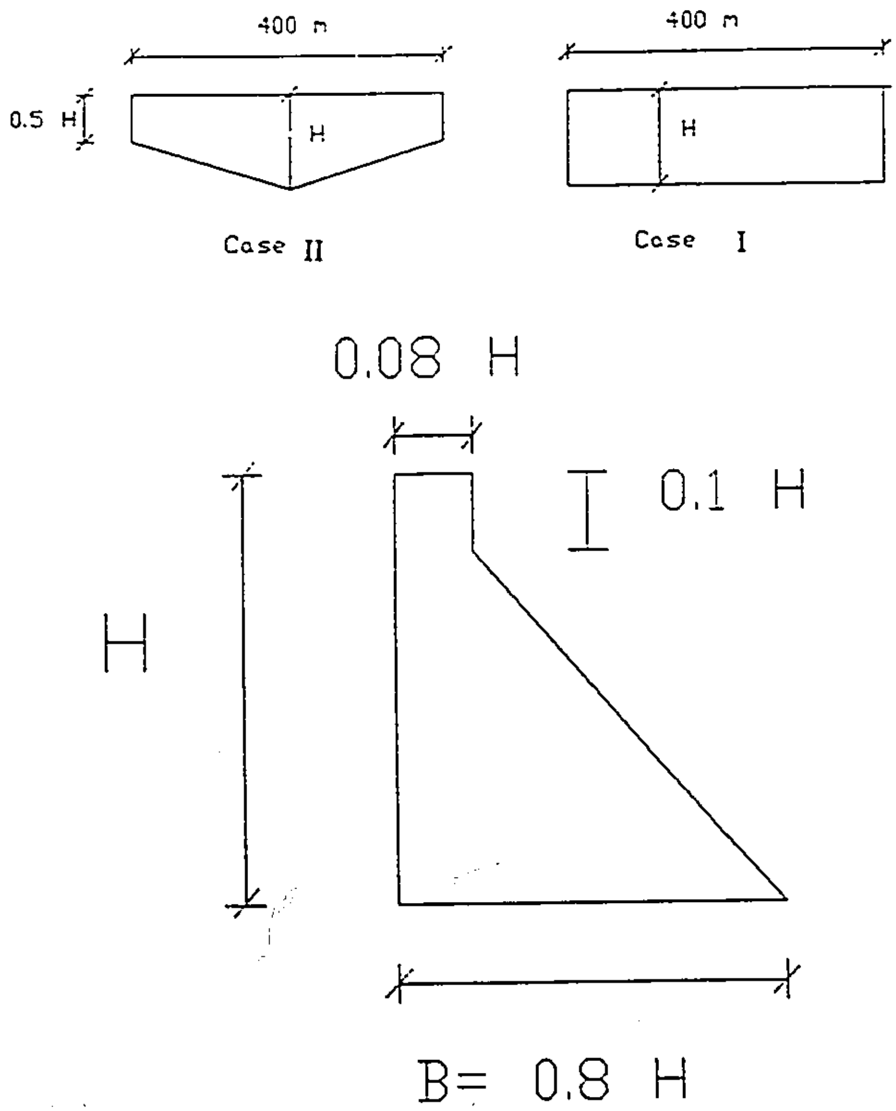

Figure (3-8) Geometry of Cases I and II

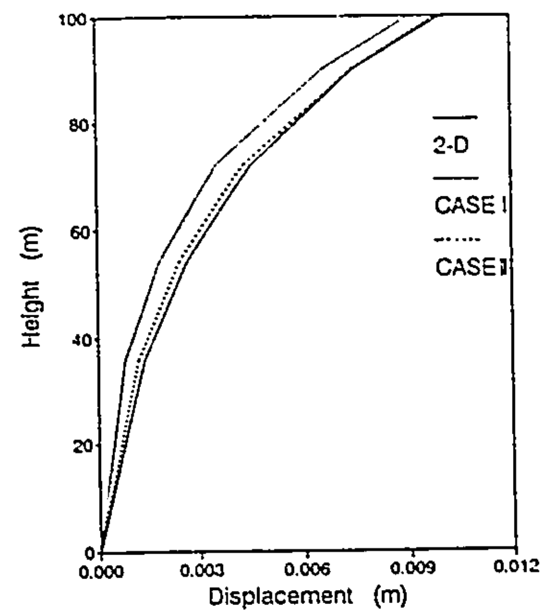

Figure (3-9) Envelope of Horizontal Displacements for Critical Monolith

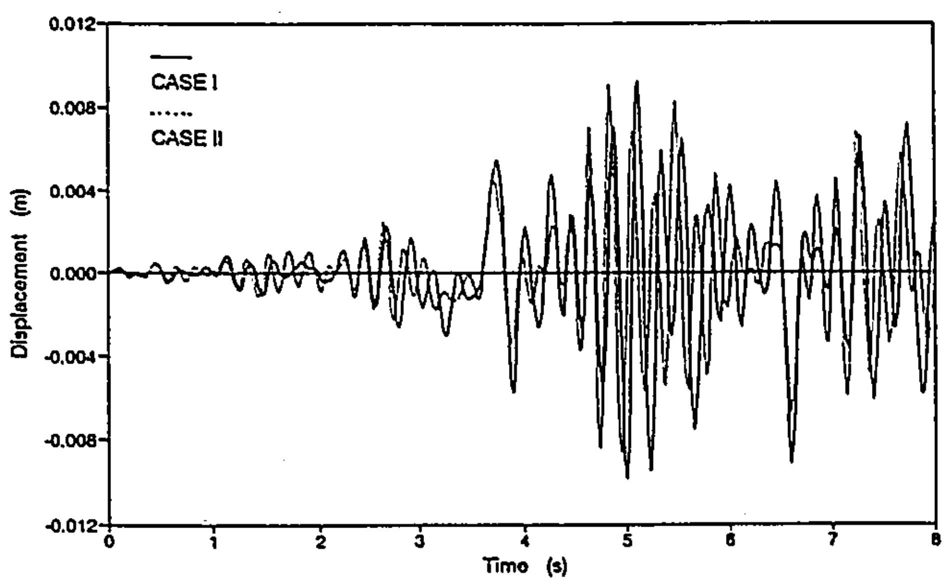

Figure (3-10) Time History of the Top Displacement H=100 m Taft Record

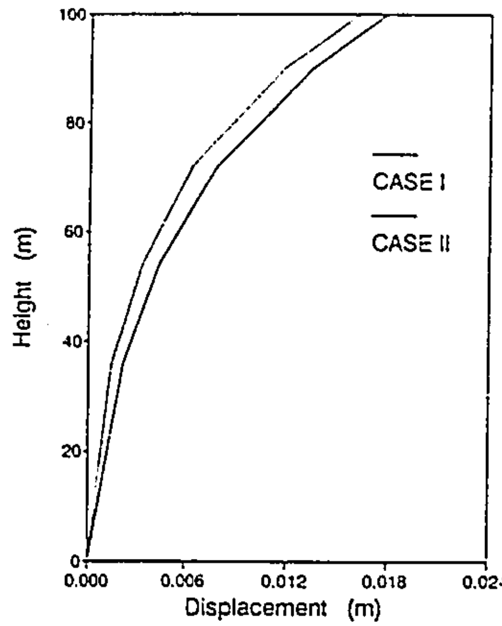

Figure (3-11)a Envelope of Horizontal Displacements for Critical Monolith

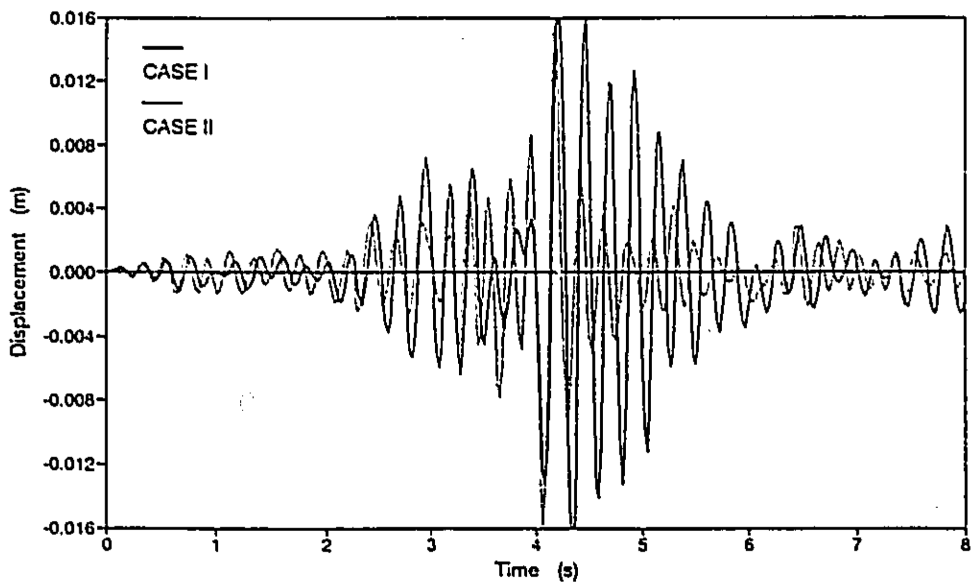

Figure (3-11)b Time History of the Top Displacement H=100 m, Parkfield Record

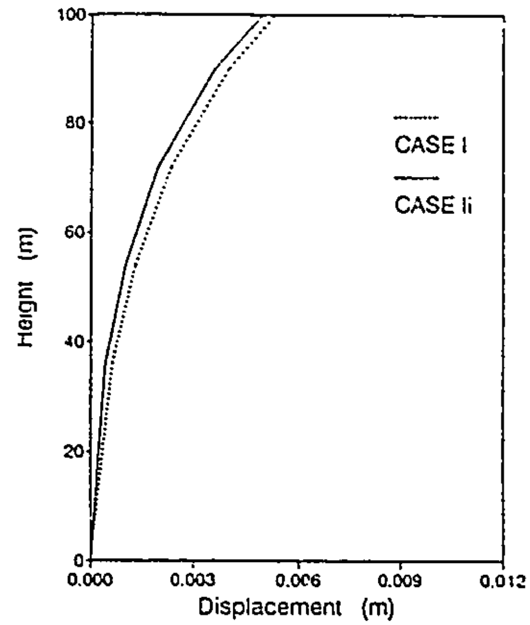

Figure (3-12)a Envelope of Horizontal Displacements for Critical Monolith

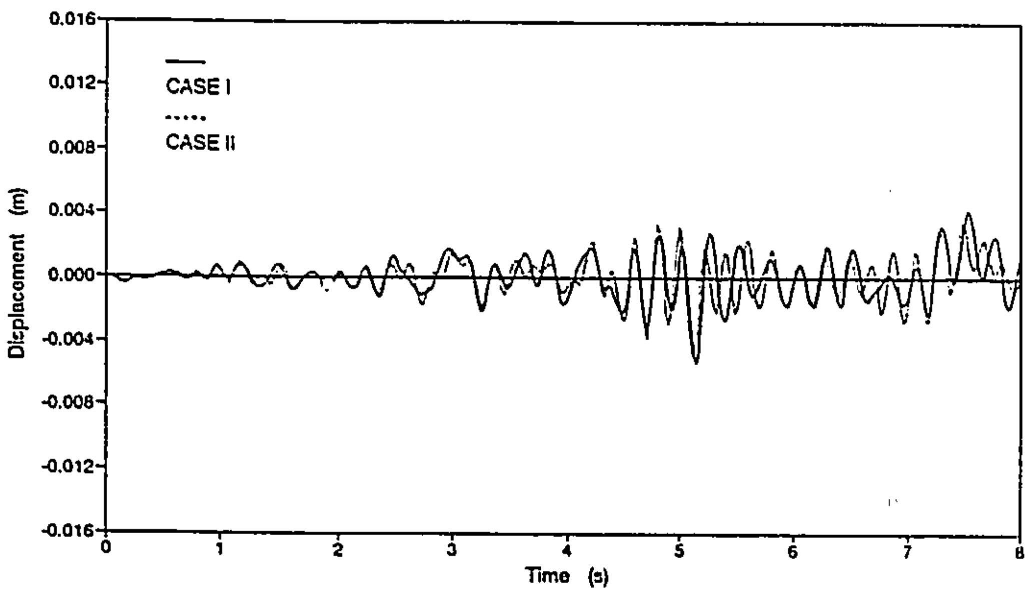

Figure (3-12)b Time History of the Top Displacement H=100, Long Beach Record

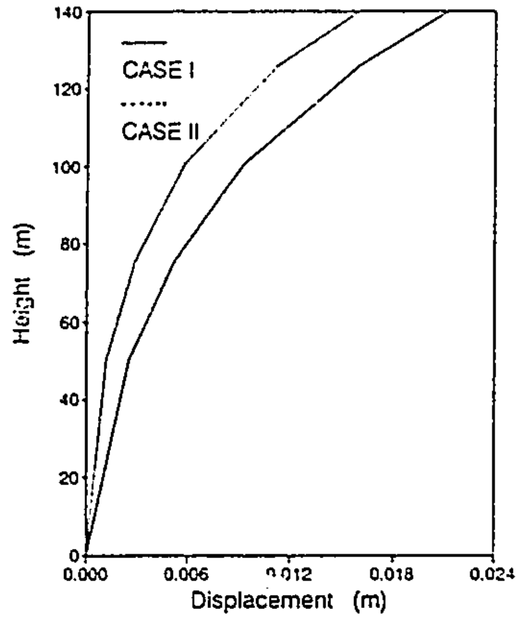

Figure (3-13)a Envelope of Horizontal Displacements for Critical Monolith

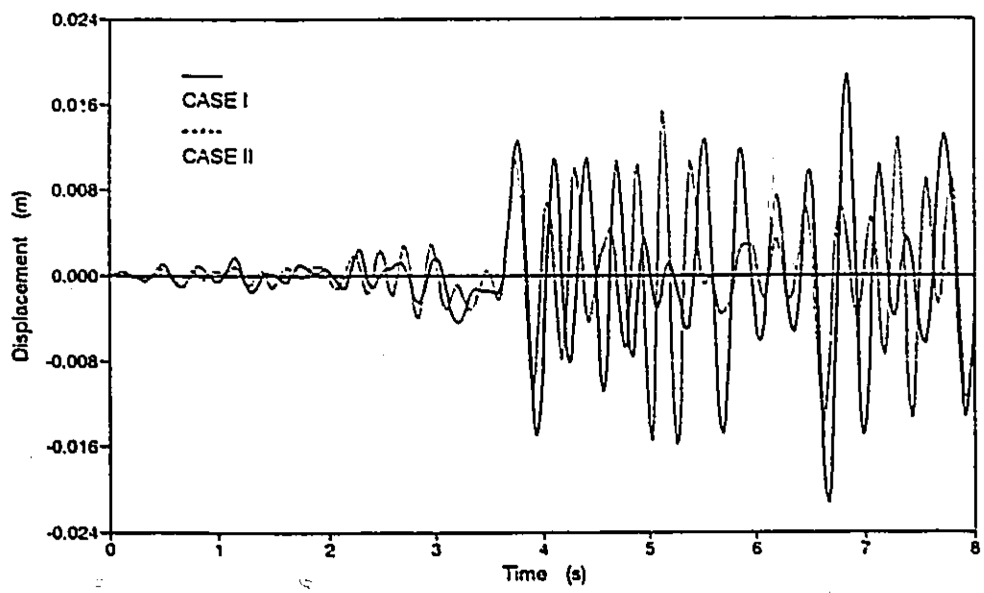

Figure (3-13)b Time History of the Top Displacement H=140 m,

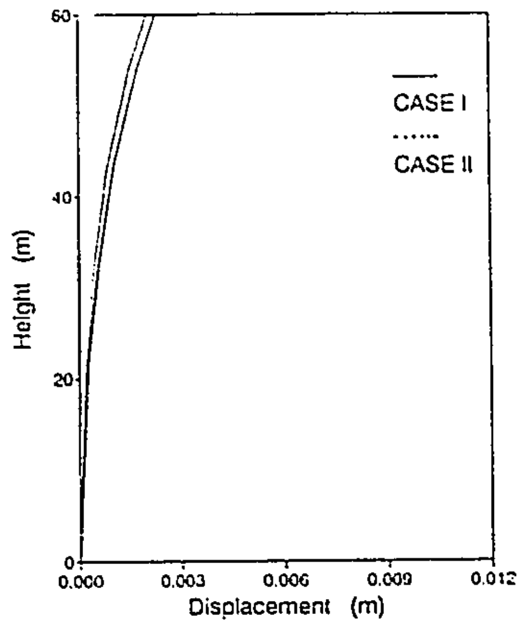

Figure (3-14)a Envelope of Horizontal Displacements for Critical Monolith

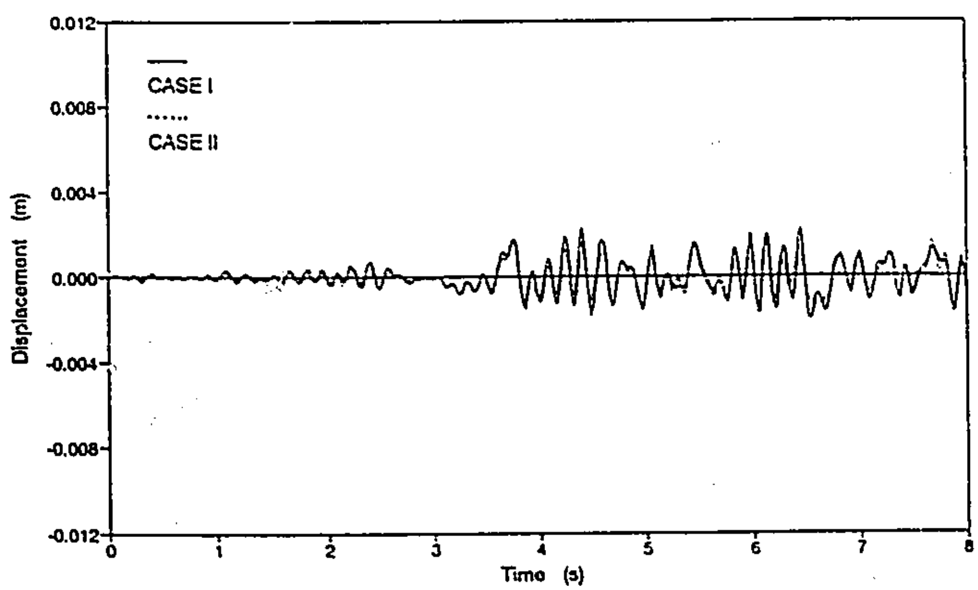

Figure (3-14)b Time History of the top Displacement H=60 m,

CHAPTER 4

DAM - RESERVOIR - FOUNDATION SYSTEM

4.1 GENERAL

Concrete Gravity dams are complex structures which can be divided into three major components; dam, reservoir and foundation. During seismic ground motion it is expected that the three domains interact and the response of the dam structure is affected by the reservoir and foundation. Many studies have been carried out in the literature to include these interactions and to determine their impact on the analysis. It was concluded in these studies that the dam-reservoir-foundation interaction is important and should be included in the analysis. This chapter summarizes the procedure used to include the two interactions separately. Then it describes the overall analysis of the dam including these interactions as well as monoliths interaction previously described in chapter 3. Some of the results obtained to show the effect of different interactions are also included.

4.2 SOIL - STRUCTURE INTERACTION

One of the principal criteria in choosing dam sites is the type of foundation rock at the proposed location. Although it is usually the case to prefer rigid rock sites to build gravity dams on, it is not always possible. In some cases concrete gravity dams have been constructed on foundation material with enough flexibility such that soil-structure interaction effects become significant. The foundation flexibility have been included in the analysis of the structure and is represented by massless springs at the monolith base as shown in figure (4-1). As a result, its contribution in the analysis of gravity dams is included as added dynamic stiffness at the base of the dam. Depending on the type and geometry of soil layers, different procedures can be used to model the soil domain. Two main approaches have been used in the literature; finite element mesh for soils with limited depth to the rigid rock and visco-elastic half space for soil layers which extend to large depths with the same properties. Either of the two approaches can be implemented in the analysis depending on the foundation conditions. However, using the finite element idealization for the foundation increases dramatically the number of degrees of freedom and consequently the time and effort required to carry out the analysis. In this study, the dynamic stiffness matrix of the soil is calculated using the visco-elastic half space model. This representation has the advantage of reducing the degrees of freedom for the soil to that at the base of the dam (r_d) and at the base of the reservoir (r_r) as shown in figure (4-1). The equations of motion for the foundation soil is written in the form:

$$S(\omega) \cdot r_f(\omega) = F(\omega) \tag{4-1}$$

where, $S(\omega)$ is the dynamic stiffness matrix of the foundation soil, $r_f(\omega)$ and $F(\omega)$ are the vectors of displacements and forces at the foundation level respectively. Dividing the degrees of freedom at the foundation level into these under the dam (r_d) and the reservoir (r_r), equation (4-1) can be written in the form:

$$\begin{bmatrix} S_{dd}(\omega) & S_{dr}(\omega) \\ S_{rd}(\omega) & S_{rr}(\omega) \end{bmatrix} \begin{bmatrix} r_d(\omega) \\ r_r(\omega) \end{bmatrix} = \begin{bmatrix} F_d(\omega) \\ F_r(\omega) \end{bmatrix} \tag{4-2}$$

where the subscripts d and r refer to dam and reservoir respectively. As the analysis is more concerned with the dam, the soil interface with the dam and reservoir will be reduced to that at the dam base using static condensation. The vector $r_r(\omega)$, displacements at the reservoir bottom, can be written in the form:

$$r_r(\omega) = S_{rr}^{-1}(\omega)\ [F_r(\omega) - S_{dr}(\omega) r_d(\omega)] \tag{4-3}$$

As a result, equation (4-1) can be reduced to one single equation which only include the degrees of freedom at the dam base:

$$S_f(\omega)\ r_d(\omega) = F_d(\omega) - S_{dr}(\omega)\ S_{rr}^{-1}(\omega)\ F_r(\omega) \tag{4-4}$$

where,

$$S_f(\omega) = S_{dd}(\omega) - S_{dr}(\omega)\ S_{rr}^{-1}(\omega)\ S_{dr}(\omega) \tag{4-5}$$

The dynamic stiffness matrix $S_f(\omega)$ is computed from a separate analysis of the foundation rock region (Dasgupta and Chopra, 1979). It is available in the form of data which differs depending on the foundation damping and the exciting frequency. Compatibility of interaction displacements between the two substructures, dam and foundation at the base of the dam requires that:

$$r_b(\omega) + r_d(\omega) = 0 \tag{4-6}$$

where, $r_b(\omega)$ is the vector of displacements at the dam base. Similarly, the equilibrium of interaction forces between the two substructures at the dam base requires that

$$R_b(\omega) + F_d(\omega) = 0 \tag{4-7}$$

where, $R_b(\omega)$ is the vector of forces at the dam base. Using both the compatibility and equilibrium conditions, the two substructures can now be related. The foundation stiffness matrix is written in the global form:

$$S_f(\omega) = \begin{bmatrix} 0 & 0 \\ 0 & S_f(\omega) \end{bmatrix} \tag{4-8}$$

where, zero's correspond to the degrees of freedom above the dam base. As a result, equation (3-1) in chapter 3 can be written, including soil-structure interaction, in the form:

$$-\omega^2 \begin{bmatrix} m & 0 \\ 0 & m_b \end{bmatrix} + \left((1+i\eta) \begin{bmatrix} k & k_b \\ k_b & k_{bb} \end{bmatrix} + \begin{bmatrix} 0 & 0 \\ 0 & S_f(\omega) \end{bmatrix} \right) \begin{Bmatrix} r(\omega) \\ r_b(\omega) \end{Bmatrix} = - \begin{Bmatrix} ml \\ m_b l_b \end{Bmatrix} + \begin{Bmatrix} R(\omega) \\ R_b(\omega) \end{Bmatrix} \tag{4-9}$$

Details of combining monoliths interaction with foundation interaction are described later in section 4.3 which covers the overall analysis of the system including different interactions. Results to show the importance of soil-structure interaction when monoliths interaction is considered, are included in this section. Figure (4-2) shows two cross sections; rectangular and triangular, and two longitudinal profiles, uniform and nonuniform. Different combinations of the cross sections and longitudinal profiles are used in the analysis as shown in table (4-1). The material properties of the structures are listed in table (4-2) and are kept constant through the analysis unless mentioned otherwise. The ground motion used in carrying out the analysis is the horizontal component of the Taft ground motion as described in chapter 3.

Comparisons of the natural frequencies of gravity dams including and excluding soil- structure interaction are shown in tables (4-3) and (4-4). Table (4-3) shows the natural frequencies of the dam of rectangular section with uniform and nonuniform longitudinal profiles. Table (4-4) shows the natural frequencies of the dam with triangular section with uniform and nonuniform longitudinal profiles. The natural frequencies of the structure decreases when including soil-structure interaction leading to a more flexible structure. The amount of reduction depends on the ratio of Young's modulus of foundation to that of concrete but is not affected by the longitudinal profile of the structure. Table (4-5) shows the natural frequencies for dam of rectangular cross section with uniform profile and variable values of the foundation Young's modulus. Table (4-6) shows the natural frequencies for a dam triangular cross section with nonuniform profile and variable values for the foundation Young's modulus. Figure (4-3) shows the envelope of maximum displacements evaluated for different values of the foundation Young's modulus. It is noted that as the ratio of the Young's modulus of the foundation to that of the dam increases, the effect of soil structure interaction decreases. It is also noted that both rectangular and triangular cross sections have the same behaviour when including the soil flexibility. Figure (4-4) shows the time history of the crest displacement for the critical monolith with rectangular cross-section including and excluding foundation interaction, a) uniform longitudinal profile and b) nonuniform longitudinal profile. Figure (4-5) shows the envelope of horizontal displacements of the critical monolith with rectangular cross-section including and excluding soil structure interaction, a) uniform longitudinal profile and b) nonuniform longitudinal profile. In both figures the magnification of the response as a result of including soil structure interaction is noted. Figure (4-6) shows the crest displacement profile of the dam with rectangular cross-section; a) rigid foundation and b) flexible foundation. The case of uniform profile produces the same results obtained from typical two dimensional analysis. For the case of nonuniform profile, using such an analysis significantly overestimates the response of the critical monolith and is not capable of producing the longitudinal deflection profile of the structure. Including monoliths interaction increases the stiffness of the structure when including soil structure interaction. Figure (4-7) shows the time history of the crest displacement for the critical monolith of triangular section including and excluding (NR) foundation interaction, a) uniform longitudinal profile and b) nonuniform longitudinal profile. Figure (4-8) shows the envelope of horizontal displacements of the critical monolith for the triangular section including and excluding soil structure interaction, a) uniform longitudinal profile and b) nonuniform longitudinal profile.

4.3 RESERVOIR-STRUCTURE INTERACTION

The main objective of including the hydrodynamic water pressures during ground motion is to study its effect on the response of the dam. Although many studies have been carried out on gravity dams including reservoir interaction, only a few presented practical solutions for the hydrodynamic pressures on the dam. Other studies spend too much effort on the analysis and behaviour of the reservoir systems while oversimplifying the dam structure and in some cases neglecting its flexibility. To include the hydrodynamic pressure in the current procedure, the following assumptions are used:

a) Water is linearly compressible with small amplitude irrotational motion.

b) The upstream face of the dam is vertical

c) The reservoir is assumed to be infinitely long with uniform cross-section. It is also assumed that wave propagation is only allowed in the upstream-downstream direction.

d) Water pressure at the free surface is zero. (neglecting the effect of surface waves) The hydrodynamic pressure on the upstream face of the dam during harmonic excitation is controlled by the wave equation:

$$\frac{\partial^2 p}{\partial x^2} + \frac{\partial^2 p}{\partial y^2} + \frac{\omega^2}{c^2} p = 0 \tag{4-10}$$

where,

P is the hydrodynamic water pressure

c is the wave propagation velocity in water

Three boundary conditions are introduced to obtain a closed form solution of the governing differential equation. One of the boundary conditions is the upstream face of the dam. The horizontal and vertical mode shapes of the dam alone as well as the generalized degrees of freedom Z_j are used to represent the motion of the dam. The boundary conditions are:

a) At monolith face:

$$\frac{\partial}{\partial x}P(0,y,\omega)=-[\delta_{xl}+\sum_{j=1}^{J}\psi_{xj}(y)Z_j(\omega)] \tag{4-12}$$

b) At reservoir bottom:

$$\frac{\partial}{\partial y}P(x,0,\omega)=-[\delta_{xl}-\omega^2 q_h(x,\omega)+\sum_{j=1}^{J}\psi_{yj}(x)\tilde{Z}_j(\omega)] \tag{4-13}$$

where,

Ψ is the structure mode shapes

q represents reservoir bottom absorbtion

δ_{xl} is the Kronker delta function

This equation is the same when the soil is assumed rigid with two modifications; effect of soil flexibility on the reservoir - foundation interaction and its effect on the dam -foundation interaction. Two mechanisms contribute to the effective damping of the dam - water system: the first is the energy dissipation in the dam alone, represented by the hysteretic damping and the second is the added damping due to radiation and absorption of hydrodynamic pressure waves at the reservoir bottom.

c) At the free surface:

$$P(x,H,\omega)=0 \tag{4-14}$$

where, H is the water depth. This boundary condition is a direct result of neglecting the effects of surface wave.

Due to the linear nature of the problem, the hydrodynamic pressure on the upstream face of the dam can be represented by the superposition of two components; the pressure due to the horizontal or vertical motion with rigid dam and the pressure due to the flexibility of the dam.

$$P(x,y,\omega)=P_o(x,y,\omega)+\sum_{j=1}^{J} Z_j(\omega)P_j(x,y,\omega) \tag{4-15}$$

where, P_0 is the complex frequency response function for the hydrodynamic pressure when the excitation is the ground motion and the dam is assumed rigid

P_j is the corresponding function when the excitation is the acceleration of the dam in its j's mode of vibration without the motion of the reservoir floor.

The solution of the wave equation with the two sets of boundary conditions, as presented by Fenves and Chopra (1984), leads to:

$$P_0^x(0,y,\omega) = -2\rho H\sum_{n=1}^{\infty} \frac{\mu_n^2(\omega)}{H[\mu_n^2(\omega) - (\omega q)^2] + i(\omega q)\sqrt{\mu_n^2(\omega) - \frac{\omega^2}{C^2}}} \frac{I_{on}(\omega)}{\sqrt{\mu_n^2(\omega) - \frac{\omega^2}{C^2}}} Y_n(y,\omega) \tag{4-16}$$

$$P_0^y(0,y,\omega) = \frac{\rho C}{\omega}\frac{1}{\cos\frac{\omega H}{C} + iqC\sin\frac{\omega H}{C}}\sin\frac{\omega(H-y)}{C} \tag{4-17}$$

$$P_j(0,y,\omega) = -2\rho H \sum_{n=1}^{\infty} \frac{\mu_n^2(\omega)}{H[\mu_n^2(\omega) - (\omega q)^2] + i(\omega q)} \frac{I_{nj}(\omega)}{\sqrt{\mu_n^2(\omega) - \dfrac{\omega^2}{C^2}}} \Upsilon_n(y,\omega)$$

(4-18)

where, ρ is the water density and $I_{jn}(\omega)$ and $I_{on}(\omega)$ are defined by the two equations:

$$I_{jn}(\omega) = \frac{1}{H}\int_0^H \psi_j(y)\ \Upsilon_n(y,\omega)\ dy \tag{4-19}$$

$$I_{0n}(\omega) = \frac{1}{H}\int_0^H \Upsilon_n(y,\omega)\ dy \tag{4-20}$$

and the eigenvalues μ and eigenvectors $Y_n(y,\omega)$ of the reservoir can be calculated using the following equations:

$$e^{2i\mu_n(\omega)H} = -\frac{\mu_n(\omega) - \omega q}{\mu_n(\omega) + \omega q} \tag{4-21}$$

$$\Upsilon_n(y,\omega) = \frac{1}{2\mu_n(\omega)}([\mu_n(\omega)+\omega q]e^{i\mu_n(\omega)y} + [\mu_n(\omega)-\omega q]e^{-i\mu_n(\omega)y}) \tag{4-22}$$

4.4 RESPONSE OF THE SYSTEM

The equations of motion of the dam including soil, reservoir and monoliths interaction subjected to harmonic ground excitation in the vertical or lateral directions can be written in the form:

$$S(\omega)\ Z(\omega) = L(\omega) \tag{4-23}$$

where,

Z(ω) is the vector of generalized coordinates

S and L functions can be defined as follows:

$$S_{nj}(\omega)=[-\omega^2+(1+i\eta_s)]+\psi_n[S_f(\omega)-(1+i\eta_s)S_f(\omega)]\psi_j+\omega^2\psi_n R_j(\omega) \tag{4-24}$$

$$L_n = -\psi_n{}^T m_c l_c + \psi_n{}^T R_0(\omega) - \psi_{bn}{}^T S_{rq}(\omega) S_{qq}{}^{-1} Q_0(\omega) \tag{4-25}$$

Hydrodynamic terms appear on both sides of the equation as added loads on the right and added masses on the left. The added load terms are associated with hydrodynamic pressures on the dam face due to ground accelerations while the dam is rigid. Added mass terms arise form hydrodynamic pressures due to motions of the dam relative to its base. The hydrodynamic terms depend on the excitation frequency, a consequence of the water compressibility.

These two equations include only the effective terms of hydrodynamic and soil - structure interaction forces as evaluated by Fenves and Chopra (1984). The resulting equations are single complex equations each one has only one variable (the modal response) which can easily be solved. The transformation of the modal response from the time domain to the frequency domain is done using the Fourier transform:

$$Z_j(t) = \frac{1}{2\pi} \int_{-\infty}^{\infty} Z(\omega)\, Ag(\omega)\, e^{i\omega t}\, d\omega \tag{4-26}$$

where:

$$A_g(\omega) = \int_0^T a_g(t) e^{-i\omega t} dt \tag{4-27}$$

In which T is the duration of the ground motion. The displacement response to the horizontal and vertical components of ground motion, simultaneously, is obtained by transformation of the generalized coordinates to the nodal displacements:

$$r_c(t) = \sum_{j=1}^{J} Z_j(t)\, \psi_j \tag{4-28}$$

To examine the importance of the interactions described in this chapter along with the monoliths interaction, the two example dam structures used with soil-structure interaction are used again including the effects of hydrodynamics, soil-structure interaction and monoliths interaction. Figure(4-9) shows the time history of the crest displacement of the critical monolith for a dam with rectangular section and uniform profile. The solid line represents the dam without hydrodynamics on rigid foundation while the dotted line represents the response including hydrodynamics. Figure (4-10) shows the same relationship for a dam with nonuniform longitudinal profile. Having the same properties except for the longitudinal profile, the difference between the two figures show the effect of the monoliths interaction when the hydrodynamics effect is included. Figure (4-11) shows the time history of the crest displacement of the critical monolith for a dam with rectangular section and uniform profile. In this case the dotted line represents the response of the dam when all interactions are included. Figure (4-12) shows the same relationship for a dam with nonuniform longitudinal profile. The reduction in the response of the structure of the nonuniform longitudinal profile compared to the one with uniform profile is noted. Figure (4-13) shows the envelope of the maximum displacements of the critical monolith for a structure with rectangular section and uniform profile. Figure (4-14) shows the same relationship for a structure with nonuniform profile. It is noted that the response of the dam when including both hydrodynamics and soil structure interaction is the highest. A reduction in the response of the structure as a result of the nonuniform profile is also noted. Figure (4-15) shows the time history of the maximum displacement for a structure with typical triangular section and uniform longitudinal profile including and excluding hydrodynamics. Figure (4-16) shows the same relation for a structure with variable longitudinal profile. Both the increase in response as a result of including hydrodynamics and the decrease due to including monoliths interactions are noted. Figure (4-17) shows the envelope of maximum displacements at the upstream face of the critical monolith for a structure with triangular section and uniform profile. The solid line represents the response of the dam without interactions while the light dotted represent the effect of hydrodynamics and the heavy dotted represent both hydrodynamics and soil interactions. Figure (4-23) shows the same relation for a structure with nonuniform profile where the height at the end is equal to half the height at the middle.

The results obtained show the importance of including soil-structure as well as reservoir-structure interactions. It also shows that for structures with nonuniform longitudinal profile, the effect of monoliths interaction is important and should be included. Triangular cross sections seems to be less sensitive to the effect of monoliths interaction than rectangular sections. The reason for this is that the effect of the adjacent monoliths to the critical one reduces when triangular sections are used instead of rectangular. Unless the base width of each monolith is kept the same, the effect of monoliths interaction on triangular sections will be less than that of rectangular sections.

4.5 SUMMARY

This chapter described the part of analysis related to including soil-structure interaction as well as hydrodynamic effects. Both interactions were included in the analysis and their effect on the overall analysis of gravity dams were considered. Soil-structure interaction was included by modelling the foundation domain as a visco-elastic half space. The hydrodynamic effects on the dam were included by solving the second order differential equation assuming an infinitely long reservoir. It is noted that both interactions significantly alter the response of the structure and as a result must be included in the analysis. The overall analysis of the structure including the three interactions: monoliths interaction, as described in chapter 3, soil-structure interaction and reservoir-dam interaction was described. The results obtained including the three interactions simultaneously show a significant variation in the response of the structure from that obtained by considering the critical monolith alone. The effect of the monoliths interaction is dependent on the strength and stiffness of contraction joints located among the monoliths. The behaviour of these joints is essential for the analysis of dams including monoliths interaction as will be described in details in chapter 5.

Table (4-1) Cases Studied with Dam-Reservoir-Foundation Interactions

Case	Section Shape	B m	H_e m	H_c m	Soil	Hydrodynamic effects
UR	Rect	60	100	100	Rigid	No
URS	Rect	60	100	100	Flexible	No
URW	Rect	60	100	100	Rigid	Yes
URSW	Rect	60	100	100	Flexible	Yes
NR	Rect	60	60	100	Rigid	No
NRS	Rect	60	60	100	Flexible	No
NRW	Rect	60	60	100	Rigid	Yes
NRSW	Rect	60	60	100	Flexible	Yes
UT	Trngle	80	100	100	Rigid	No
UTS	Trngle	80	100	100	Flexible	No
UTW	Trngle	80	100	100	Rigid	Yes
UTSW	Trngle	80	100	100	Flexible	Yes
NT	Trngle	80	50	100	Rigid	No
NTS	Trngle	80	50	100	Flexible	No
NTW	Trngle	80	50	100	Rigid	Yes
NTSW	Trngle	80	50	100	Flexible	Yes

Table (4-2) Material Properties used in the Analysis

Material	Property	Symbol	Value	Units (SI)
Dam	Young's modulus	E_c	34×10^6	kN/m^2
(Concrete)	Poisson's ratio	υ_c	0.20	-
	Unit Weight	γ_c	24.3	kN/m^3
	Hysteretic Damping	η_c	0.10	-
Reservoir	Unit Weight	w	10.0	kN/m^3
(Water)	Wave Velocity	C	1470	m/sec
Foundation	Reflection Coefficient	α_f	1.0	-
(Rock)	Young's Modulus	E_f	34×10^7	kN/m^2
	Unit Weight	γ_f	26.4	kN/m^3
	Poisson's Ratio	υ_f	0.33	-
	Hysteretic Damping	η_f	0.10	-

Table (4-3) Natural Frequencies of Rectangular Dam Section with Uniform and Nonuniform Longitudinal Profiles (rad/s)

Mode	Case			
	UR	URS	NR	NRS
1	19.08	13.44	24.64	17.96
2	20.92	15.86	32.53	24.20
3	25.28	21.09	37.28	28.55
4	30.38	26.72	41.89	33.45
5	35.19	31.75	44.51	37.47

Table (4-4) Natural Frequencies of Triangular Dam Section with Uniform and Nonuniform Longitudinal Profiles (rad/s)

Mode	Case			
	UT	UTS	NT	NTS
1	28.79	22.01	33.18	26.19
2	29.82	23.42	41.26	34.33
3	32.51	26.95	45.17	38.16
4	36.15	31.39	48.98	42.00
5	39.93	35.76	51.39	44.60

Table (4-5) Natural Frequencies (rad/s) of the Structure with Rectangular Section

Mode	E_f/E_d			
	1	3	5	20
1	13.44	16.38	17.28	19.08
2	15.86	18.46	19.27	20.92
3	21.09	23.20	23.87	25.28
4	26.72	28.57	29.16	30.38
5	31.75	33.51	34.06	35.19

Table (4-6) Natural Frequencies (rad/s) of the Structure with Triangular Section

Mode	E_f/E_d			
	1	3	5	10
1	17.97	21.49	22.55	24.64
2	24.20	28.59	29.92	32.53
3	28.55	33.06	34.47	37.29
4	33.45	37.59	38.98	41.89
5	37.47	40.96	42.11	44.51

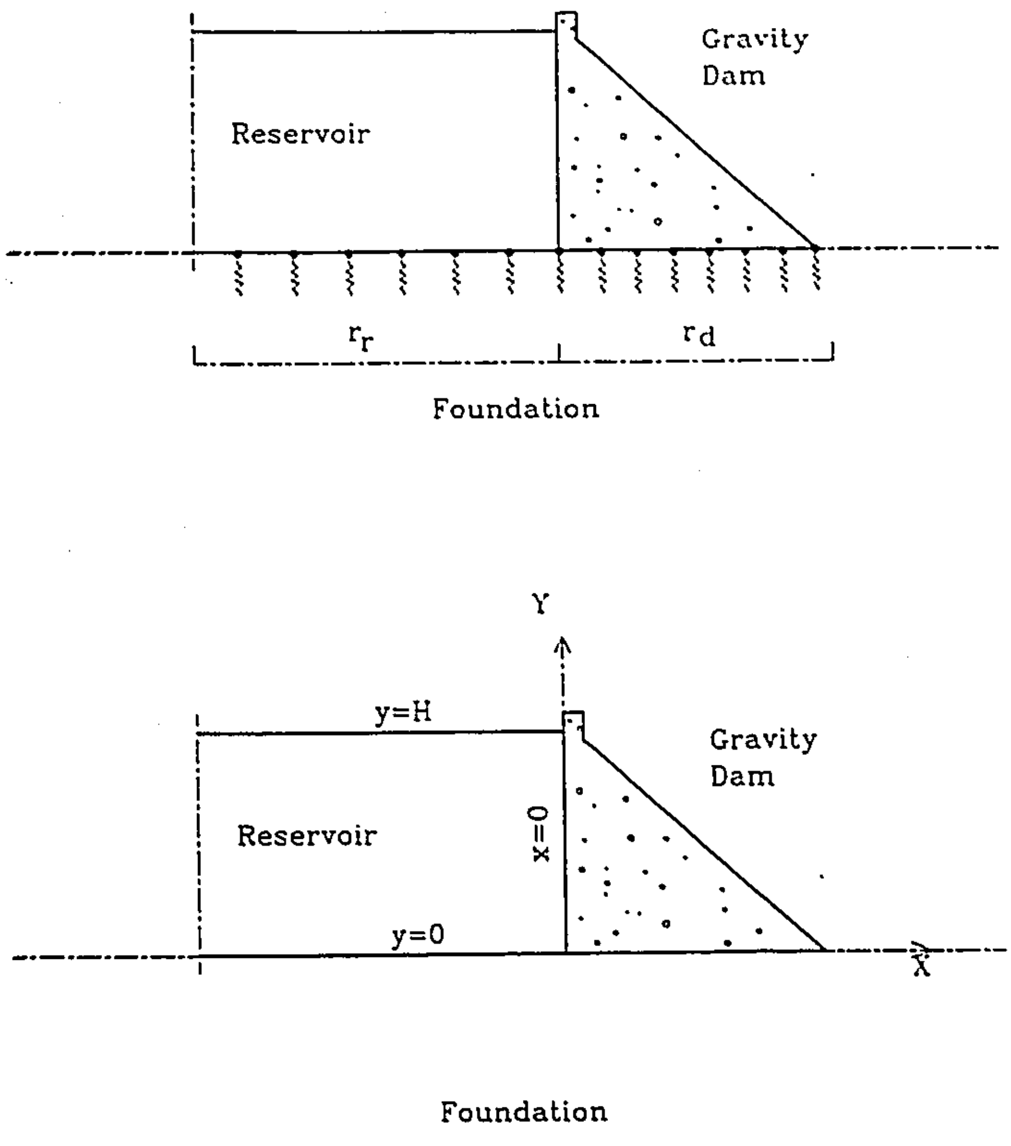

Figure (4-1) Dam-Reservoir-Foundation Interaction

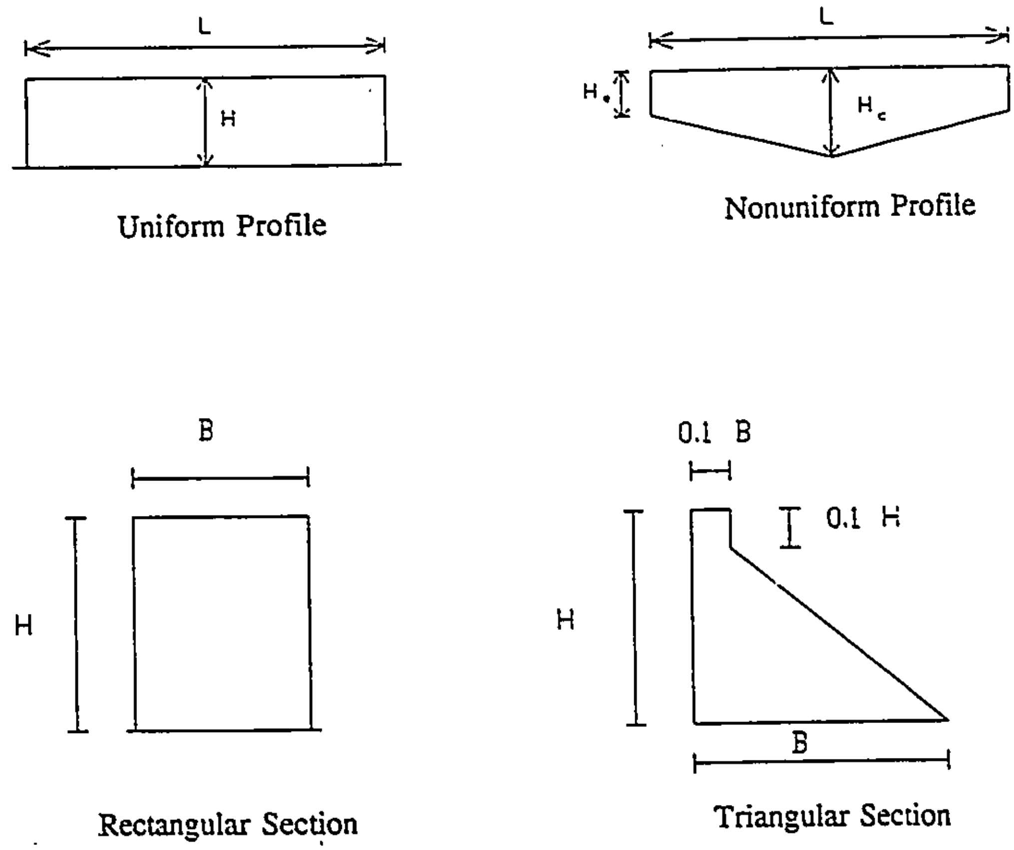

Figure (4-2) Geometry of the Model Structure

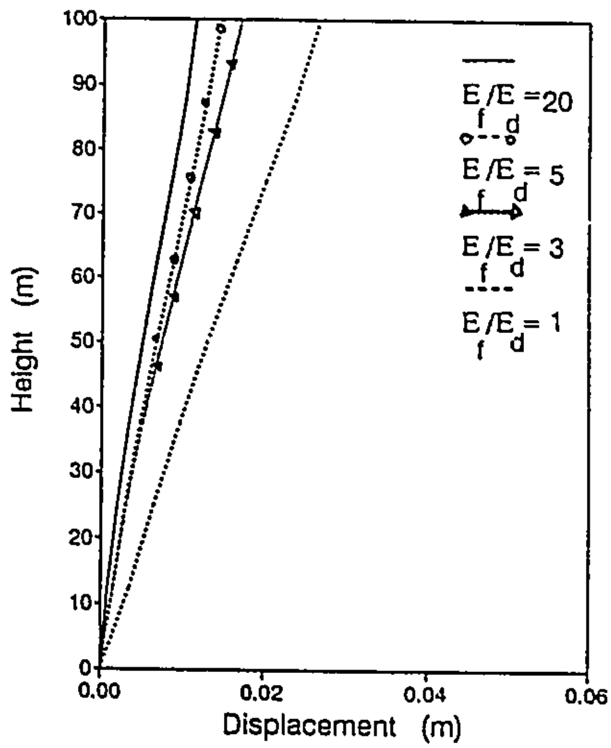

Figure (4-3) Envelope of Horizontal Displacement of the Critical Monolith

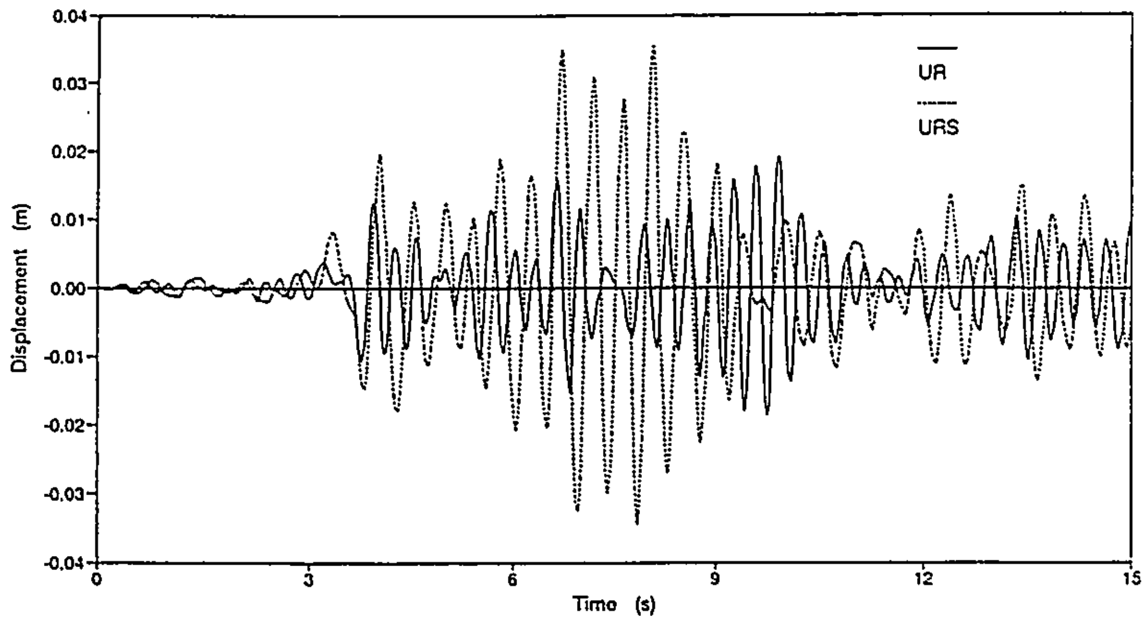

a) Uniform Profile

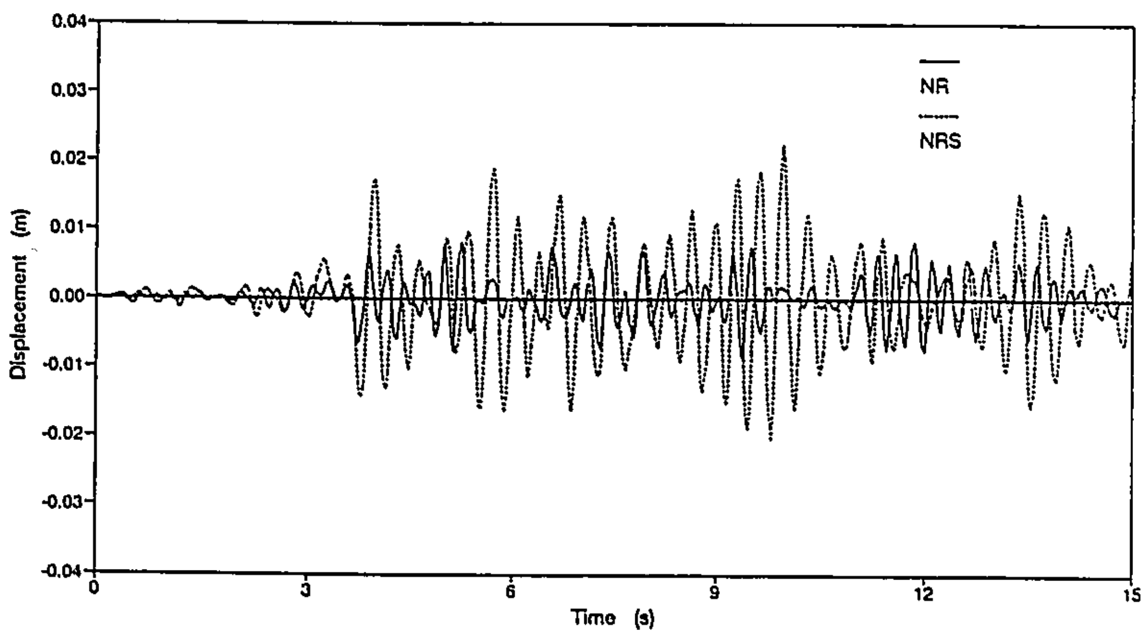

b) Nonuniform Profile

Figure (4-4) Crest Displacement Time History of the Critical Monolith

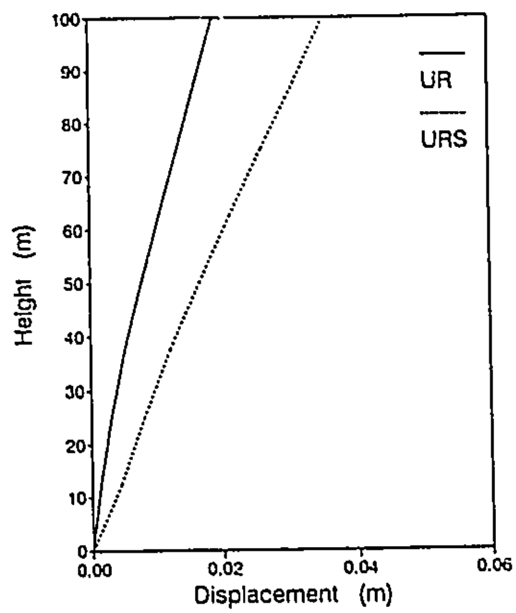

a) Uniform Profile

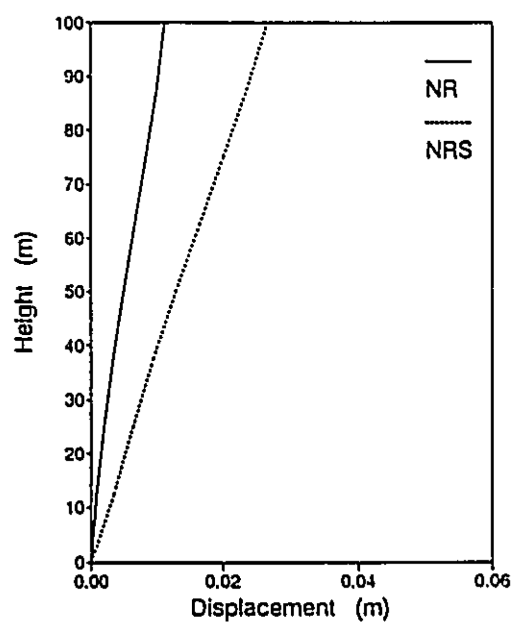

b) Nonuniform Profile

Figure (4-5) Envelope of Horizontal Displacement of the Critical Monolith

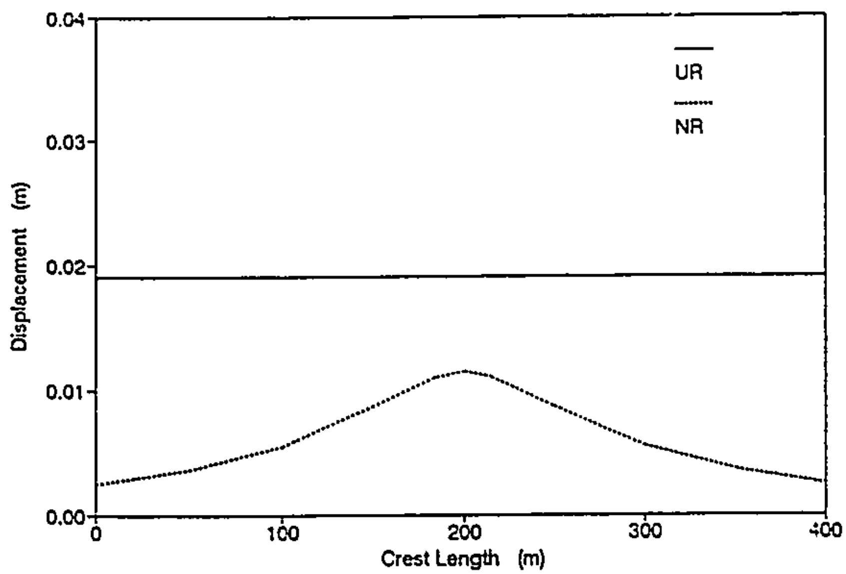

a) Rigid Foundation

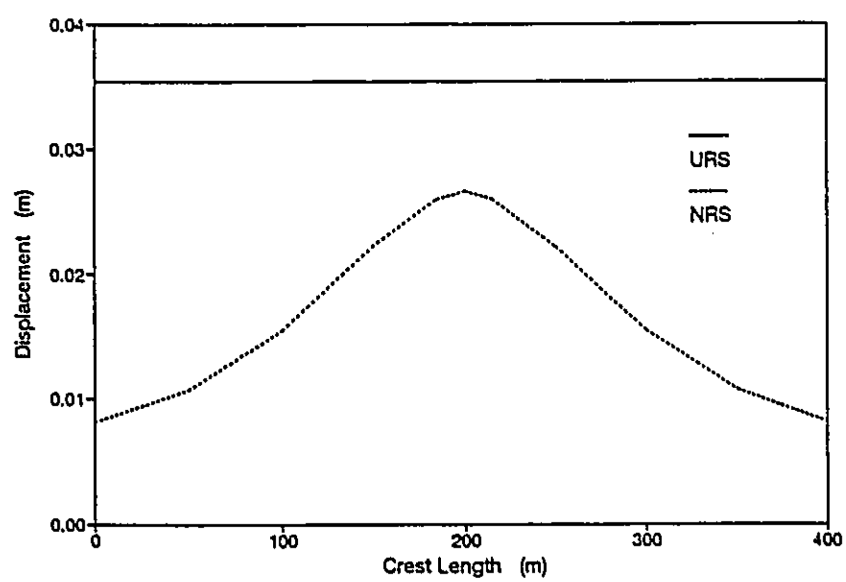

b) Flexible Foundation

Figure (4-6) Crest Displacement along the Dam Longitudinal Axis

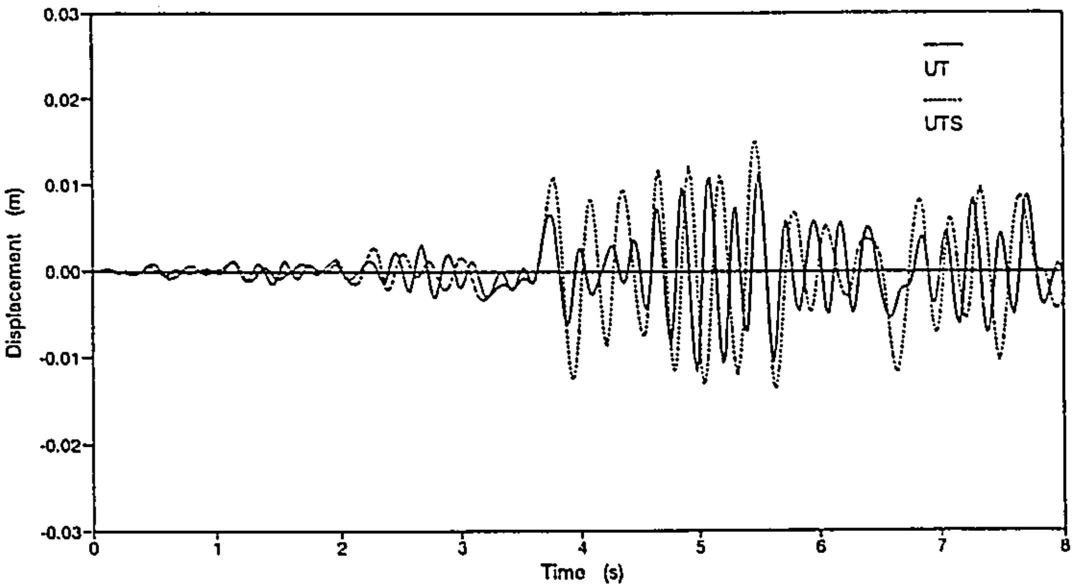

a) Uniform Profile

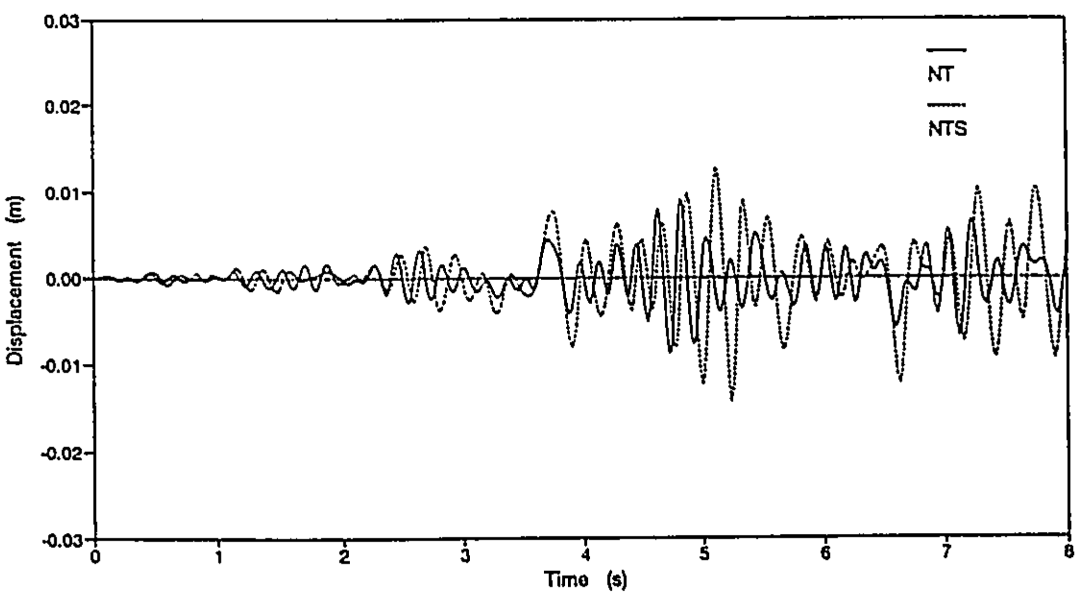

b) Nonuniform Profile

Figure (4-7) Crest Displacement Time History of the Critical Monolith

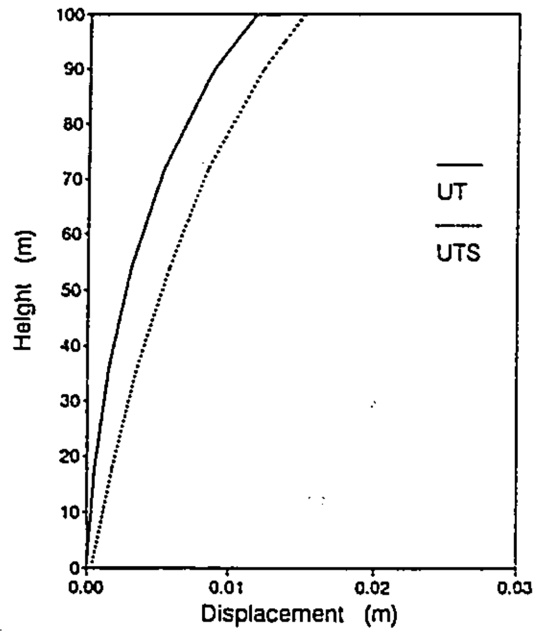

a) Uniform Profile

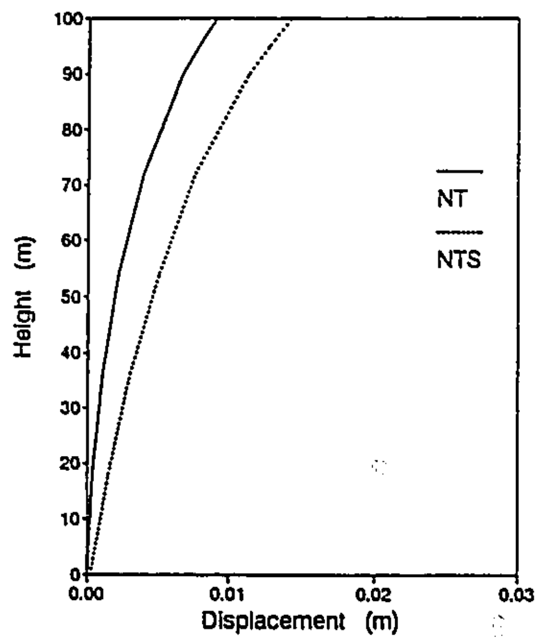

b) Nonuniform Profile

Figure (4-8) Envelope of Horizontal Displacement of the Critical Monolith

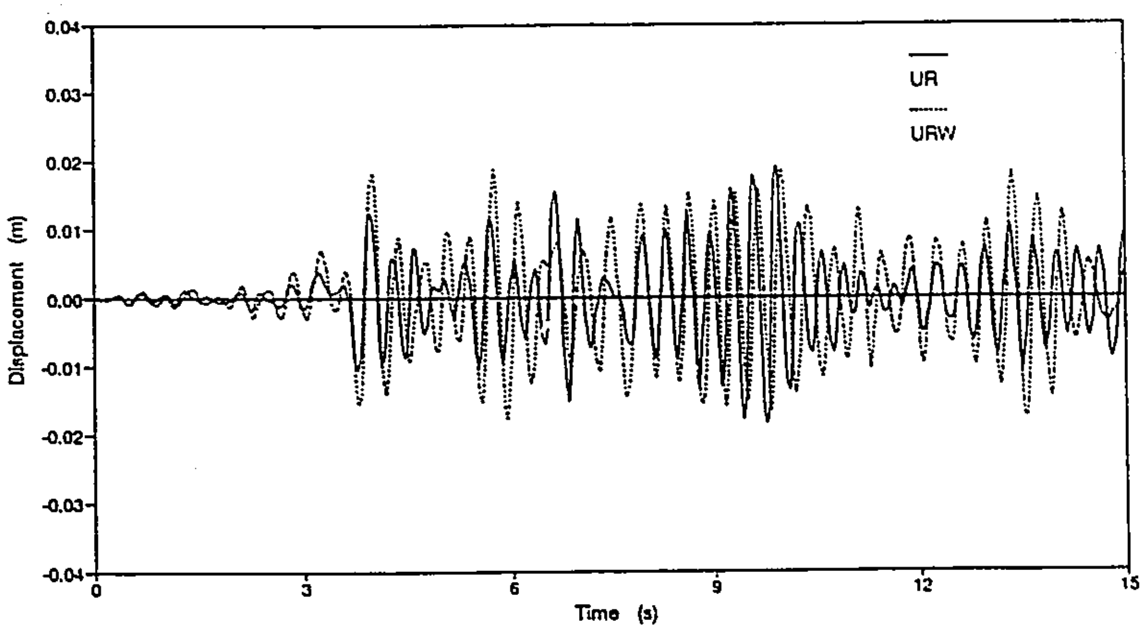

Figure (4-9) Crest Displacement Time History of the Critical Monolith of Rectangular Section (Uniform Profile)

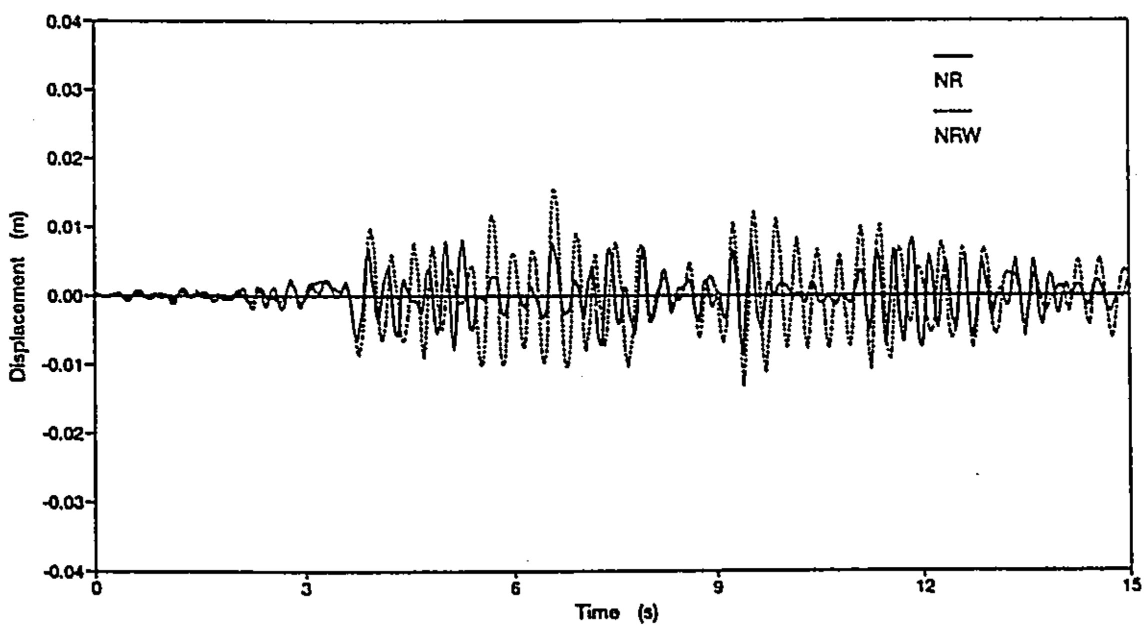

Figure (4-10) Crest Displacement Time History of the Critical Monolith of Rectangular Section(Non-uniform Profile)

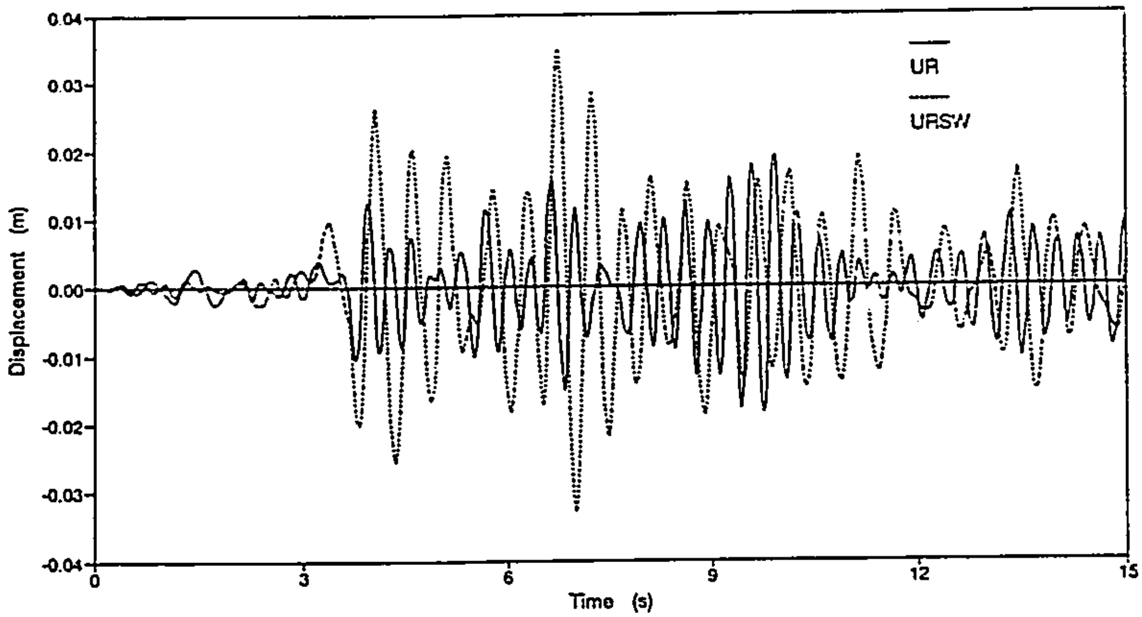

Figure (4-11) Envelope of Horizontal Displacement of the Critical Monolith of Rectangular Section (Uniform Profile)

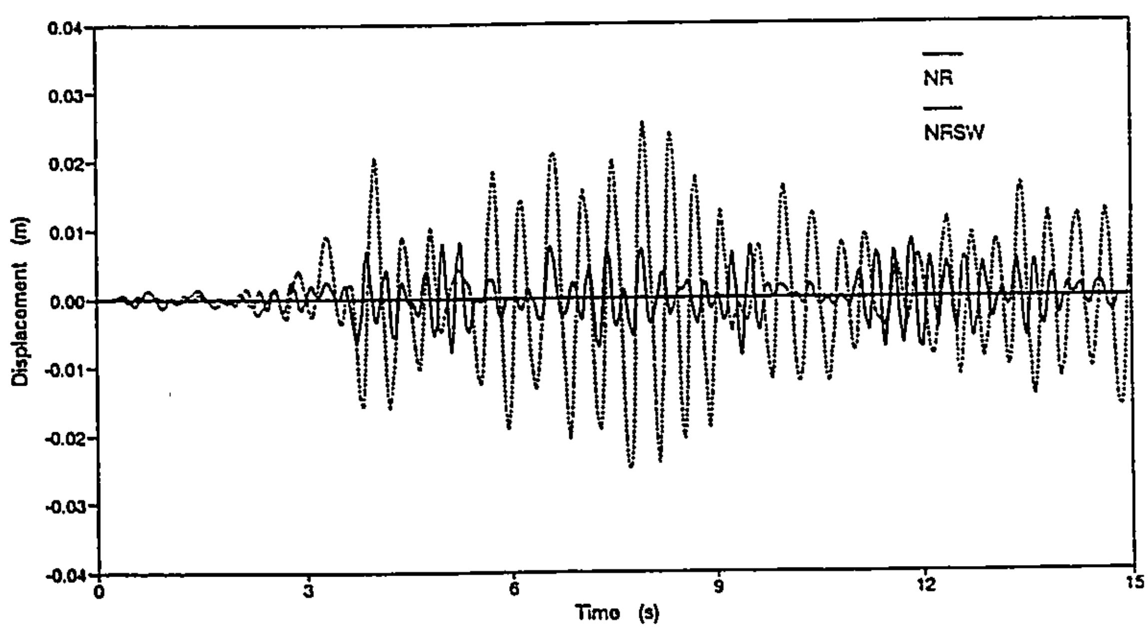

Figure (4-12) Crest Displacement Time History of the Critical Monolith of Rectangular Section (Non-uniform Profile)

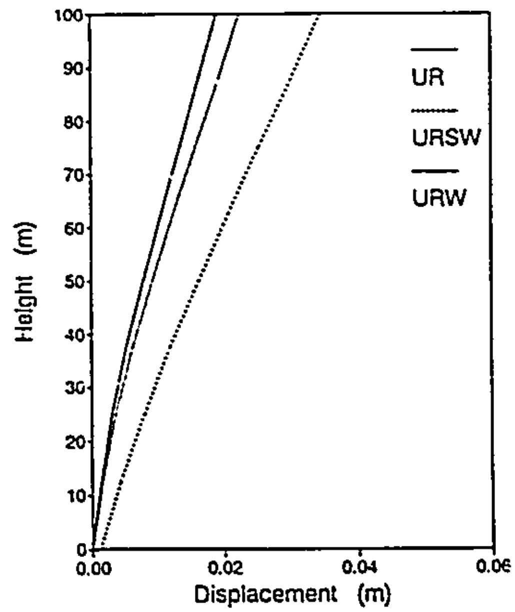

Figure (4-13) Envelope of Horizontal Displacement of the Critical Monolith of Rectangular Section (Uniform Profile)

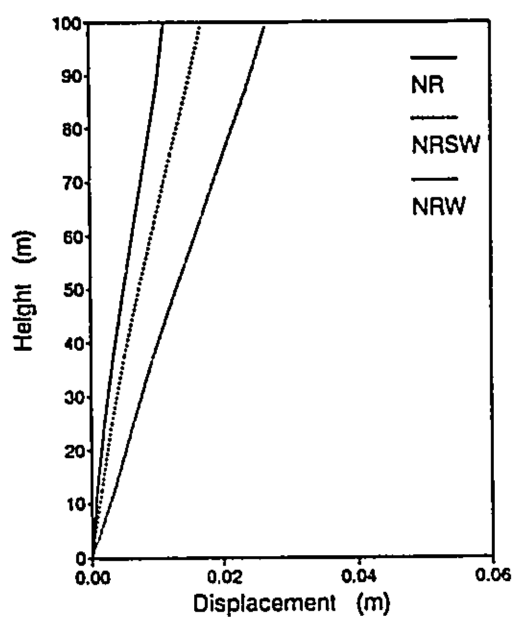

Figure (4-14) Envelope of Horizontal Displacement of the Critical Monolith of Rectangular Section (Non-uniform Profile)

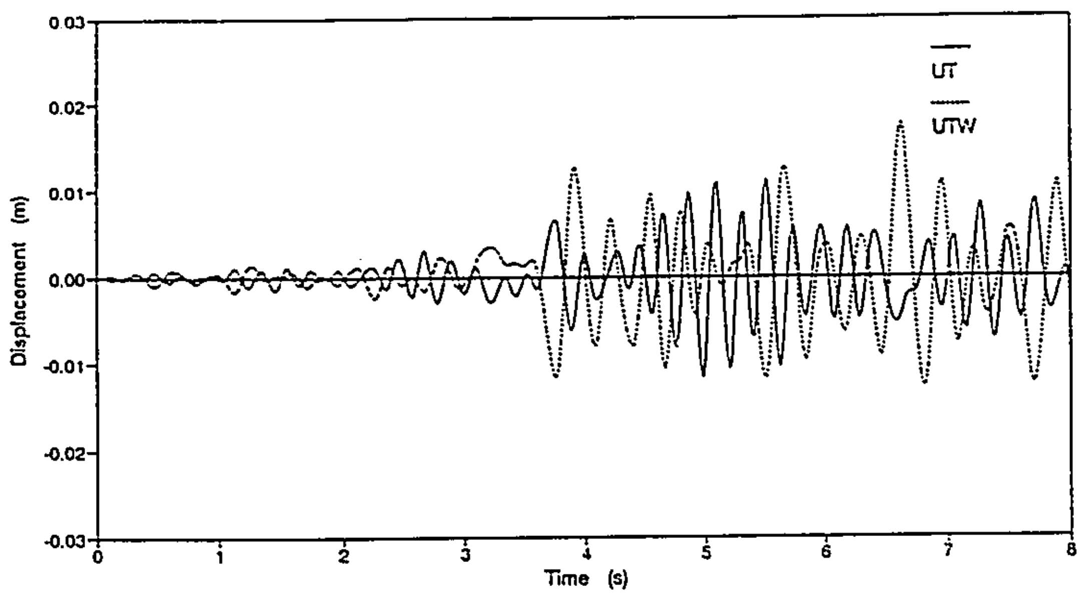

Figure (4-15) Crest Displacement Time History of the Critical Monolith of Traingular Section (Uniform Profile)

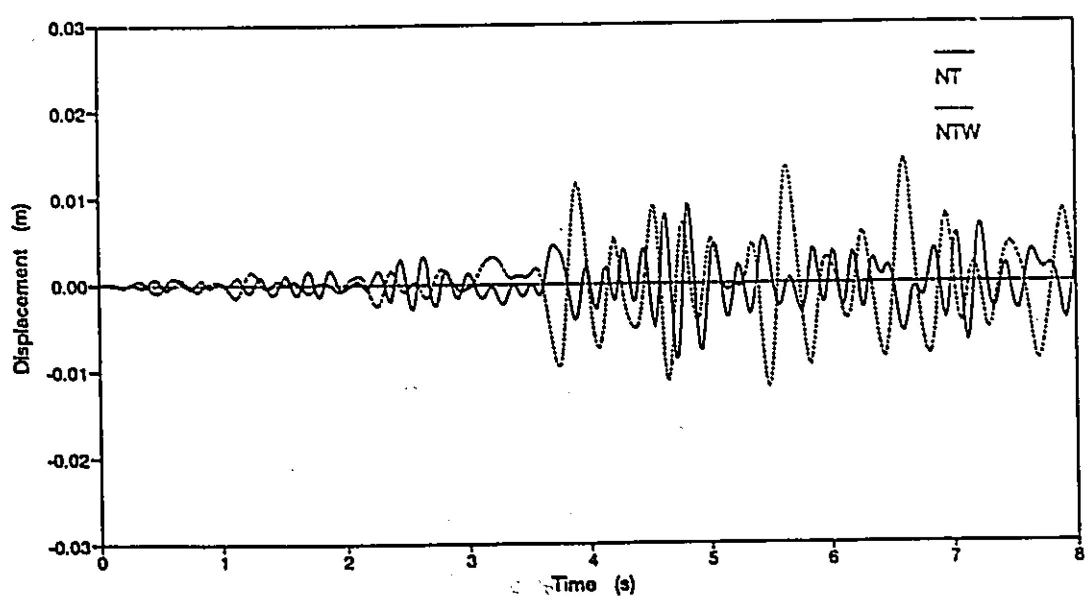

Figure (4-16) Crest Displacement Time History of the Critical Monolith of Traingular Section (Non-uniform Profile)

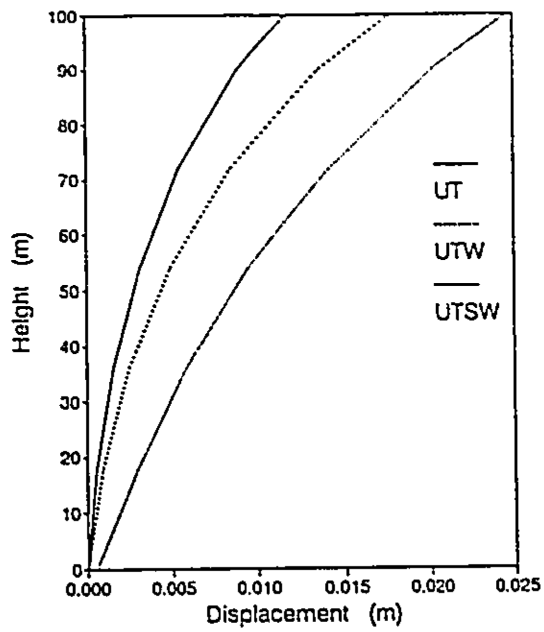

Figure (4-17) Envelope of Horizontal Displacement of the Critical Monolith of Triangular Section (Uniform Profile)

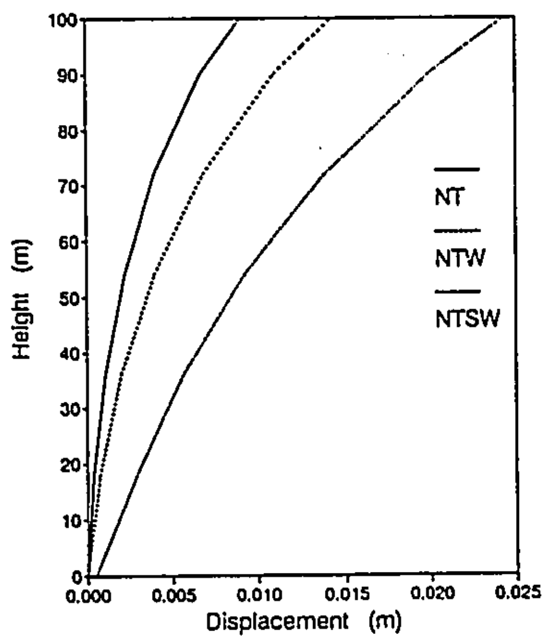

Figure (4-18) Envelope of Horizontal Displacement of the Critical Monolith of Traingular Section (Non-uniform Profile)

CHAPTER 5

CONTRACTION JOINTS

5.1 GENERAL

A procedure was developed in chapters 3 and 4 to include the effect of monoliths interaction on the response of concrete gravity dams. The principal mechanism which affects the interaction between different monoliths is the shear transfer at the vertical joints between them. These joints are provided in order to prevent tensile cracks caused by chemical or thermal expansion or contraction of concrete and also to facilitate the concrete placement work. As it serves different objectives, it is called by different names e.g. vertical construction joints, contraction joints or expansion joints. Assuming that the shear strength of these joints is very small, its effect was neglected in the literature resulting in a two dimensional planar analysis of the critical monolith. However, recent simplified studies (Rashed and Iwan, 1984) show that the shear behaviour of contraction joints can play a major role in the earthquake response of concrete gravity dams. In this chapter, different types of contraction joints are discussed. The shear behaviour and strength of these joints are studied and compared. The effect of using different types of joints on the overall behaviour of the structure is also included. The chapter is concluded with a summary of the obtained results and recommendations.

5.2 TYPES OF CONSTRUCTION JOINTS

Construction joints, used in concrete gravity dams to facilitate the construction of the structure can be divided into two groups: vertical joints and horizontal joints. Horizontal joints, although a potential weak link in the structural system, are relatively much stiffer than the vertical joints because of the normal pressure, weight, applied to these joints. Moreover, there are microcracks in the vertical joints due to shrinkage and chemical effects in concrete. The extent of interaction among the monoliths depends on the shear strength of the contraction joint which consequently depends on the type of joint used in the dam construction. Three types of joints are used in construction; i) smooth joints, ii) keyed joints and iii) reinforced joints, as shown in figure (5-1). A brief description of each type is included in this section. The three types are shown in figure (5-2).

5.2.1 Smooth Joints

Smooth joints are the first type to be used in the construction of concrete gravity dams. This is the cheapest and simplest type of construction joints. The joint surface is smooth and does not require any additional effort. As shown in figure (5-1), this type is subdivided into three groups according to the construction method as follows:

i- without gap between the monoliths. In practice, after casting and curing of the first monolith, the second monolith is casted next to it without gaps.

ii- with a gap, in which a gap is left between the two monoliths to allow for expansion of the concrete.

iii- with a grouted gap, in which the gap left between the two monoliths is injected with grout after the dam has been cured to a few degrees below mean ambient temperature.

5.2.2 Keyed Joints

In this type of joints shear keys are used in construction to prevent water seepage through vertical construction joints during medium to strong seismic motion which is a major drawback of smooth joints. Shear keys, as shown in figure (5-2), have different shapes and distribution. There is not enough research carried out on the effect of its shape on the response of the dam. Similar to the smooth joints, this type of joints can be subdivided to the same subgroups mentioned previously. In spite of the fact that it is relatively more expensive than smooth joints, this type is preferred in the construction of dams to provide enough resistance to water seepage.

5.2.3 Reinforced Joints

Reinforced joints, which could be smooth or keyed, are the most expensive type of joints. Reinforcement is usually provided in the form of shear dowels across the interface between the two surfaces. While smooth and keyed joints are normally used for massive structures, such as gravity dams, reinforced joints are mostly used for precast structures. Because it is rarely used in gravity dams construction, it is not covered in this study.

5.3 FORCE TRANSFER AT CONTRACTION JOINTS

Limited experimental test results are available in the literature for the kind of joints discussed herein. The majority of these tests were done as a part of research in precast concrete. In this type of research, as found in other structural reinforced concrete elements, reinforcing steel is extensively used. Such reinforcing steel can contribute to the shear strength of joints in two ways; direct contribution in which the shear strength of reinforcing bars is added to the shear strength of concrete and indirect contribution in which the force in the steel bars provide a clamping force to the joints creating additional friction strength and increasing its aggregate interlocking strength. Reinforcing bars also provide ductility to the contraction joints and improve the behaviour when subjected to repeated loading. However, typical joints used in the construction of concrete gravity dams are unreinforced. Another difficulty with the data available in the literature is that the conditions of concrete in-situ especially for the older dams can be different from laboratory testing under controlled conditions. For these reasons among others an upper and lower bound approach is suggested. The upper and lower bounds of shear stress-shear strain relationship are shown in figure (5-3). In this chapter other relationships will be discussed and can be used for different types of joints. However, it is up to the designer to chose the specific relations which produce acceptable results for the specific case under consideration.

Shear carrying capacity of vertical joints depends on many factors, such as the shape of joint, area of shear keys, characteristic strength of in-situ grouting (if any) and other technological factors such as shrinkage and creep. From the experimentally obtained values of shear stiffness, it is observed that the area of shear keys in a joint does not have any significant effect as a parameter, although its influence in determining the shear capacity of such joints cannot be ignored. Shear stiffness of a joint is found to be dependent mainly on the strength of the joint concrete, reinforcement percent (if any) and the level of slip deformation (Chakrabati et al, 1985). Shear forces are transferred through joints in three forms; cohesion, friction and aggregate interlock.

5.3.1 Cohesion

Shear is transferred by the bond between the old surface and the new surface of concrete. For monolithic concrete, the cohesion factor is found to be 0.2 f_c, e.g. 20% of the concrete compressive strength. A reduction of 60% in cohesion compared with monolithic concrete was obtained. In their experimental study on smooth construction joints under shear and axial load, Clark and Gill (1985) used modified Coulomb failure criteria to write a formula for the shear strength. The only parameter which was found to have any significant statistical correlation with c/f_{cu} was the age of the first half of the joint when the second half was cast. They introduced the following formula to be used for the calculations of the concrete cohesion at the contraction joints:

$$C_c = .06\, f_c \tag{5-1}$$

where,

C_c is the shear strength due to cohesion

f_c is the compressive strength of concrete

5.3.2 Friction

Shear transmitted by friction is a function of the normal stresses as well as the angle of friction of the joint:

$$\tau = \sigma \tan\phi \tag{5-2}$$

where,

τ is the shear strength due to friction

σ is the normal stress on the contact surface

ϕ is the angle of internal friction

An angle of friction of 37° was suggested by Clark et Gill (1985). For smooth contraction joints, based on the assumption of no axial forces transferred through the joint, friction will have negligible effect. For keyed joints, friction exists in some parts of the keys as such will be discussed in the following section.

5.3.3 Aggregate Interlock

Consideration of two rough interlocking faces along a crack in the general shear plan indicates that shear displacement much larger than those to be encountered along initially uncracked interfaces will now be required to effectively engage aggregate particles protruding across the shear plane. The larger the crack width, w, the larger the shear displacement, delta, and the smaller the attainable ultimate strength. It is also evident that as the shear displacement increases, the concrete masses on either side of the crack will be pushed apart; hence the crack width will tend to increase. Unless the tendency of the crack width to increase is controlled by an effective clamping or restraining force, very little shear can be transmitted. In gravity dams, this clamping force is provided by the weight of the monoliths. The design for interface shear transfer can be based on traditional concepts of friction. For large shear stresses the concrete in the interlock mechanism can be expected to break down. The upper limit by ACI code is 0.2 f'_c or 5.5 N/mm^2 to guard against a concrete failure. After the development of cracks, repeated loading will cause deterioration of the interface roughness, with a corresponding reduction in the equivalent coefficient of friction. To determine the relationship between shear transfer by interlocking of aggregates and the associated shear displacement, other factors need to be identified. One of these factors is the available contact area against which aggregate particles projecting across the crack may bear. The larger this area is the greater will be the force likely to be transmitted for the same displacement. This contact area increases if the crack width is reduced or the shear displacements increased and/or a larger proportion of coarse aggregate is present.

5.4 SHEAR STRENGTH AND STIFFNESS OF JOINTS

In this study, it is assumed that only shear stresses are transferred across contraction joints. Due to the existence of cracks in these joints, tension stresses cannot be transmitted. Compression stresses may or may not exist depending on many parameters. However, its effect on the analysis is neglected to simplify the problem to that of shear transfer only. This simplification is on the conservative side as compression stresses, if exist, will generally add to the shear strength of the joint. In the elastic range, the rigidity of the three types of joints is the same. The shear carrying capacity of the three types of joints depends on many factors, such as shape of joint, area of shear keys, characteristic strength of in-situ concrete, percent of transverse reinforcement in the joint and other factors like shrinkage and creep.

The purpose of this part is to extend the formula suggested by Clark and Gill (1985) to evaluate the shear strength of keyed joints using an analytical procedure. In this study the geometry and number of keys are considered. The simplified proposed formula is evaluated by assuming a failure mechanism and calculating the force required to cause the failure. Two cases of keyed joints are considered; i) no cohesion between the adjacent monoliths which may result from using ungrouted joint or as a result of grouting which was precracked before loading. In this case, it is considered appropriate to neglect the shear strength due to cohesion and friction, i.e. only the interlocking shear will be considered. ii) Grouted uncracked joint in which the shear forces are resisted by the three mechanisms; cohesion, friction and interlocking.

i) Ungrouted or precracked joints

Figure (5-4) shows two adjacent monoliths, A and B, separated by a keyed contraction joint. The total shear force to be transferred across the surface (1-6) is F. As the surface is precracked, or ungrouted, the force can only be transferred along surface (2-3). The maximum force F_1 which can be transferred along surface (2-3) is controlled by the bearing strength of concrete. The shear force F_2 along surface (2-5) is limited by the monolithic shear strength of surface (2-5).

$$F_1 = a \cot\alpha \, f_b \tag{5-3}$$

$$F_2 = .17\ (2a+b)\ f_c \tag{5-4}$$

where, f_b and f_c are the bearing and compression strength of concrete respectively. a and b are the dimensions of keys and α is their slope angle. These formulas are based on the coulomb failure criteria. Using these formulas the maximum shear carrying capacity of each joint can be estimated. The maximum force which can be transferred is the minimum of F_1 and F_2 which consequently, depends on the geometry of shear keys. For most geometries F_2 controls the failure mechanism. The previous formula is based on the assumption of one key per unit length of the monolith width. For n keys per unit length, the shear capacity of the joint is multiplied by n. It should be mentioned that for ungrouted joints the effect of impact can be included as an impact factor of 1.2. The stiffness of these joints can be evaluated using the results presented by Park and Paulay (1975) as shown in figure (5-5). It is noted that shear stiffness is a function of the crack width, or gap width, which should be estimated before carrying out the analysis. The maximum capacity of the joint is almost the same regardless of the crack width as long as the clamping force keeps the crack width to a constant value.

ii) Grouted or no gap joints: This type of joints are created in two ways either by grouting the space between the adjacent monoliths or if the second monolith was cast against the first monolith without a space. The shear strength in this case is expected to be higher as the effect of cohesion and friction are included. Figure (5-6) shows shear transfer mechanism between two adjacent monoliths A and B. The joint shear strength, in this case, is expected to be higher as the effect of cohesion and friction are included. The total shear force which can be resisted by this type of joint, F, is transferred along surface (1-6). Along surfaces (1-2), (3-4) and (5-6), the shear forces are transferred through the interface by cohesion. Another form of shear transfer is keys interlock along surface (2-3) and monolithic cohesion along surface (2-5). The following formula define the shear force transferred along each surface.

$$F_1 = a \cot\alpha \, f_b \tag{5-5}$$

$$F_2 = .17 \, (2a+b) \, f_c \tag{5-6}$$

$$F_3 = .06 \, (L-2a-b) \, f_c \tag{5-7}$$

$$F_4 = .06 \, b \, f_c \tag{5-8}$$

Because these forces result from different types of shear and because each type requires different slip to transfer shear, it does not add to each other. Forces F_3 and F_4 are cohesion forces, which require small shear slip compared to interlocking shear, this resisting shear forces at the early stage. When shear slip increases, these sections are expected to fail before section (2-3) start to resist shear by interlocking. Shear stiffness is governed by shear interlocking and is estimated using the formula obtained from experimental results (Chakrabati et al, 1985):

$$K = 2.40 \, f_c^{0.68} - 0.06 \, f_c^{1.66} \, s - 250 \, s + 15 \tag{5-10}$$

where, s is the shear slip (cm) and K is the shear stiffness (kg/cm^2).

For both types of joints, factors as quality deterioration and erosion will affect the shear strength of concrete. This effect can be included in these formula through the value of the compression strength of concrete.

5.5 JOINT EFFECT ON THE OVERALL BEHAVIOUR

As shown in the previous sections, different types of contraction joints can have different behaviour and as a result its effect on the overall behaviour of the structure is expected to vary. Contraction joints with different characteristics are used in the analysis of the two structures described in the previous chapter; one with rectangular section and the other with triangular section. Its stiffness is included in the formation of the stiffness matrix of the structure as discussed in chapter 3.

Four types of joints are used for comparison; joint A with keyed uncracked joint, joint B is keyed joint with crack width= 0.13 mm, C is keyed joint with crack width = 0.62 mm and D is a smooth joint. The shear capacity of the smooth joint is very small and as a result it is neglected. The stiffness and shear capacity of keyed joints are evaluated using figure (5-5) and equations (5-3) and (5-4). Table (5-1) shows the natural frequencies of the structure with rectangular section and uniform profile. Table (5-2) shows the natural frequencies of the structure with rectangular section and nonuniform profile. Table (5-3) shows the natural frequencies of the structure with triangular section and nonuniform profile. It is noted that as the crack width increases, the effect of monoliths interaction on the natural frequencies decreases. For smooth joints, the natural frequencies estimated in these tables are the same as those calculated using typical two dimensional analysis. Figure (5-7) shows the maximum displacement of the structure calculated for different types of joints ranging from zero stiffness (to represent smooth joints) to very high stiffness (representing rigid joints). It is noted that as the rigidity of the joint decreases the maximum displacement of the critical monolith increases. Figure (5-8) shows the vertical envelop of maximum horizontal displacement for the critical monolith of the structure with nonuniform profile. Figure (5-9) shows the maximum principal stresses of the structure calculated for different types of joints ranging from zero stiffness to infinite stiffness. It is noted that the response of the dam increases as the crack width in the keyed joints increases until it reaches maximum value for the smooth joints. For structures with uniform profile, the variation in the joint stiffness affects the higher modes of vibration especially those representing the third dimension of the structure. However, the response of the dam is not affected and a typical two dimensional analysis would give the same results.

5.6 SUMMARY

In this chapter, different types of contraction joints have been evaluated. The shear strength of each joint as well as the shear stiffness were estimated for each type based on the available experimental results in the literature as well as by postulating different failure mechanisms. Due to the wide variation of parameters in construction joints, a bound principle, which uses the experience of the designer is also suggested. It was noted that smooth joints usually have a small capacity in resisting shear forces among the monoliths and as a result each monolith will tend to vibrate independently from the adjacent ones. This type of behaviour usually results in higher displacements and stresses in the critical monolith. Also water seepage through the failed joint is another reason to abandon this type of joints. On the other hand, keyed joints were shown to have higher strength in resisting shear stresses. The stiffness of the joint depends on the width of the crack or the gap left between monoliths. It is concluded that when keyed joints are introduced in the construction of gravity dams, the effect of monoliths interaction is significant and affects the behaviour of the dam. The results obtained in this chapter are necessary to complete the analysis procedure developed in chapters 3 and 4 for including monoliths interaction.

Table (5-1) Natural Frequencies (rad/s) of the Structure with Rectangular Section (Uniform Profile)

Mode	Joint Type			
	A	B	C	D
1	19.08	19.08	19.08	19.08
2	20.92	20.48	19.56	19.18
3	25.28	23.93	20.86	19.45
4	30.38	28.16	22.68	19.87
5	35.19	32.29	24.66	20.36

Table (5-2) Natural Frequencies (rad/s) of the Structure with Rectangular Section (Nonuniform Profile)

Mode	Joint Type			
	A	B	C	D
1	28.79	24.07	22.19	20.25
2	29.82	31.29	27.26	24.00
3	32.51	35.55	29.34	24.22
4	36.15	39.81	33.24	28.80
5	39.93	41.73	33.48	28.82

A is keyed joint without cracks
B is keyed joint with crack width = .13
C is keyed joint with crack width = .62
D is smooth joint

Table (5-3) Natural Frequencies (rad/s) of the Structure with Triangular Section
(Nonuniform Profile)

Mode	Joint Type			
	A	B	C	D
1	33.18	32.78	31.39	29.77
2	41.26	40.08	36.41	33.46
3	45.17	43.63	38.44	33.65
4	48.98	47.14	41.05	37.75
5	51.39	49.34	41.45	37.77

A is keyed joint without cracks
B is keyed joint with crack width = .13
C is keyed joint with crack width = .62
D is smooth joint

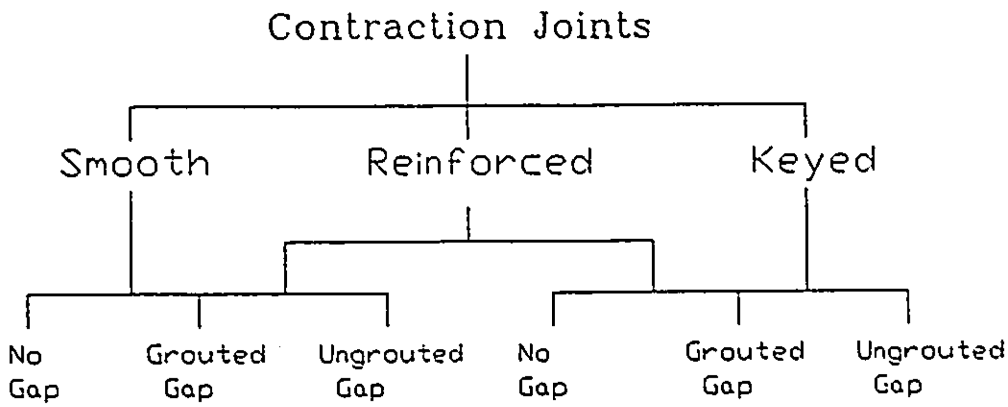

Figure (5-1) Classification of Contraction Joints

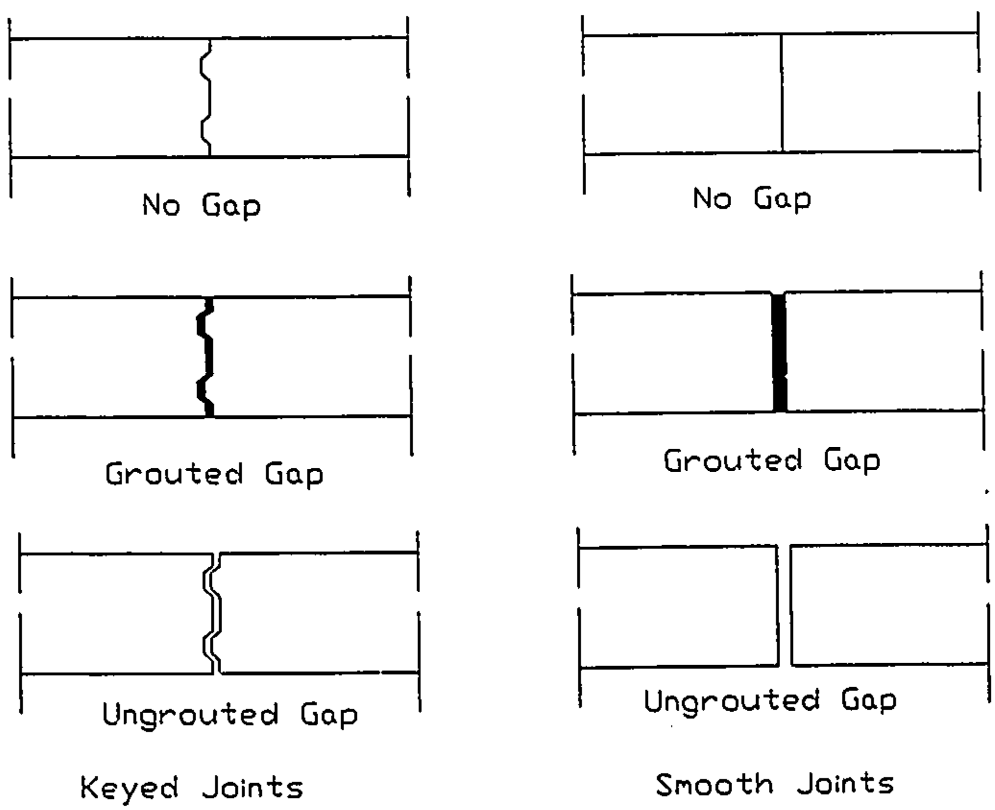

Figure (5-2) Different Types of Contraction Joints

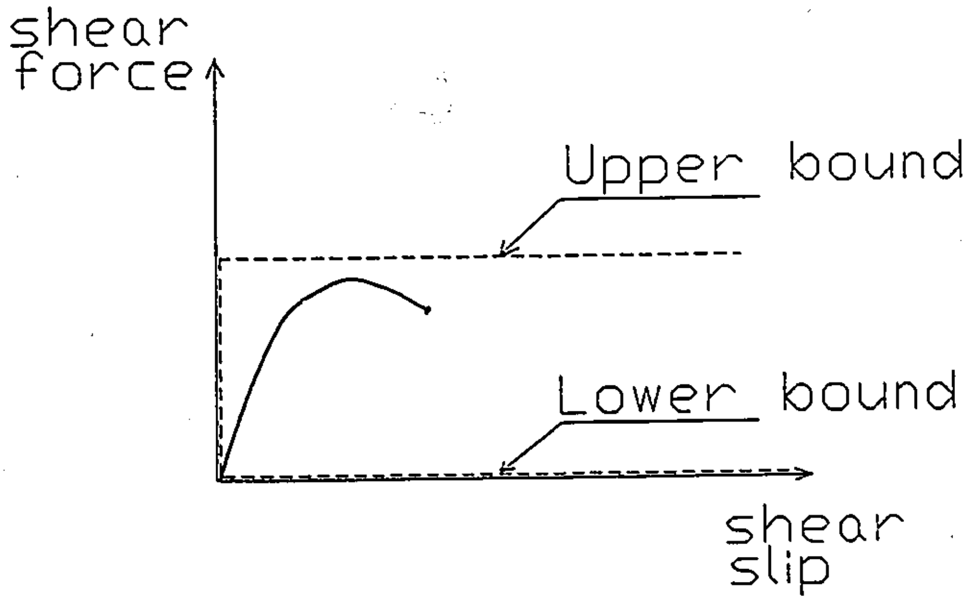

Figure (5-3) Upper and Lower Bounds of Shear Strength

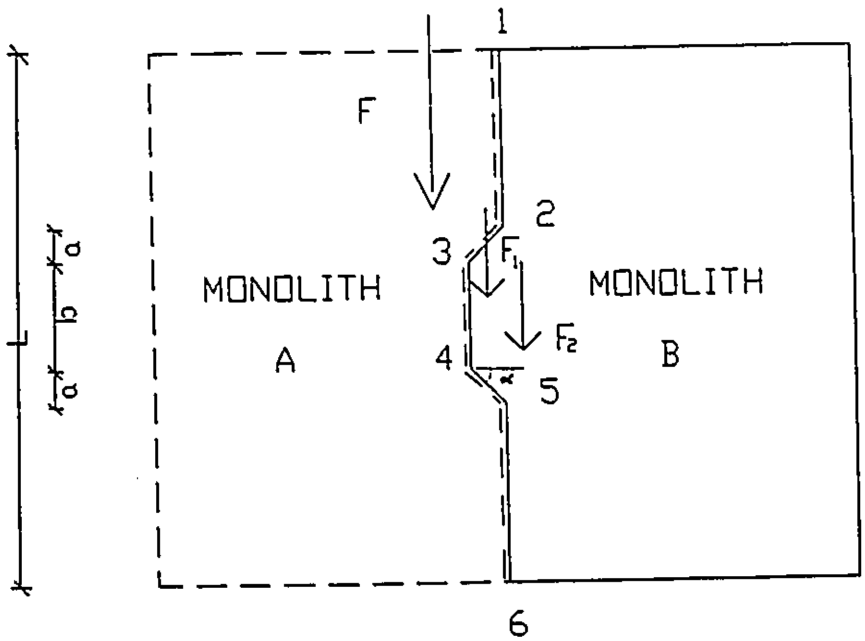

Figure (5-4) Shear Transfer Mechanism in Cracked Joints

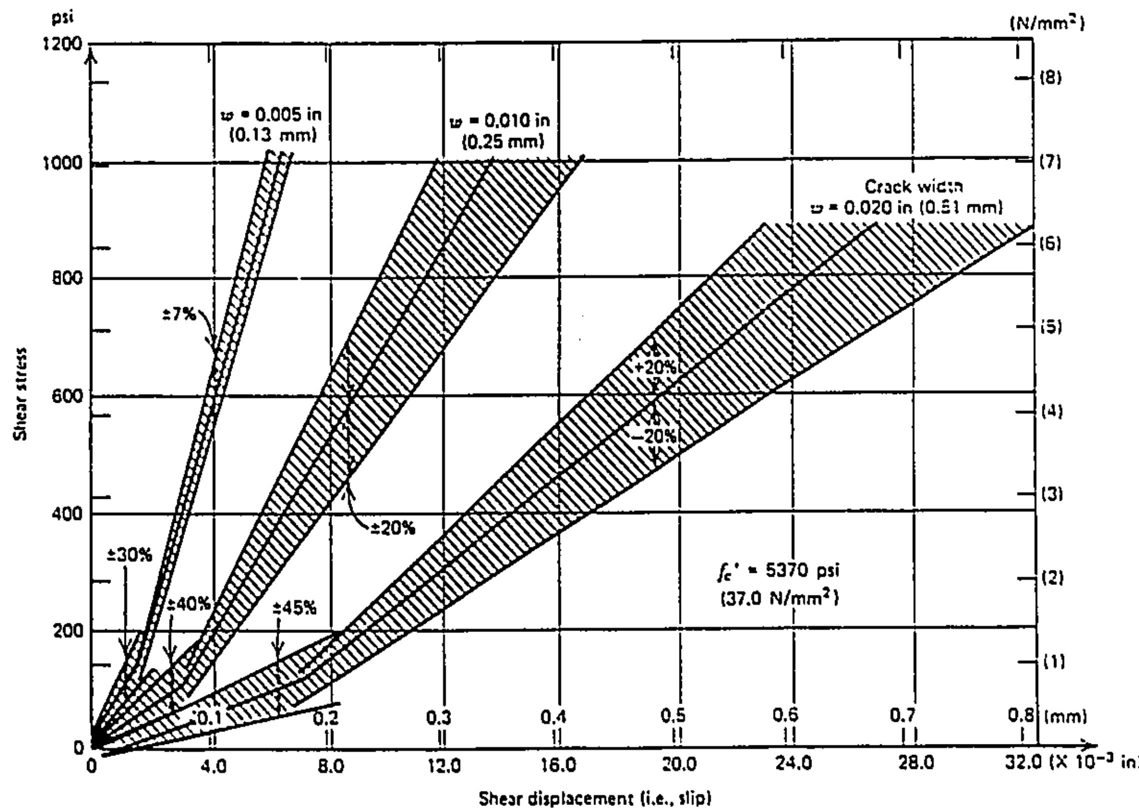

Figure (5-5) Typical Mean Shear Stress-Shear slip relationships for Aggregate Interlock Mechanism (Park and Paulay, 1975)

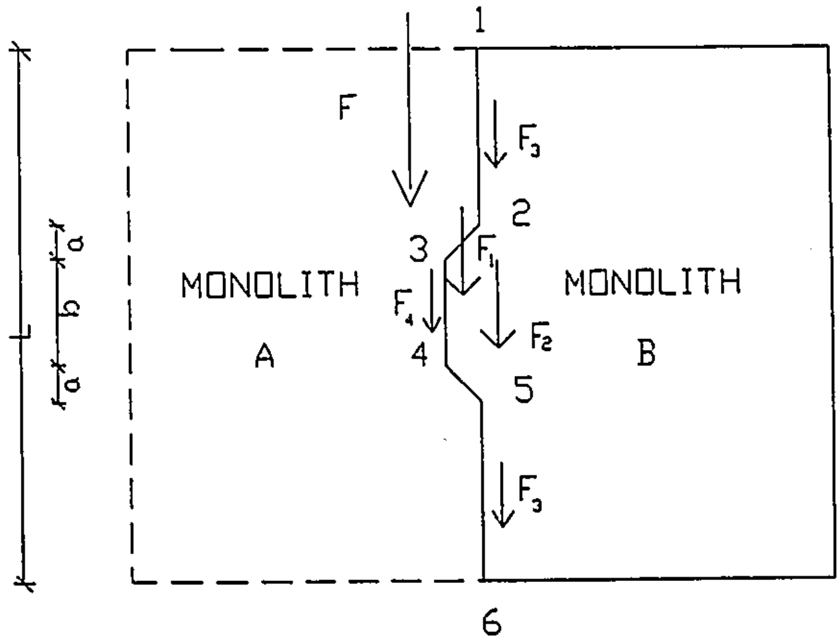

Figure (5-6) Shear Transfer Mechanism in Uncracked Joints

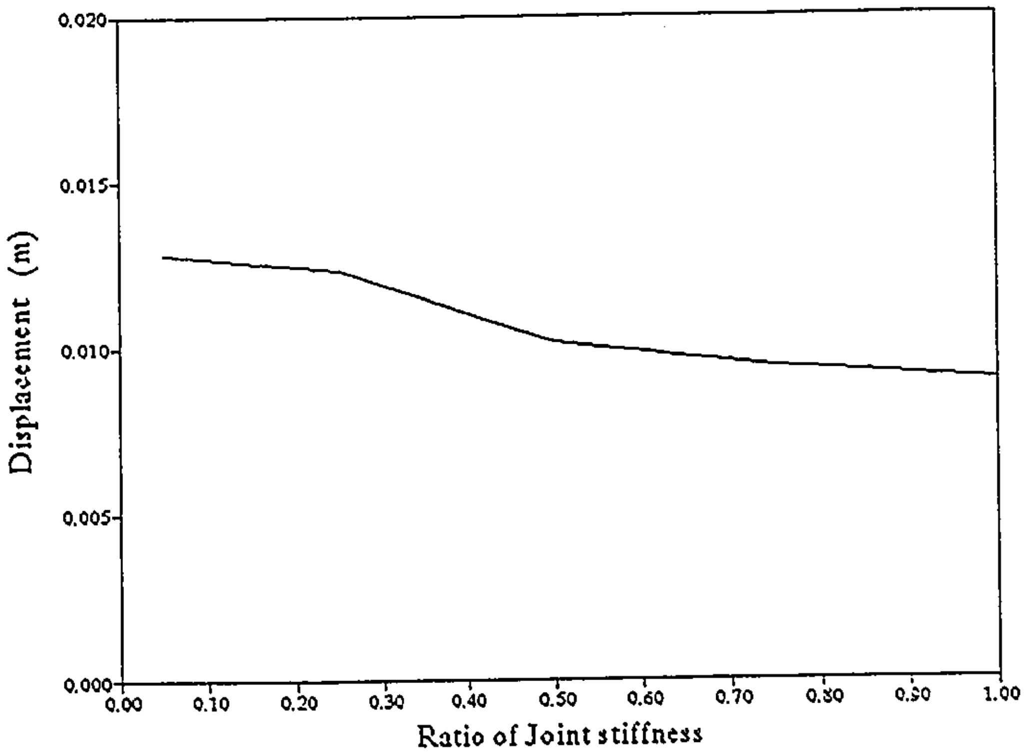

Figure (5-7) Crest Displacement of the Model Structure
with Different Joint Stiffness

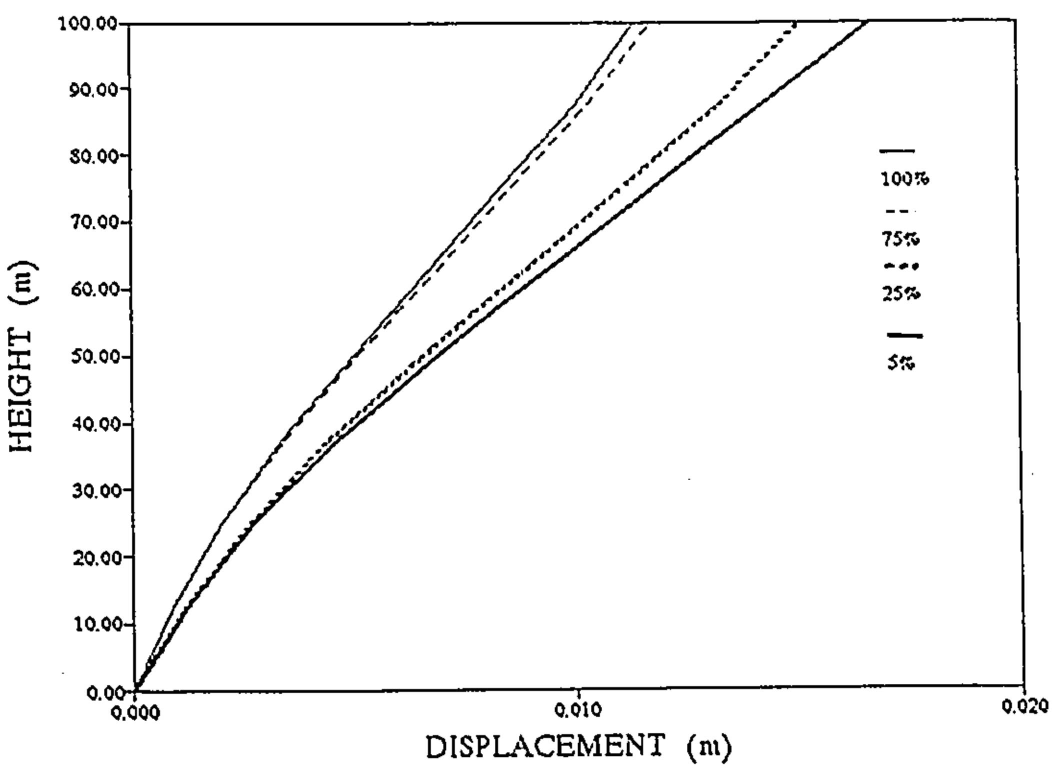

Figure (5-8) Displacement Profile of the Critical Monolith with Different Joint Stiffness

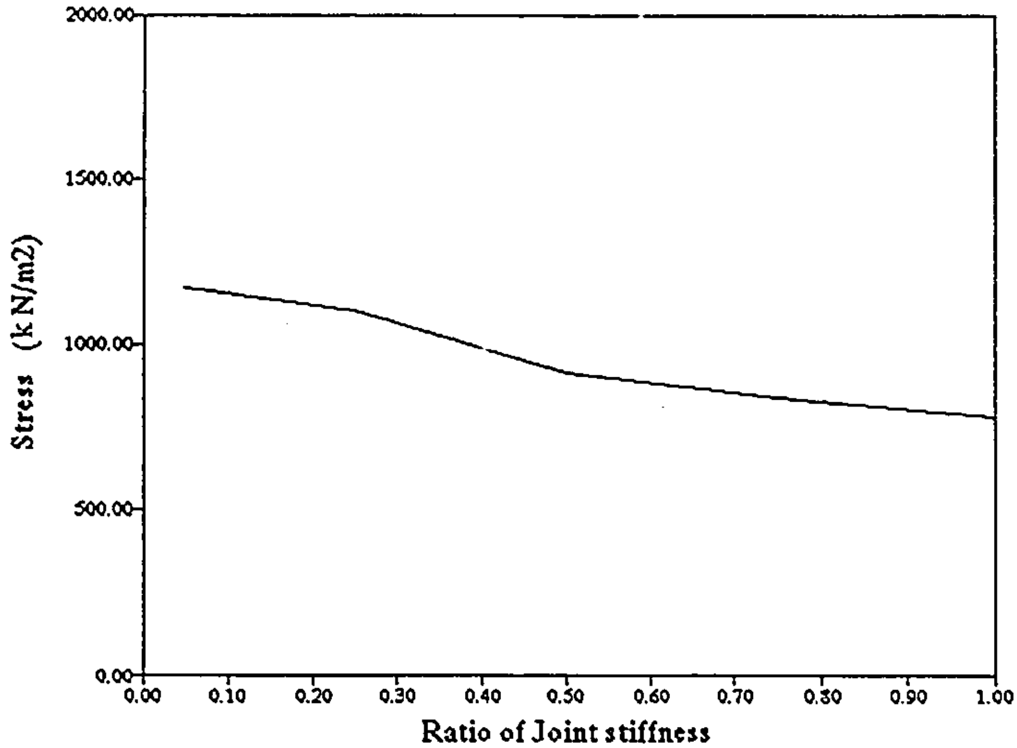

Figure (5-9) Maximum Stresses within the Model Structure
with Different Joint Stiffness

CHAPTER 6

INFLUENCE OF THE LONGITUDINAL PROFILE ON THE RESPONSE OF CONCRETE GRAVITY DAMS

6.1 GENERAL

The effect of monoliths interaction on the overall response of concrete gravity dams have been shown to be important. In, chapter 5, it was demonstrated that the behaviour of contraction joints is a significant factor in this interaction. In cases of strong interaction, the response of a monolith is also affected by the longitudinal profile of the dam. The longitudinal profile is described by the profile of the canyon cross-section, the end conditions of the dam at the two sides of the canyon and the existence of overflow monoliths with the nonoverflow monoliths. In a typical two dimensional analysis of gravity dams, these parameters have no effect on the overall response as the monoliths interaction is neglected. As a result, these parameters have not been studied in the literature except for a very few cases which tackled these parameters in an indirect fashion (Rashed and Iwan, 1984).

In this chapter, each of these parameters is studied separately to obtain its effect on the response of gravity dams. The results obtained were analyzed and some conclusions have been reached. It was shown that including the effect of monoliths interaction usually increases the natural frequencies of the dam. The response to the Taft ground motion which is used through this study is studied. However, the results obtained using other earthquake records may be different. The response of a structure depends on both the dynamic characteristics of both the structure and the exciting ground motion. Different earthquake records are used in calculating the response of the dam. Figure (6-1) shows a sketch of the factors affecting the response of the dam.

6.2 CANYON CROSS-SECTION

Natural canyon cross-section may have different shapes depending on the location of the dam. The designer has little control on this parameter as it is one of several factors in selecting sites for gravity dams. Figure (6-2) shows three different longitudinal profiles of existing concrete gravity dams. The profiles shown are for: Pine Flat Dam, in california, Blackbrook dam, in England, and Hsinfengkiang dam, in China. The canyon usually has the greatest depth near the middle and decreases towards the ends. To mathematically model the exact shape of the canyon is a complicated issue and is usually not required. Three parameters are suggested to describe the shape of the canyon; width, maximum depth at the middle and the depth at the two ends. For simplicity the shape shown in figure (6-3) is used in the analysis.

The effect of canyon cross-section is examined by analyzing two different cross sections of the monolith; rectangular and triangular, as shown in figure (6-3). The rectangular section will be referred to as structure A and the triangular section is referred to as structure B. Two ratios are considered to control the effect of canyon cross-section: the ratio of the monolith depth at the end (h) to the that at the critical monolith (H) and the ratio of the crest length (B) to the critical depth of the dam (H). The case of full reservoir, flexible foundation as well as keyed contraction joints stiff enough to transfer shear forces among monoliths is analyzed. The material properties for concrete, water and foundation used in the present analysis are the same as given in table (4-2).

6.2.1 (h/H) Ratio:

Four h/H ratios are considered, 0.75, 0.5, 0.25 and 0.05 . Table (6-1) shows the natural frequencies of a dam of rectangular section, structure A, for different longitudinal profiles. As the (h/H) ratio decreases, the natural frequencies of the structure increases gradually to reach its maximum at very small end height. This is predictable as the decrease in the (h/H) ratio translates into a steeper slope for the longitudinal profile which consequently increases the effects of monoliths interaction. In this particular case, the increase in the fundamental frequency from uniform profile to the case with the most steep profile reached 65%. Table (6-2) shows the natural frequencies of the dam with triangular cross-section, structure B, for different longitudinal profiles. The same observation can be made as the decrease in the (h/H) ratio caused an increase in the natural frequencies of the structure. However, the percentage of increase in this case, 27%, is smaller than that for the rectangular section. This can be explained since the width to height ratio in triangular sections, for typical gravity dams cross-section, is kept constant for all the monoliths while for rectangular sections, as used by Rashed and Iwan, the width is kept constant for all monoliths regardless of the height. As a result, for the case of rectangular sections, monoliths at the ends are stiffer than triangular section for the same h/H ratio. For this reason, its contribution to the natural frequencies of the structure are more significant. It is noted that as the ratio of the height at the end / the maximum height (h/H) decreases the effect of monoliths interaction increases. When the height at the ends reaches its maximum, the longitudinal profile of the dam becomes uniform with constant depth and the effect of monoliths interaction vanishes. On the other hand, it is noted that for small ratios of h/H, the natural frequencies of the structure tends to increase leading to a more stiff structure.

Figure (6-5) shows the envelope of maximum displacement for the dam with rectangular cross section and different longitudinal profiles. The time history of crest displacement at the critical monolith of a dam with h/H ratio of 0.75 and 0.05 are shown in figure (6-6). The response of the dam decreases as the ratio of (h/H) decreases. A reduction of 37% was obtained in the maximum displacement at the dam crest when the (h/H) ratio was decreased from 0.75 to 0.25. The percentage of reduction in the dam response depends on other factor such as the exact profile of the canyon and the dynamic properties of the exciting ground motion. The same general trend of reduction in the dam response with decreasing h/H ratio is obtained for dams with typical triangular sections. The envelope of maximum displacement for the dam with triangular cross section and different longitudinal profiles is shown in figure (6-7). Figure (6-8) shows the displacement time history of the critical monolith's crest for a dam with end depth / maximum depth (h/H) ratio of 0.75 and 0.05 . In the case of steep canyon slopes, the lateral load on the dam is distributed in both the horizontal and vertical directions instead of being carried in the vertical direction only as the case in uniform longitudinal profile.

6.2.2 (L/H) Ratio:

The dam length / maximum height (L/H) ratio is another measure of the canyon cross-section. Dams with high (L/H) ratio usually are categorized in the uniform longitudinal profile category, as the effect of the (h/H) ratio is reduced. one of the examples of such a case is Aswan Dam, Egypt, which has a maximum height of 40 m and a length of about 1000 m. However, for smaller values of (L/H) ratio, it is expected that both (h/H) ratio and the type of end conditions will have a more significant effect on the response. Four values of the (L/H) ratio are considered in this section; 2,3,4 and 5. In all cases, the h/H ratio is taken as 0.5 and the end conditions are considered to be free. The height of the critical monolith (H) is kept constant at 100 m while the length of the structure was assigned different values of 200, 300, 400 and 500 m to give the L/H ratios of 2,3,4 and 5. The natural frequencies of the dam with rectangular cross-section for different longitudinal profiles are listed in table (6-3). As the (L/H) ratio increases from 2 to 5, the frequencies are reduced by about 44%. In this type of analysis, the lateral load resulting from earthquake ground motion is distributed in two directions; vertical and longitudinal along the length of the dam. Decreasing the (L/H) ratio leads to a reduction in the lateral path of transferring the load which leads to a stiffer support for the structure. Table (6-4) shows the natural frequencies of the dam with triangular section for different (L/H) ratios. A reduction of 41 % in the values of the frequencies is obtained when the (L/H) ratio is increased from 2 to 5.

Figure (6-9) shows the time history of the crest displacement of the critical monolith. The maximum displacement at the critical monolith crest for structures with rectangular section and different values of (L/H) are plotted in figure (6-10). Figure (6-11) and (6-12) show the same relationship for the structure with triangular section. The increase in the (L/H) ratio is associated with an increase in the crest displacement of the structure. For high values of L/H, the response of the structure obtained by including or excluding monoliths interaction are almost the same. However, the response differs as the (L/H) ratio decreases. From the response analysis presented, it can be observed that the influence of the (L/H) ratio is dependent on two other parameters; namely h/H ratio and the end conditions. Also, increasing (L/H) leads to increasing the maximum stresses within the dam as a direct result of carrying the load in a single direction. However, the stresses near the dam crest decrease slightly as a result of the elimination of the lateral support of the critical monolith.

6.3 End conditions

The effect of the dam boundary conditions at the canyon sides on the response are evaluated. In some cases, the end monoliths may be supported by different types of earth formations. Usually the end monoliths are built or anchored to earth or rock sides at least at one side of the structure. The existence of earth or rock boundary may cause some restraints on the displacements of the end monoliths. This may cause a degree of fixation for the nodes of end monolith. Although side boundary conditions are main factors in the analysis of arch dams, this parameter has always been neglected when designing gravity dams as a direct result of using typical two dimensional analysis. The effect of end conditions is structurally modeled in this analysis by fixing the vertical and horizontal displacement of end monoliths.

The results presented so far in this chapter were calculated assuming free end conditions of the dam. In this section, the same structures were analyzed again assuming fixed end conditions. The evaluation of the effect of end conditions is dependent on the two ratios (h/H) and (L/H). Table (6-5) shows the natural frequencies of the dam with rectangular cross-section for fixed end conditions. Table (6-6) shows the natural frequencies for a triangular dam section. It is noted that as the ratio of the depth at the end to the maximum depth decreases the effect of monoliths interaction increases. When the depth at the ends reaches its maximum, the longitudinal profile of the dam becomes uniform with constant depth and the effect of monoliths interaction vanishes. On the other hand, it is noted that for small (h/H) ratios, the natural frequencies of the structure tends to increase leading to a more stiff structure.

Figure (6-13) shows the envelope of maximum displacement for the dam with rectangular cross section and different h/H ratios. Figure (6-14) shows the same relationship for a dam with triangular cross-section. It is noted that assuming fixed end conditions results in a reduction in the response of the dam. As the h/H ratio decreases, the effect of end conditions decreases as a result of the reduction in the stiffness of the end monolith. The response of the structure using different (L/H) ratios is shown in figures (6-15) and (6-16). The same trend is obtained when comparing the two figures. As the (L/H) ratio decreases, the effect of end conditions increases. However, the effect of end conditions was proved to be of less importance than the canyon cross-section.

6.4 OVERFLOW MONOLITHS

Concrete gravity dams are usually built with two types of monoliths; overflow monoliths and nonoverflow monoliths. The first type is designed to allow water spillage over it and usually has a geometry as shown in figure (6-17). The nonoverflow type is designed to retain water in the upstream reservoir. The overflow monoliths are shorter in height and has a greater width. As a result, they are stiffer than nonoverflow monoliths and offer more resistance to lateral loads. Nonoverflow monoliths have been well studied in the literature as it is more suspectable to earthquake damage than overflow monoliths. There are no references in the literature concerning the evaluation of the response of dams with overflow monoliths. This is mainly due to the typical two dimensional model assumption used in analyzing the dam. The geometry as well as the location of the overflow monoliths are the main parameters which may affect the response of the dam.

The dimensions of the cross section shown in figure (6-17) are used to represent overflow monoliths for both dams of rectangular and triangular cross sections. The natural frequencies of the structure are listed in table (6-7). Figure (6-18) shows the maximum displacement at the dam crest for the two cases; case C without overflow monoliths and case D with overflow monoliths. The crest displacements time histories of the critical monolith are plotted in figure (6-19). It is noted that the existence of overflow monoliths in dam construction leads to a stiffer structure with lower response. The overflow monoliths with its lower height and higher width forms a partial support for the critical monolith which distribute more load in the lateral direction.

6.5 FREQUENCY CONTENT OF THE GROUND MOTION

Earthquake ground motions are different in their magnitude, peak acceleration and frequency content. Although it is understood that no earthquake is repeated in the same way, it is a normal practice of structural engineers to study the behaviour of structures subjected to previously recorded earthquakes. The response of the same structure is expected to be different when subjected to two different earthquake ground motion records. As the dam response analysis in this study was carried out using a single earthquake, it is prudent to investigate the implications of using several records of different characteristics.

Different parameters are used to categorize seismic ground motion records. Among these parameters are; magnitude, peak acceleration, velocity or displacements, duration and intensity of ground motion. Another parameter which was found to be efficient and representative of the frequency content of the ground motion is the A/V ratio (the peak ground acceleration in g's to the peak ground velocity in m/s). Tso et al (1992) concluded that the A/V ratio is a reasonable parameter to indicate the dynamic characteristics of earthquake ground motions resulting from different seismic events. The A/V ratio correlates well with magnitude - distance relationship; as ground motions close to the epicentre of small or moderate earthquakes usually have high A/V ratio whereas those distant from the epicentre of large earthquakes have low A/V ratios. As a result the A/V ratio is a good measurement of the frequency content and duration of the ground motion resulting from different environment. Ground motions having high A/V ratios are usually of short duration with seismic energy in the high frequency range, whereas those with low A/V ratios usually have long duration with seismic energy in the low frequency range. It was also found that A/V ratio is a better index to represent the intensity of ground shaking at a site for building design, as compared to peak ground acceleration. As a result the earthquake records available in the literature were classified according to their A/V ratios in three categories: high, intermediate and low A/V ratios. Three records to represent each group were applied to the two cross-sections of gravity dams. Table (6-8) shows the details of these records including its location, peak acceleration, peak velocity and A/V ratio. Figure (6-20) shows the time histories of these records and figure (6-21) shows the response spectrum for 10% damping ratio. The records were normalized to have the same peak velocity of the Taft ground motion, PGV= 0.177 m/s, which was used through this study.

As monoliths interaction is expected to shift the natural frequency of gravity dams to a higher frequency, the dam response is affected by the frequency content of different ground motions. In this study, the effect of the A/V ratio of earthquake records on the overall response of concrete gravity dams is evaluated. The results obtained show that the A/V ratio has a significant effect on the response of the system. Figures (6-22) to (6-24) show the envelope of maximum horizontal displacements for the critical monolith subjected to records with high, intermediate and low A/V ratios. Part a of each figure, designated structure A, represents the results for structures with rectangular section while part b, structure B, is for structures with triangular section. It is noted that as the A/V ratio increases, the response of the structure tends to increase. High A/V ratio records, which means high frequency content, may have more damaging potential for gravity dams due to the high natural frequency characteristics of concrete gravity dams.

6.6 SUMMARY

In this chapter, different parameters which affect the behaviour of gravity dams when including monoliths interaction have been studied. These parameters are; longitudinal profile of the dam, end conditions and the existence of overflow monoliths. The longitudinal profile of the dam is shown to increase the natural frequencies of the structure leading to a stiffer structure. In most of the cases this leads to a lower response of the critical monolith in the form of displacements and principal stresses. The effect of the longitudinal profile was represented by the ratio of end depth / maximum depth of the monolith (h/H). End conditions were considered in two forms; either free or fixed. It is noted that gravity dams with fixed end conditions tend to have higher natural frequencies and lower response. The amount of reduction in the response depends mainly on the longitudinal profile of the dam. The existence of overflow monoliths is considered and its effect on the overall analysis of the dam is modeled. This type of monolith is generally much stiffer than typical nonoverflow monoliths and provides some stiffness in the longitudinal direction. As a result, including the effect of the overflow monoliths increases the natural frequencies of the structure leading to a stiffer structure. The three parameters have been shown to have a significant effect on the response of gravity dams when including monoliths interaction. Different combination of these parameters may lead to a great amplification or reduction of the response. It was also demonstrated that the response of gravity dams differ substantially with different earthquake records. As the A/V ratio, which is an indication of the frequency content of the earthquake increases, the response tends to increase. These effects are more pronounced when monoliths interaction is included in the analysis.

Table (6-1) Natural Frequencies of Dam of Rectangular Section with Different h/H (rad/s)

MODE	h/H			
	0.75	0.5	0.25	0.05
1	23.22	27.43	31.58	35.01
2	27.72	37.19	46.26	53.06
3	32.27	44.65	59.63	65.99
4	39.92	50.82	60.22	69.47
5	41.4	51.34	70.8	74.23

Table (6-2) Natural Frequencies of Dam of Triangular Section with Different h/H (rad/s)

MODE	h/H			
	0.75	0.5	0.25	0.05
1	31.6	33.18	35.67	36.79
2	34.43	41.26	42.9	44.99
3	36.39	45.17	49.21	52.18
4	39.18	48.98	55.17	58.97
5	43.49	51.39	61.02	65.72

Table (6-3) Natural Frequencies of Dam of Rectangular Section with Different L/H (rad/s)

MODE	L/H			
	5	4	3	2
1	16.49	22.28	32.46	37.41
2	22.71	30.62	42.93	48.30
3	26.72	36.79	51.58	57.59
4	29.16	38.87	58.95	66.02
5	34.89	44.56	62.28	73.11

Table (6-4) Natural Frequencies of Dam of Triangular Section with Different L/H (rad/s)

MODE	L/H			
	5	4	3	2
1	19.34	26.77	40.2	46.09
2	23.67	31.91	45.56	51.29
3	26.98	35.72	50.02	55.6
4	31.33	38.95	53.99	59.47
5	36.61	42.89	57.34	62.91

Table (6-5) Natural Frequencies of Dam of Rectangular Section with Fixed End Conditions (rad/s)

MODE	L/H		h/H	
	5	2	0.75	0.05
1	17.71	40.41	25.70	35.01
2	26.74	50.31	33.24	53.06
3	30.21	59.43	43.43	65.99
4	34.90	69.40	44.50	69.47
5	42.10	75.12	55.16	74.23

Table (6-6) Natural Frequencies of Dam of Triangular Section
with Fixed End Conditions (rad/s)

MODE	L/H		h/H	
	5	2	0.75	0.05
1	19.44	48.79	33.64	36.79
2	24.82	53.29	38.03	44.99
3	30.49	57.67	40.51	52.18
4	36.69	61.52	45.19	58.97
5	37.20	65.33	54.18	65.72

Table (6-7) Natural Frequencies of Dams with Overflow Monoliths (rad/s)

MODE	Triangular Section		Rectangular Section	
	With Ov	Without	With Ov	Without
1	34.96	33.18	25.89	24.64
2	38.41	41.25	28.26	32.53
3	41.96	45.17	35.53	37.29
4	46.81	48.98	37.16	41.89
5	47.53	51.39	42.48	44.51

Table (6-8) Description and Data for Earthquake Records Used in the Analysis

Rec. No.	Earthquake	Date	Magn.	Site	Epic. Dist. (km)	Comp.	Max. Acc. A(g)	Max Vel. V(m/s)	A/V	Soil Cond.
H1	Parkfield California	June 27 1966	5.6	Temblor No. 2	7	N65W	.269	.145	1.86	Rock
H2	San Francisco California	Mar. 22 1957	5.25	Golden Gate Park	11	S80E	.105	.046	2.28	Rock
H3	Nahanni N.W.T., candada	Dec. 23, 1985	6.9	Site 1, Iverson	7.5	Long	1.11	.462	2.38	Rock
N1	Kern Kounty California	Jult 21 1952	7.6	Taft Linclon School Tunnel	56	S69E	.179	.177	1.01	Rock
N2	San Fernando California	Feb. 9 1971	6.4	Griffith Park Observatory, L.A.	31	S00W	.180	.205	.88	Rock
N3	Mexico Earthq.	Sept. 19 1985	8.1	La Villita, Guerrero Array	44	N90E	.123	.105	1.17	Rock
L1	Long Beach California	Mar. 10 1933	6.3	Subway Terminal, L.A.	59	N51W	.097	.237	.41	Rock
L2	San Fernando California	Feb. 9 1971	6.4	445 Figueroa St., L.A.	41	S38W	.119	.173	.69	Rock
L3	Mexico Earthq.	Sept. 19 1985	8.1	Mesa Vibradora C.U., Mexico	379	N90W	.040	.110	.36	Rock

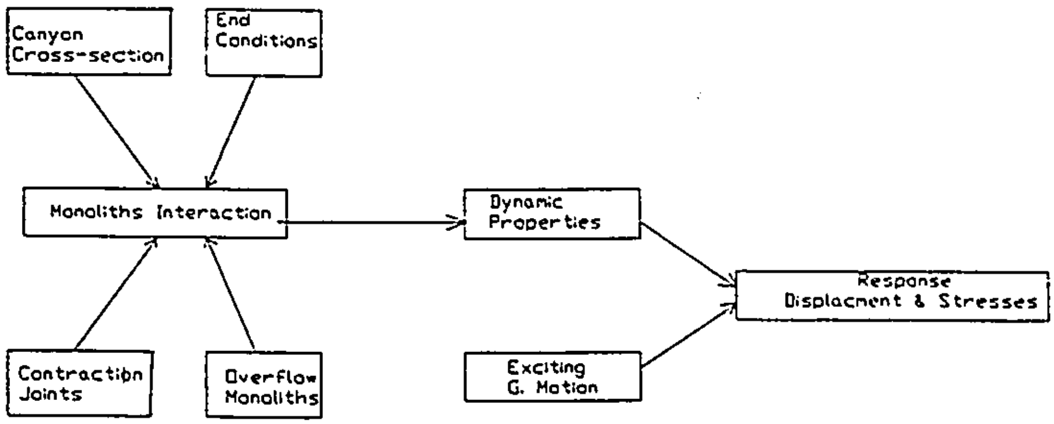

Figure (6-1) Factors Affecting Response of Gravity Dams Including Monoliths Interaction

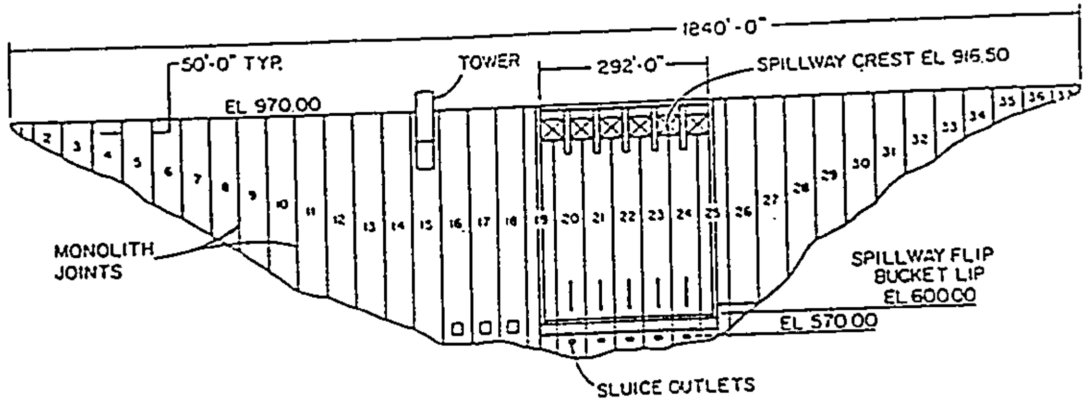

Pine Flat Dam, California
(Chopra et al, 1980)

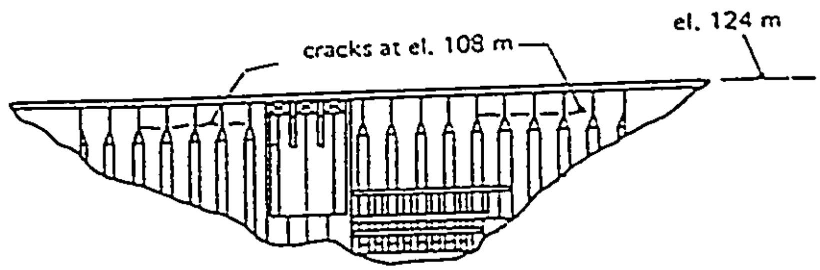

Blackbrook Dam in England
(Hansen and Roehm, 1979)

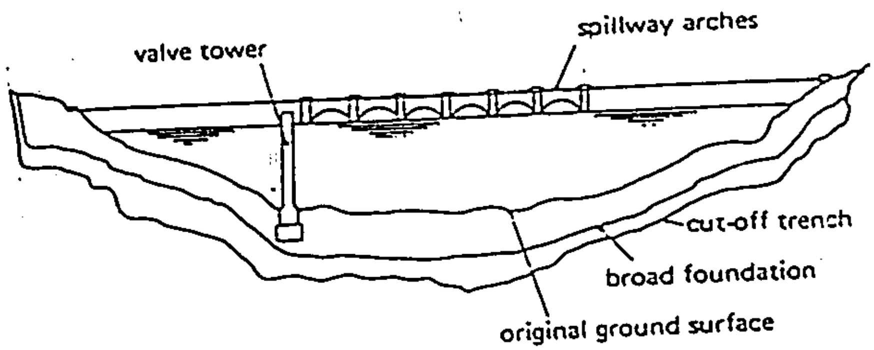

Hsinfengkiang Dam in China
(Hansen and Roehm, 1979)

Figure (6-2) Examples of Longitudinal Profiles of Concrete Gravity Dams

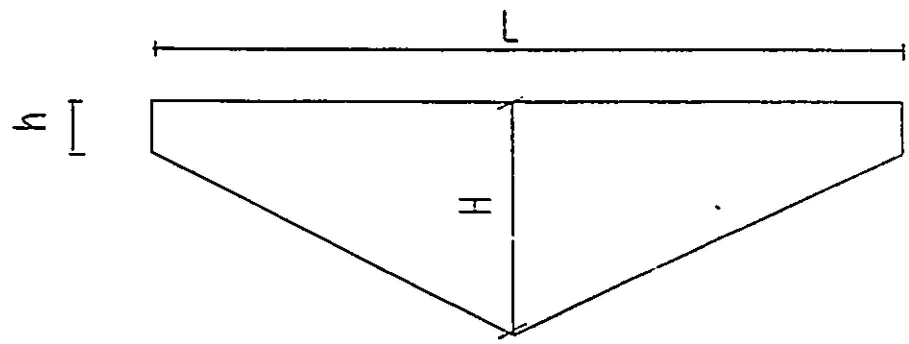

Figure (6-3) Longitudinal Profile Modelling of Gravity Dams

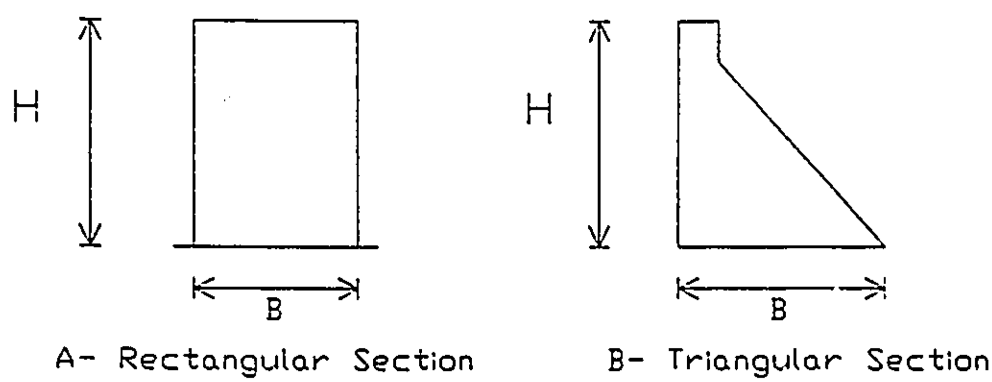

Figure (6-4) Cross-Section of Structure Cases A and B

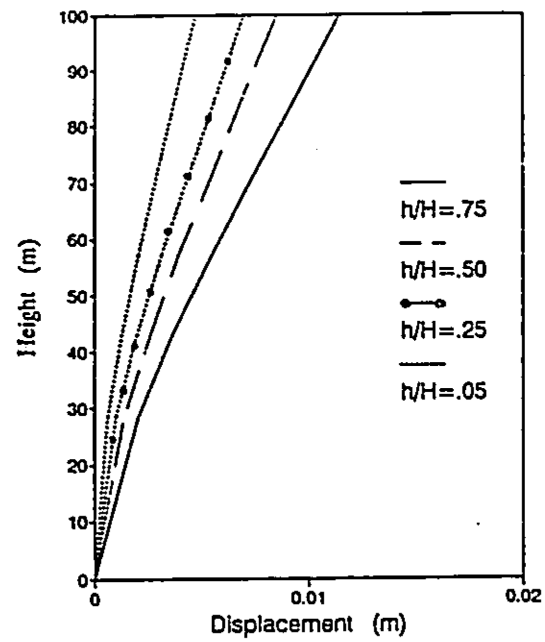

Figure (6-5) Envelope of Maximum Displacement for Structure A with different h/H ratios

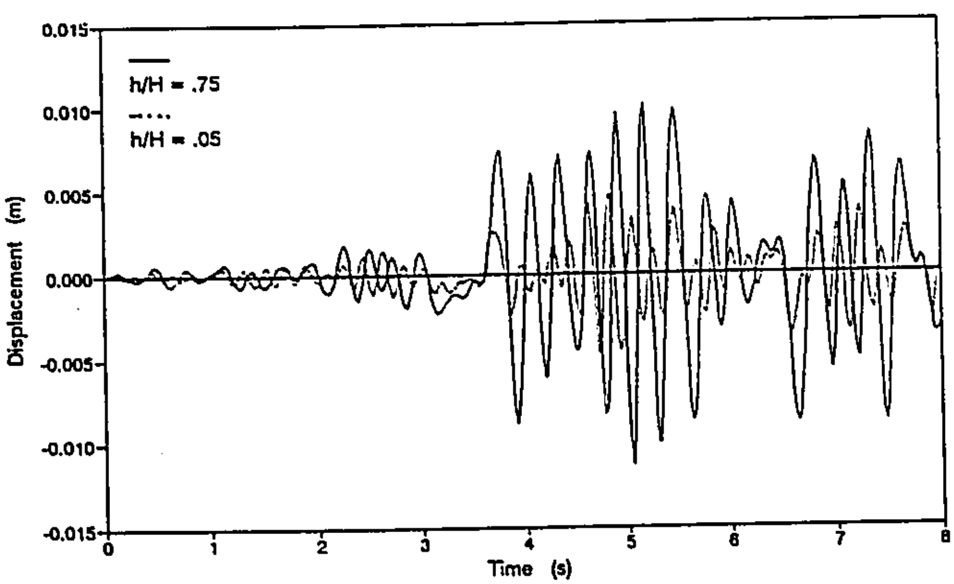

Figure (6-6) Crest Displacement Time Histories for Structure A with Different h/H ratios

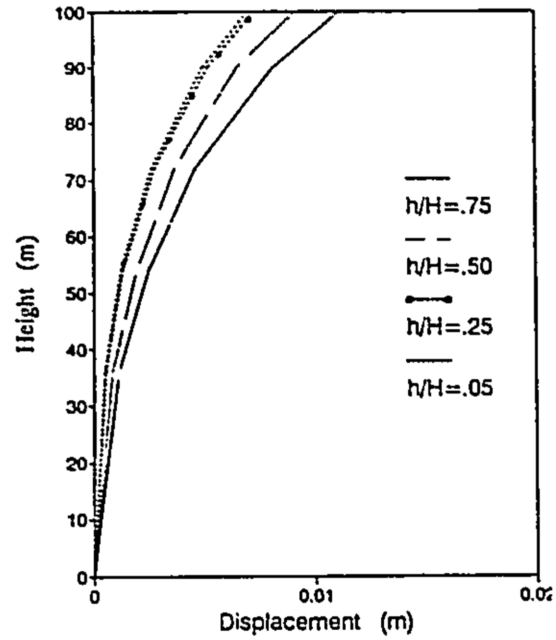

Figure (6-7) Envelope of Maximum Displacement for Structure B with Different h/H ratios

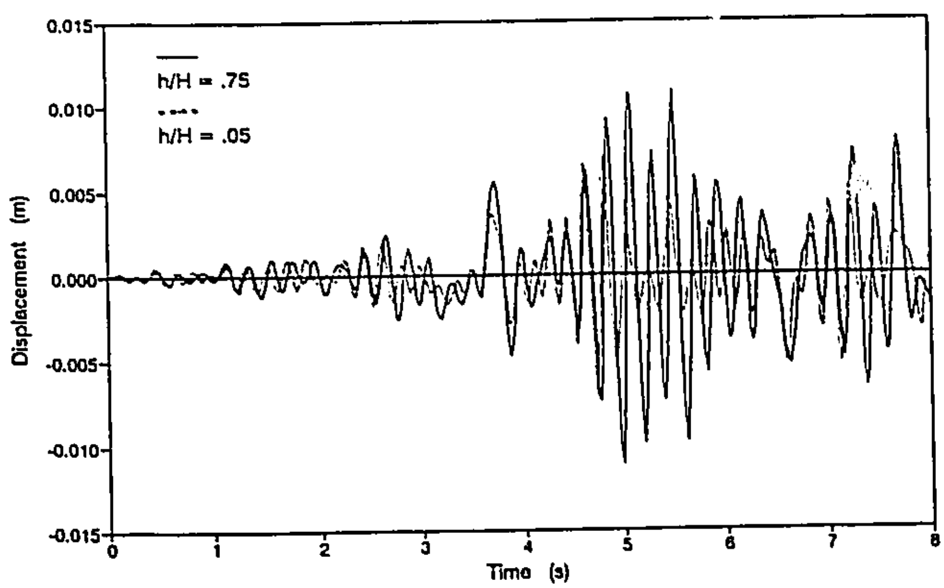

Figure (6-8) Crest Displacement Time Histories for Structure B with Different h/H ratios

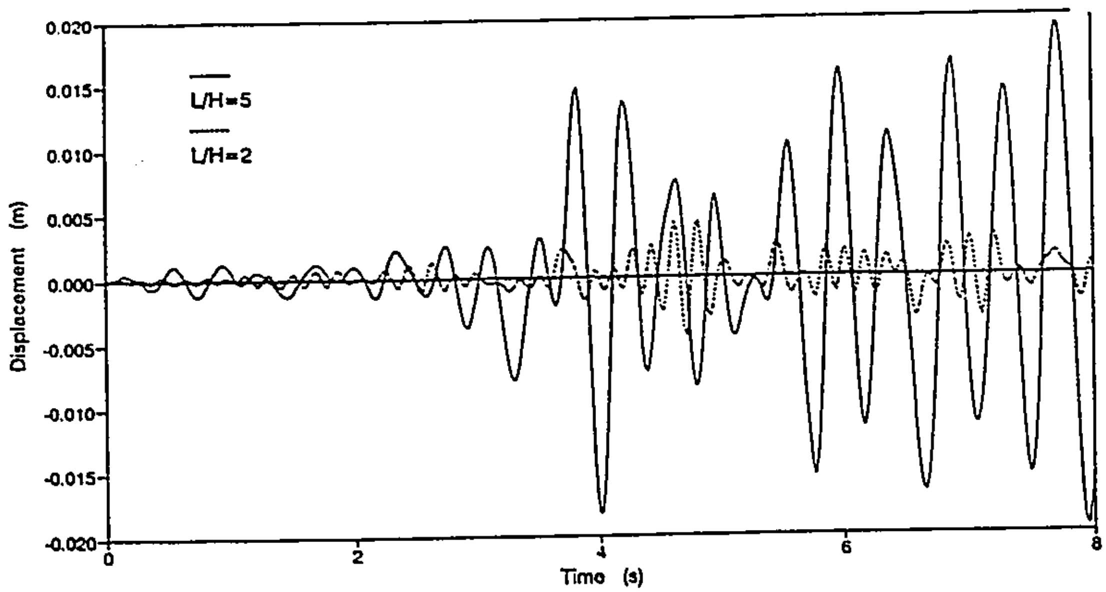

Figure (6-9) Crest Displacement Time Histories for Structure A with Different L/H ratios

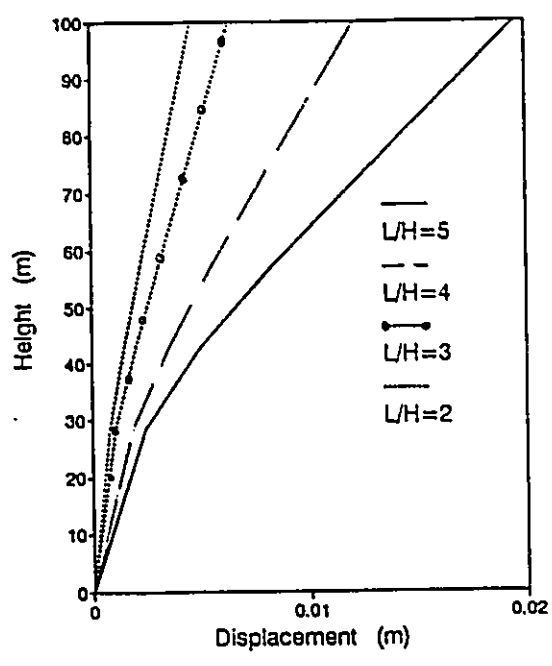

Figure (6-10) Envelope of Maximum Displacements for Structure A with Different L/H ratios

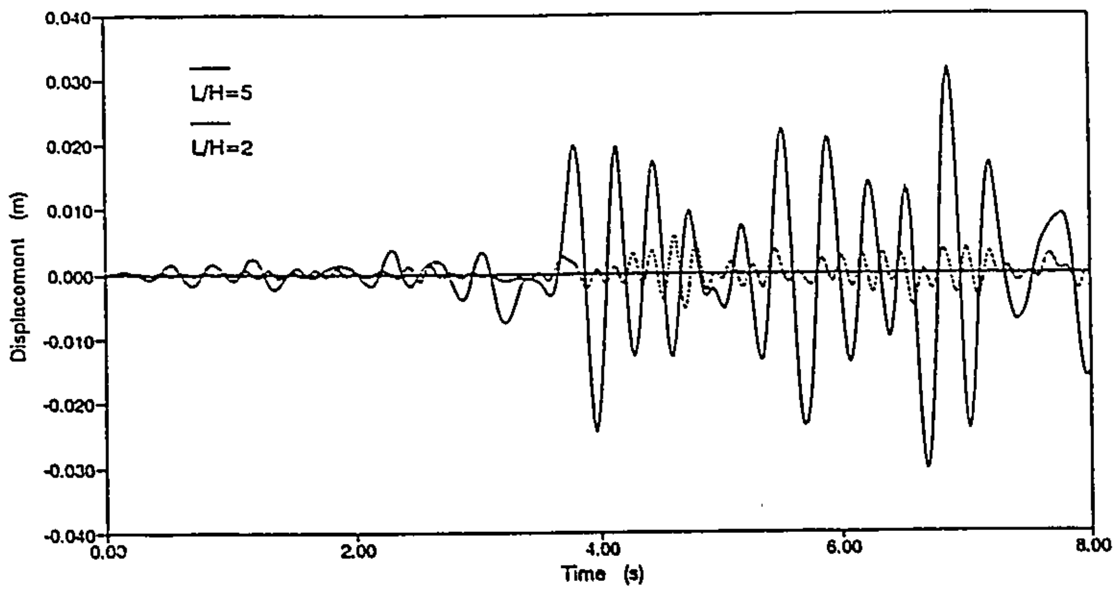

Figure (6-11) Crest Displacement Time Histories for Structure B with Different L/H Ratios

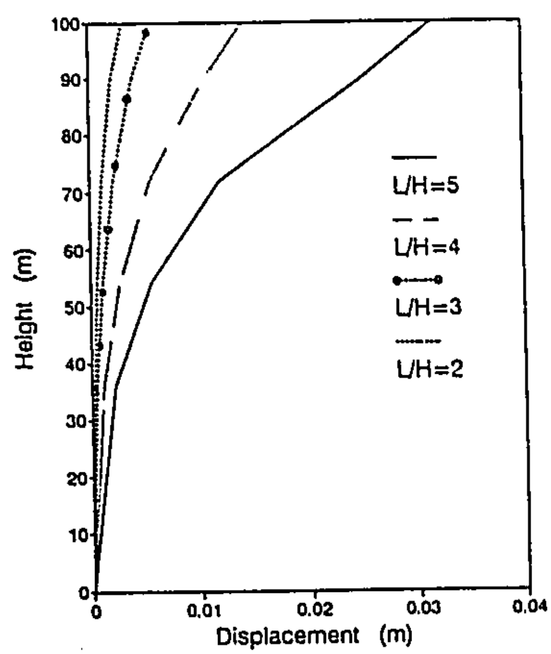

Figure (6-12) Envelope of Maximum Displacement for Structure B with Different L/H ratios

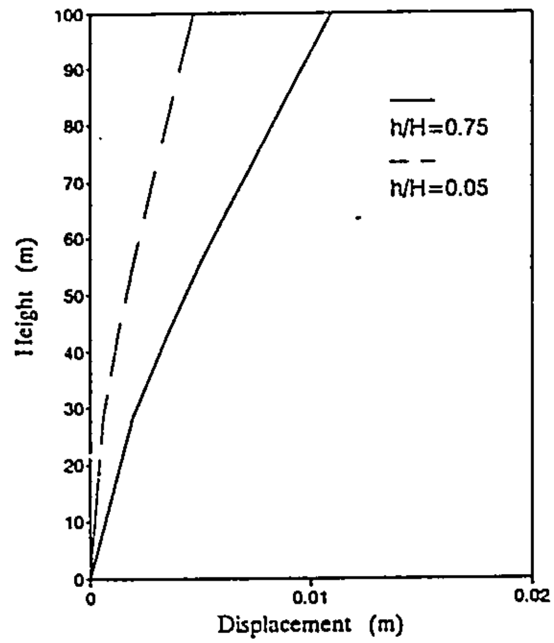

Figure (6-13) Envelope of Maximum Displacement for Structure A with Fixed End Conditions and Variable h/H

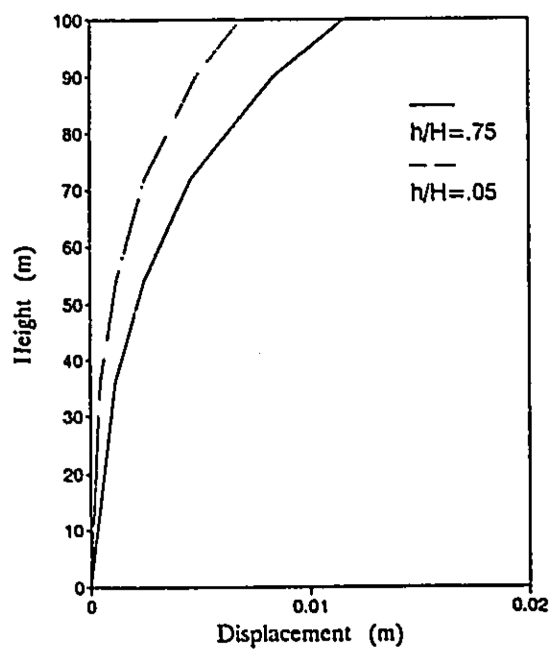

Figure (6-14) Envelope of Maximum Displacement for Structure B with Fixed End Conditions and Variable h/H

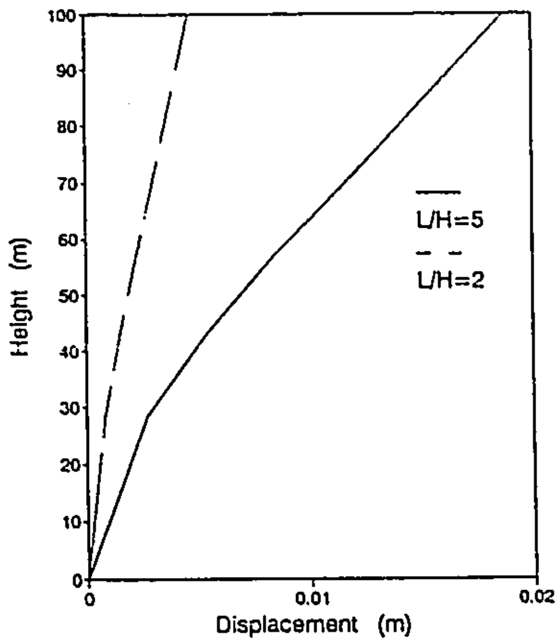

Figure (6-15) Envelope of Maximum Displacement for Structure A
with Fixed End Conditions and Variable B/H

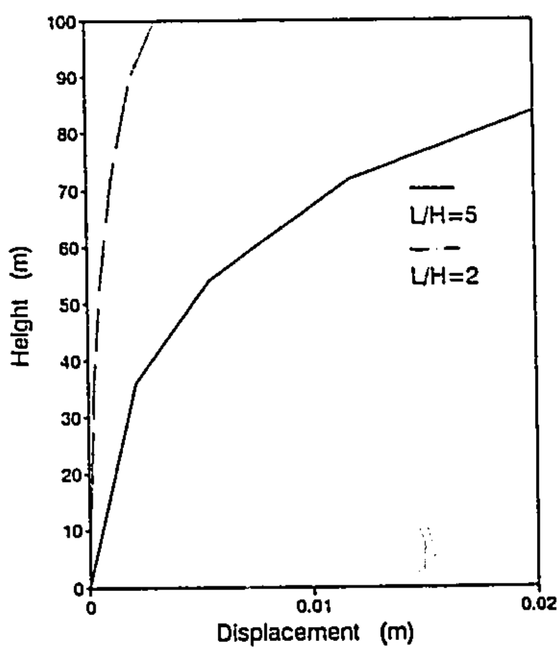

Figure (6-16) Envelope of Maximum Displacement for Structure B
with Fixed End Conditions and Variable L/H

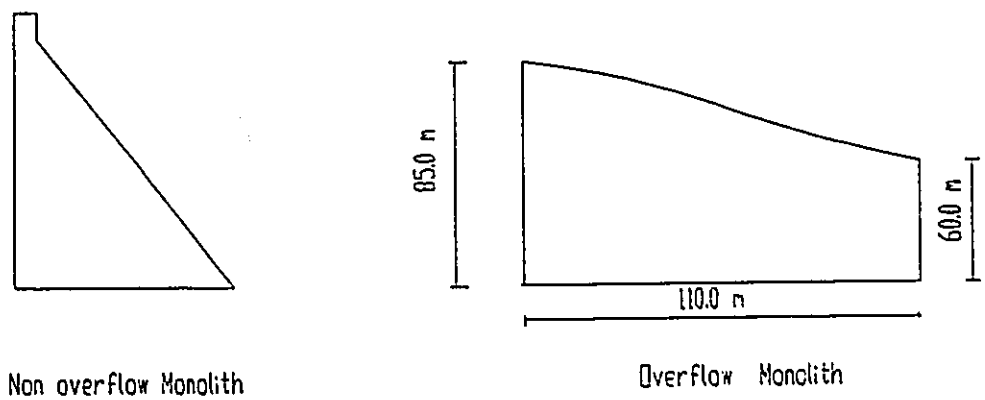

Figure (6-17) Cross-section of Overflow and Nonoverflow Monoli

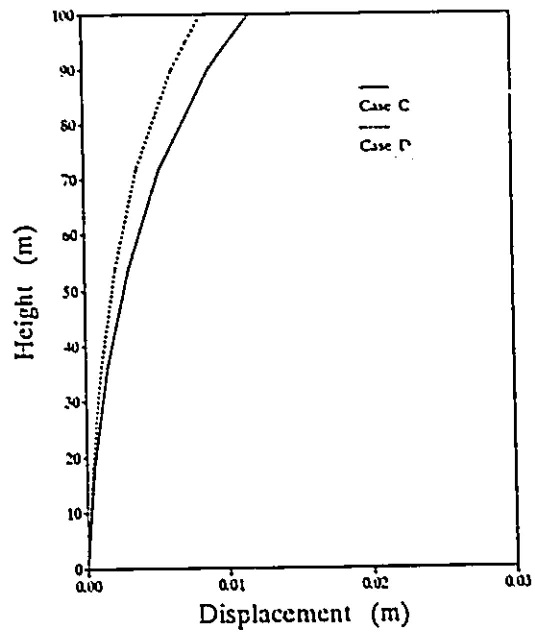

Figure (6-18) Envelope of Maximum Displacement for Structure B with Overflow Monoliths

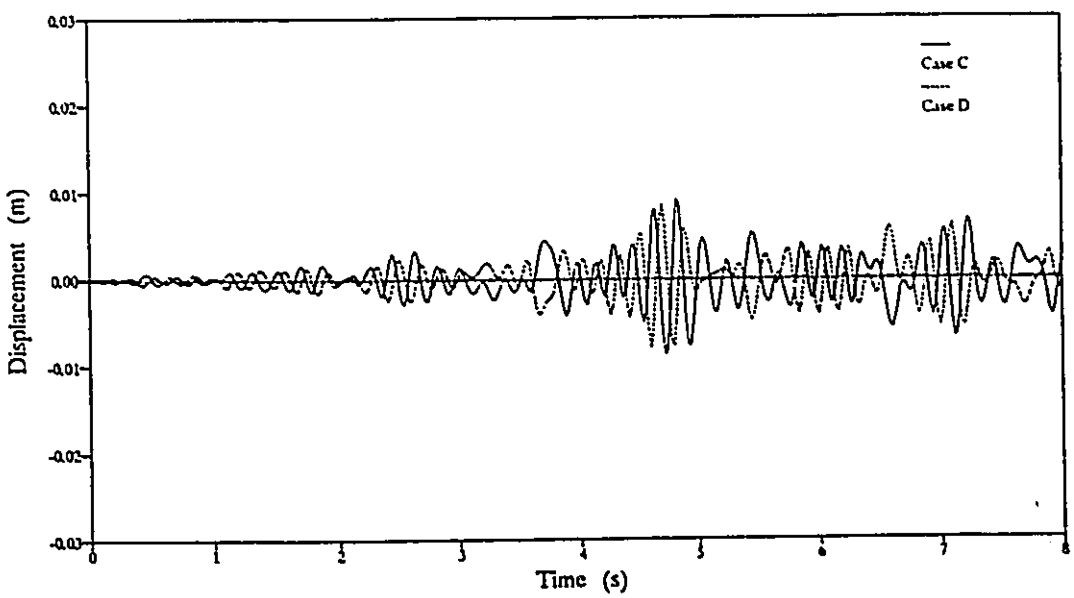

Figure (6-19) Crest Displacement Time History of Structure B with Overflow Monoliths

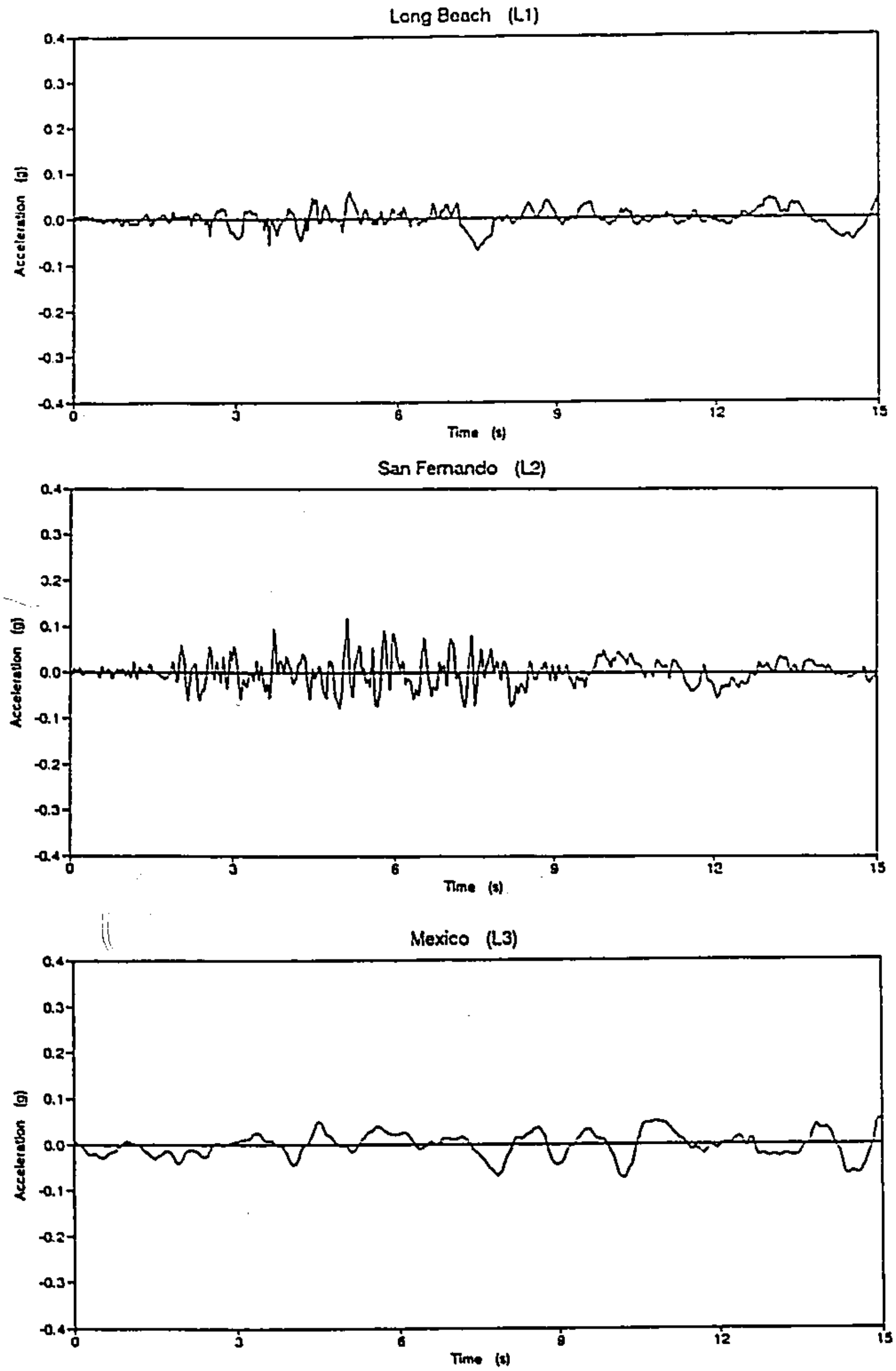

Figure (6-20) Time History Records of the Selected Earthquakes

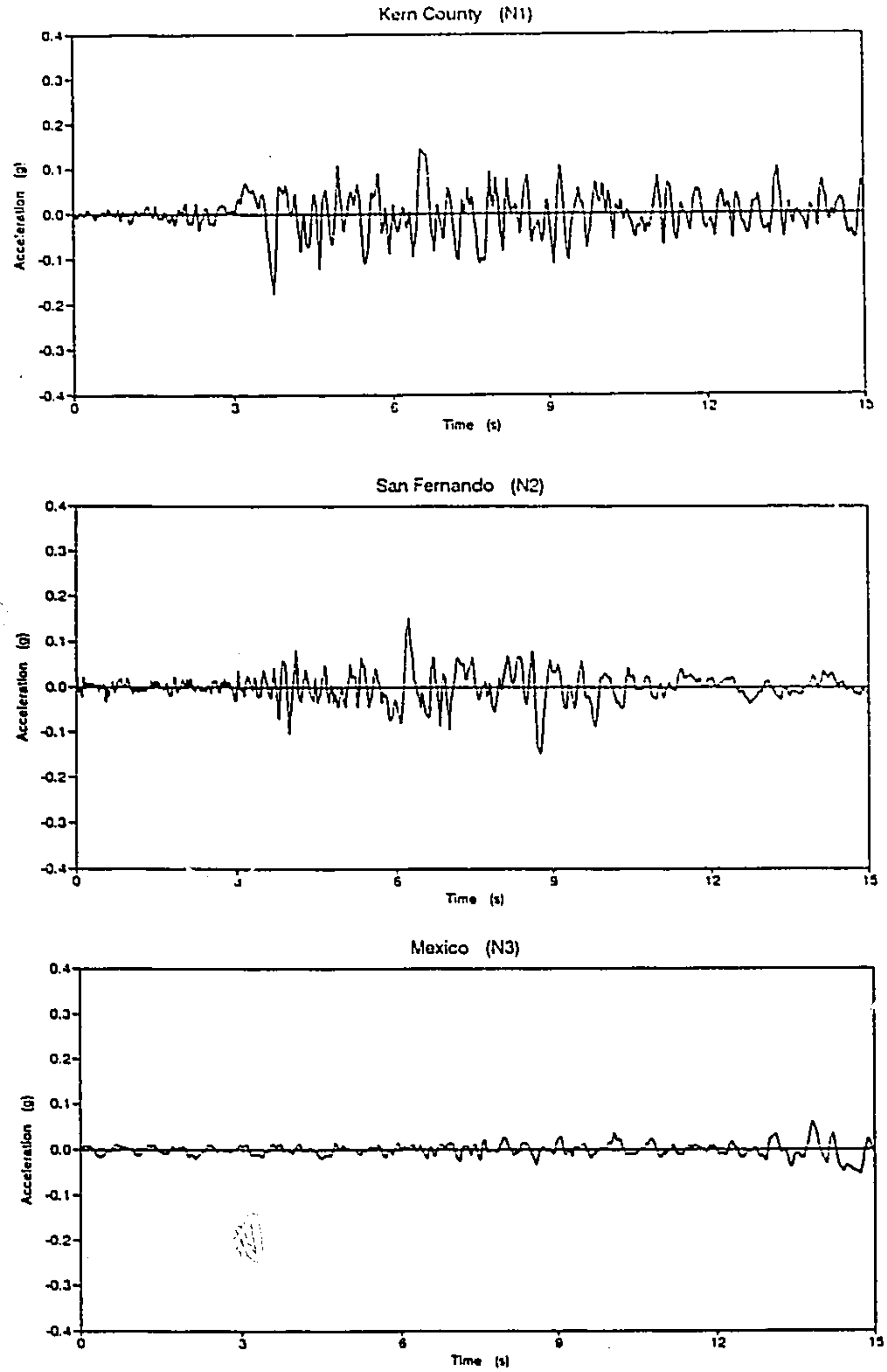

Figure (6-20) Time History Records of the Selected Earthquakes

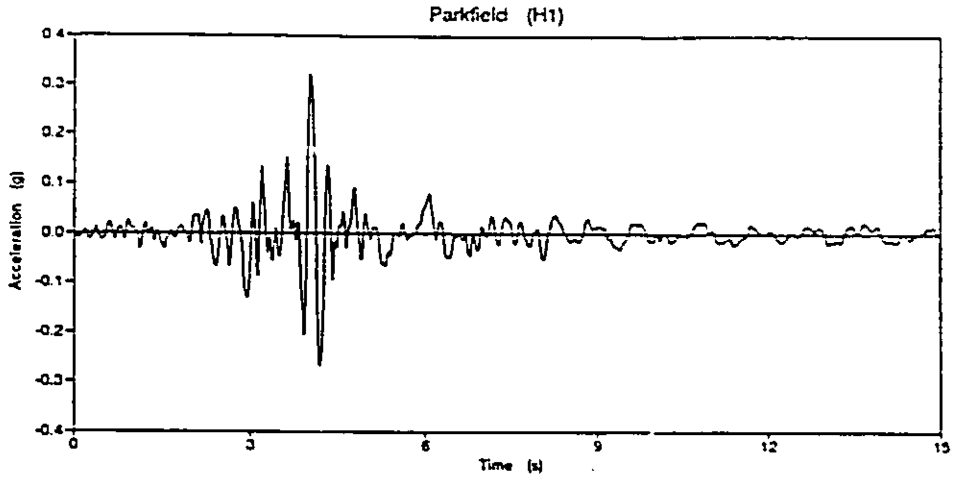

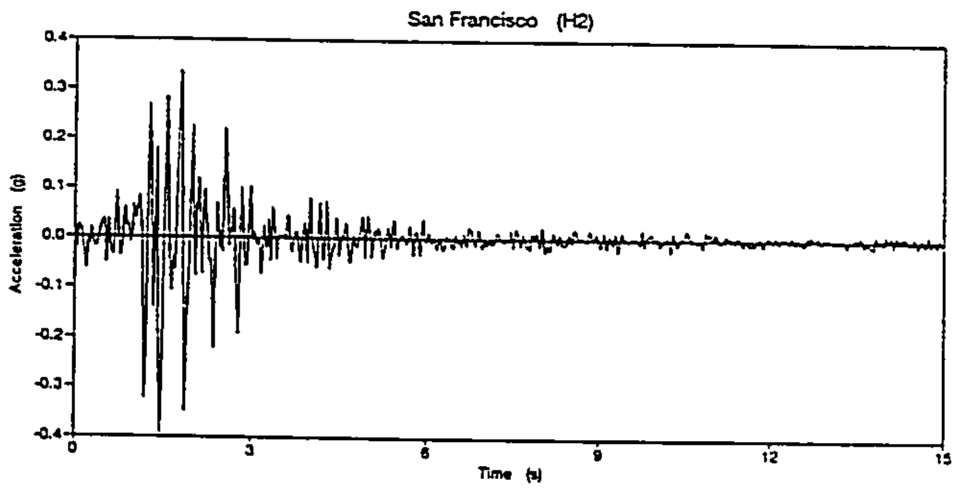

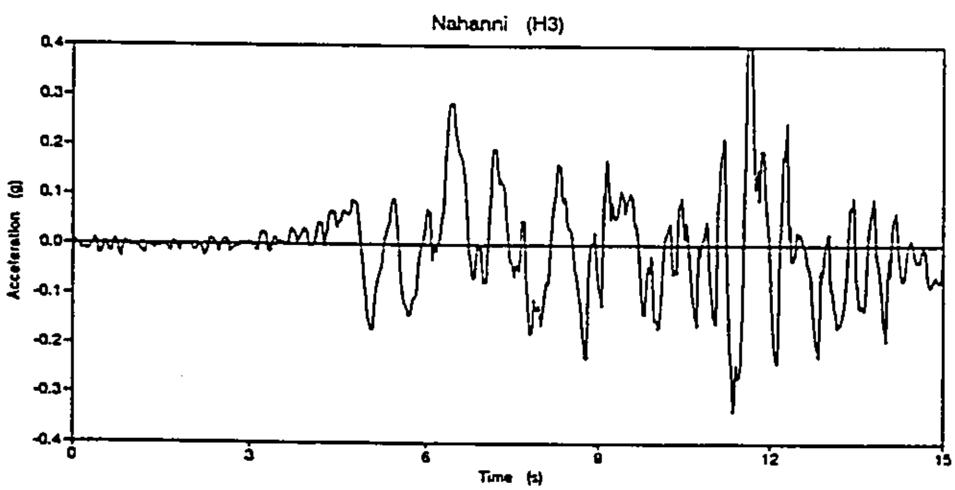

Figure (6-20) Time History Records of the Selected Earthquakes

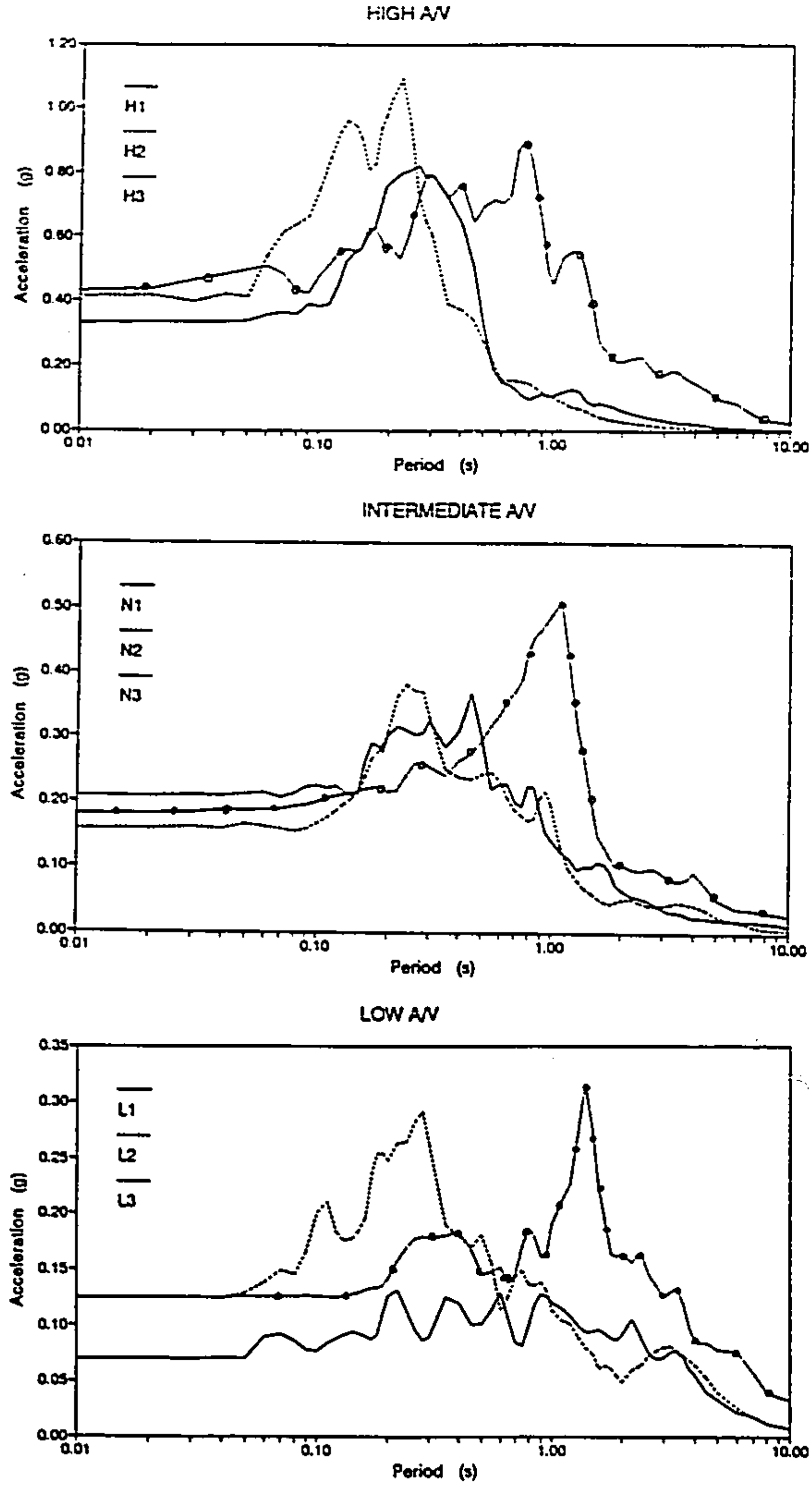

Figure (6-21) Response Spectrum for the Exciting Ground Motions
10 % Damping

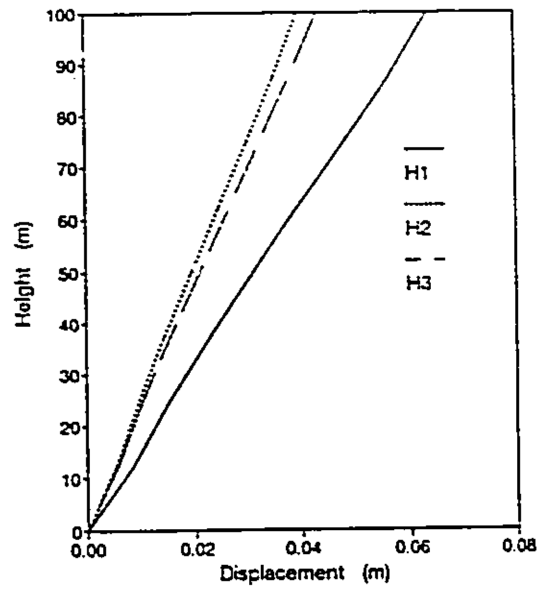

a) Structure A

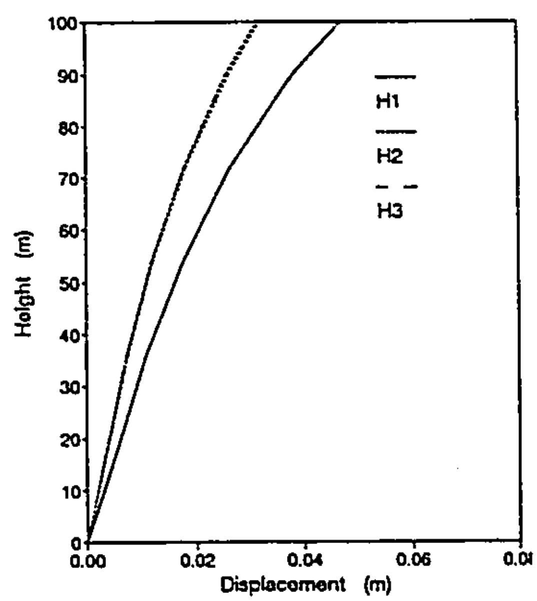

b) Structure B

Figure (6-22) Maximum Displacements of the Critical Monolith of the Structure
High A/V ratio

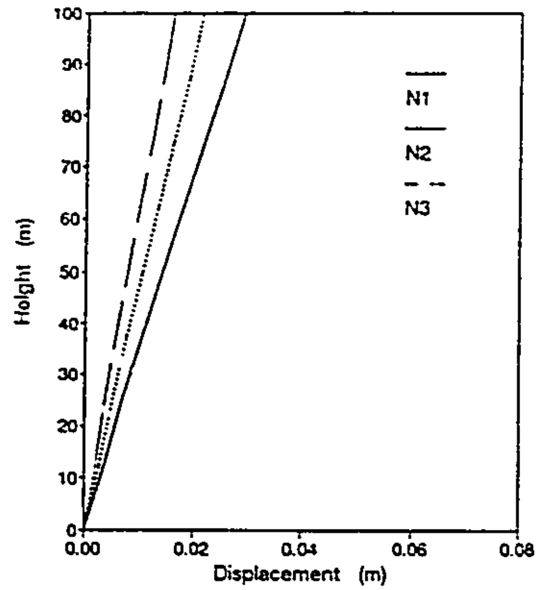

a) Structure A

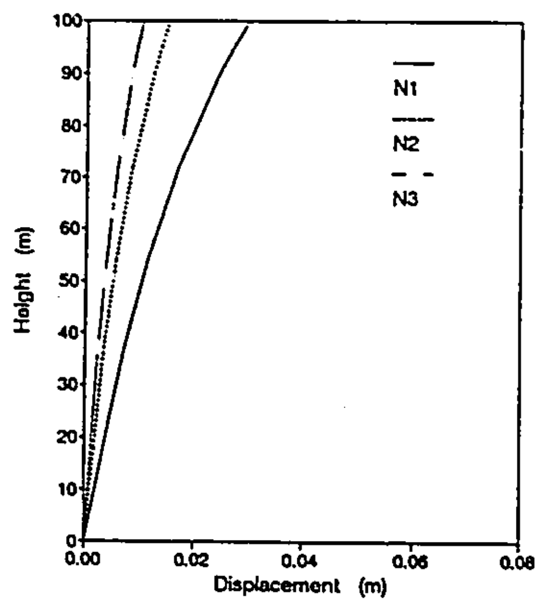

b) Structure B

Figure (6-23) Maximum Displacements of the Critical Monolith of the Structure
Intermediate A/V ratio

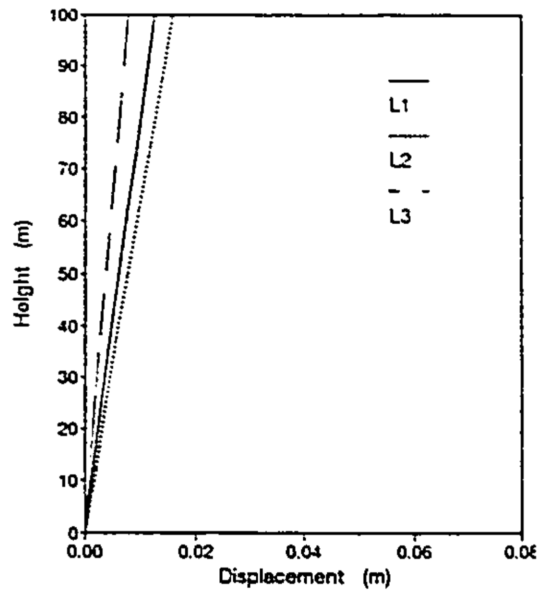

a) Structure A

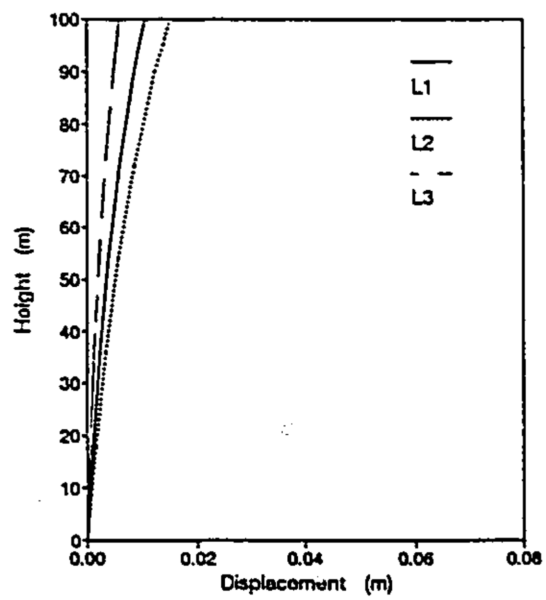

b) Structure B

Figure (6-24) Maximum Displacements of the Critical Monolith of the Structure
Low A/V ratio

CHAPTER 7

CONCLUSIONS AND RECOMMENDATIONS

7.1 GENERAL

A comprehensive study of the effect of monoliths interaction on the behaviour of concrete gravity dams with keyed contraction joints is presented. The research is carried out in three stages; a) A preliminary investigation of the importance of monoliths interaction using a simple analysis procedure. Monoliths are modeled using beam elements and the hydrodynamic effect is included using added masses. b) A more refined procedure for detailed analysis of gravity dams is developed after the preliminary study showed the significance of monoliths interaction. Each monolith is considered as a substructure and its degrees of freedom are reduced to the boundary DOF and a few Ritz vectors. Both reservoir-dam and foundation-dam interactions are included in the analysis. c) The effect of two parameters, which were found to be very significant in the dam response were evaluated. Those parameters are : the type of the contraction joint between the monoliths and the longitudinal profile of the dam structure. Gravity dams built with different types of contraction joints were analyzed to study the effect of monoliths interaction on the overall response of the dam. The longitudinal profile of the dam is described using three parameters: canyon cross-section, end conditions and overflow monoliths. From the analysis conducted in this research program, the following conclusions are reached.

7.2 CONCLUSIONS

1- A simplified procedure for the analysis of gravity dams was developed to investigate the effect of monoliths interaction. Simplicity as well as accuracy were the main motivations in developing the procedure. The procedure is recommended for preliminary evaluation of the importance of monoliths interaction for gravity dams.

2- For detailed analysis, a refined frequency domain procedure was also developed. The procedure includes reservoir - foundation - dam interaction. The results obtained using this procedure are compared to the three dimensional finite element procedure and good agreement was obtained.

3- Including the effect of monoliths interaction increases the natural frequencies of the structure and as a result will lead to a change in the overall response of the structure. The amount of change in the response depends on two factors: 1) the change in the dynamic properties of the structure as a result of including monoliths interaction and 2) the dynamic characteristics of the exciting ground motion.

4- Soil-structure and reservoir-structure interactions are shown to be important factors in the analysis of dams with keyed contraction joints. Including both interactions lead to a reduction in the natural frequency of the system and as a result significantly affects the overall response. The importance of these factors is of the same order in the case of keyed joints as that of smooth joints.

5- The geometry and material properties of contraction joints have a significant effect on the overall response of the dam. Depending on the crack width, the shear behaviour of the joints varies widely. As the crack width of the joint decreases, the shear stiffness of the joint increases and the effect of monoliths interaction increases. When cracks with small width exist, the analysis should include the effect of monoliths interaction as it significantly affects the response.

6- The effect of canyon cross-section, represented by the two ratios; h/H and L/H, is important. When the h/H ratio increases, the longitudinal profile of the dam tends to be uniform which reduces the importance of monoliths interaction. Increasing the ratio L/H leads to the same effect. It is noted that for dams with $h/H > 0.8$ or $L/H > 7.0$, the effect of monoliths interaction can be neglected and a typical two dimensional analysis would provide reasonably accurate results.

7- The end conditions of the dam affects the overall response. However, its effect is dependent on both h/H and L/H ratios. For low h/H ratios and high L/H ratios, the effect of the end conditions is minimal and can be neglected.

8- The effect of overflow monoliths is important and should be included in the analysis. The response of the structure varies depending on the location, number and geometry of overflow monoliths. In most cases, the existance of overflow monoliths will increase the natural frequencies of the structure. In the presented examples, the natural frequencies increased by approximately 15 % .

9- It was shown that the frequency content of the exciting earthquake as measured by the A/V ratio has a significant effect on the response of dams with keyed contraction joints. The results obtained in this study indicated that records with high A/V ratio have a tendency to produce higher response.

7.3 RECOMMENDATIONS

Based on the research presented in this thesis, the following recommendations for future work are suggested:

1- The results obtained in this study were based on computer analysis using a new procedure to include monoliths interaction. In order to validate the model, the results were compared to typical three dimensional model. As most of existing gravity dams have not been tested by strong ground motions, there is no actual data on the effect of monoliths interaction. It is recommended that actual performance data measurements be made on dams and tests should be carried on a three dimensional gravity dam models with a proper modelling for the contraction joints.

2- The dynamic properties of the exciting ground motions have been shown to have a significant effect on the behaviour of gravity dams. More research in this area is needed to establish the basis for selecting records for design and research purposes.

3- In selecting the design basis earthquake, it is still the trend to consider the two parameters; magnitude and peak acceleration to have the major effect on the structure. In this study, it was shown that A/V ratio may have an effect on the response of dams. More investigations in this area should be carried out to determine its importance.

4- There is a lack of experimental research in the area of the behaviour of keyed contraction joints. It is recommended that comprehensive shear tests on different types of keyed contraction joints be conducted. These tests, static and dynamic, should include the effect of some parameters as the dimensions of the keys used between the joints. The shear behaviour of the cement grouting used to fill the gaps between monoliths has a significant effect on the behaviour of the joint. More experimental tests on the properties and characteristics of this grouting is needed.

REFERENCES

Aviles, A. and Sanchez-Sesma, F. (1989). ' Water Pressures on Rigid Gravity Dams with Finite Reservoir During Earthquakes', Earthquake Engineering and Structural Dynamics, Vol. 18, pp 527-537.

Bathe, K. J., and Hahn, W. F., 1979.' On transient analysis of Fluid Structure Systems', Computers and Structures, 10 (1/2), pp 383 - 391.

Bayo, E. and Wilson, E., 1984. 'Use of Ritz Vectors in Wave Propagation and Foundation Response', Earthquake Engineering and Structural Dynamics, Vol. 12, No. 4, pp 499-505.

Bicanic, N. and Zienkiewicz, O.C., 1983.'Constitutive Model for Concrete Under Dynamic Loading ', Earthquake Engineering and Structural Dynamics , Vol. 11, pp 689-710.

Bureau, G., 1990. 'Earthquakes Put Dams to the Test', Hydro Reveiw, volume 12, , pp 12-19.

Bureau of Reclamation, 1977. 'Design Criteria for Concrete Arch and Gravity Dams', A Water Resources Technical Publication, Engineering Monograph No. 19, Office of Design and Construction Engineering and Reserarch Center, Dever, Colorado 80225.

Chakrabarti, P. and Chopra, A.K., 1973.'Earthquake Analysis of Gravity Dams Including Hydrodynamic Interaction', International Journal of Earthquake Engineering and Structural Dynamics, Vol. 2, pp 143-160.

Chakrabarti,P. and Chopra, A.K., 1974.'Hydrodynamics Effets in Earthquake Response of Gravity Dams', Journal of the Structural Division, ASCE, Vol. 100, No. ST6, pp. 1211-1224.

Chakrabati, S. C., Nayak, G. C. and Paul, D. K., 1985. 'Shear Characteristics of Cast-in Place Vertical Joints in Storeyhigh Precast Wall Assembly', ACI Structural Journal, Vol. 85, No. 1, pp 30-45.

Chen, A. C. and Chen, W., 1975.'Constitutive Relations For Concrete', Journal of the Engineering Mechanics Division, ASCE, Vol. 101, No. EM4, pp 465-480.

Chopra, A.K. , 1967.'Hydrodynamic Pressures of Dams during Earthquakes ', Journal of the Engineering Mechanics Division , ASCE, Vol. 93, No. EM6, pp. 205-223.

Chopra,A.K. ,1968.'Earthquake Behavior of Reservoir-Dam Systems', Journal of Engineering Mechanics Divsion, ASCE, Vol. 94, No. EM6, pp 1475-1500.

Chopra, A.K., 1970.' Earthquake Behavior of Reservoir-Dam Systems', Journal of Engineering Mechanics Division, ASCE, Vol. 96, No.EM4, pp 443-456.

Chopra , A.K. and Chakrabati, P., 1972. ' The Earthquake Experience at Koyna Dam and Stresses in Concrete Gravity Dams', Earthquake Engineering and Structural Dynamics, Vol. 1, No. 2, pp. 151-164.

Chopra, A.K., 1978.'Earthquake Resistant Design of Concrete Gravity Dams', Journal of the Structural Division, ASCE, Vol. 104, No. 6, pp 953-971.

Chopra , A.K., Chakrabati, P. and Gupta, S., 1980.'Earthquake Response of Concrete Gravity Dams Including Hydrodynamic and Foundation Interaction ' Report No. UCB/EERC-80/01 , Earthquake Engineering Research Center , University of California , Berkely, California.

Chopra, A.K. , 1987.'Earthquake Analysis , Design and Safety Evaluation of Concrete Dams', proceedings of the 5th Canadian Conference of Earthquake Engineering, Ottawa, pp39-62.

Clark, L. and Gill, B., 1985. ' Shear Strength of Smooth Unreinforced Construction Joints', Magazine of Concrete Research, Vol. 37, No. 131, June 1985, pp 95-100

Clough, R.W. and Penzien, J., 1975.' Dynamics of Structures ', McGraw Hill , New York.

Committee on Safety Criteria for Dams Water Science and Technology Board, 1985. 'Safety of Dams Flood and Earthquake Criteria', National Academy Press, Washington, D.C.

Dasgupta, G. and Chopra, A.K., 1979.'Dynamic Stiffness Matrices for Viscoelastic Half Planes', Journal of The Structural Engineering Divsion, ASCE, Vol. 105, No. EM5, pp 834-841.

Donlon, W. and Hall, J., 1991.' Shaking Table Study of Concrete Gravity Dam Monoliths', Earthquake Engineering and Structural Dynamics, Vol. 20, pp 769-786.

El-Aidi, B. and Hall, J., 1989. 'Nonlinear Earthquake Response of Concrete Gravity Dams Part 1 : Modelling', Earthquake Engineering and Structural Dynamics, Vol. 18, pp. 837-851.

El-Aidi, B. and Hall, J., 1989.'Nonlinear Earthquake Response of Concrete Gravity Dams Part 2 : Behavior', Earthquake Engineering and Structural Dynamics, Vol. 18, pp. 853-865.

El-Nady, A., Ghobarah, A. and Aziz, T. 1990. 'Effect of High Frequency Earthquakes on The Response of Concrete Gravity Dams'. The Canadian Society of Civil Engineering annual conference, Hamilton, Ontario, Vol.IV, pp 59-71.

El-Nady, A., Ghobarah, A. and Aziz, T. 1991. 'Simplified Three Dimensional Analysis of Concrete Gravity Dams'. The 6th Canadian Conference on Earthquake Engineering, Toronto, Ontario, pp 189-196.

El-Nady, A., Ghobarah, A. and Aziz, T. 1992. ' Analysis of Concrete Gravity Dams with Keyed Expansion Joints', International Colloquim on Structural Engineering, Cairo, Egypt, April 14-16, pp 17-28.

Fenves, G. and Loli, M., 1986.'Nonlinear Dynamic Analysis of Fluid-Structure Systems', Journal of Engineering Mechanics, ASCE, Vol. 114, No. 2, pp. 219-238.

Fenves, G. and Chopra, A.K., 1984a.' Earthquake Analysis and Response of Concrete Gravity Dams ', Report No. UCB/EERC-84/10, Earthquake Engineering Research Center, University of California, Berkely , California.

Fenves, G. and Chopra, A.K., 1984b.'A Computer Program for Earthquake Analysis of Concrete Gravity Dams', Report No. UCB/EERC-84/11, Earthquake Engineering Research Center, University of California, Berkely, California.

Fenves, G. and Chopra, A., 1985.'Simplified Earthquake Analysis of Concrete Gravity Dams: Separate Hydrodynamic and Foundation Interaction Effects', Journal of Engineering Mechanics, ASCE, Vol. 111, No. 6, pp. 715-735.

Fenves, G. and Chopra, A.K., 1987.' Simplified Analysis of Concrete Gravity Dams ', Journal of Structural Engineering, ASCE, Vol.113 , No. 8, pp. 1688-1708

Gutierrez, J.A. and Chopra, A.K., 1978.'A Substructure Method for Earthquake Analysis of Structures Including Structure-Soil Interaction', Earthquake Engineering and Structural Dynamics, Vol. 6, pp 51-69.

Guyan, R., 1965. 'Reduction of Stiffness and Mass Matrices', AIAA Journal, Vol. 3, pp 380-389.

Hall, J.F. and Chopra ,A. K., 1980.'Dynamic Response of Embankment Concrete Gravity and Arch Dams', Report No. UCB/EERC-80/39, Earthquake Engineering

Research Center, University of California , Berkely , California.

Hamdi, M. A., Ousset, Y., and Verchery, G., 1978.'A Displacement Method for Analysis of Vibrations cf Coupled Fluid - Structure Systems'. International Journal of Numerical Methods in Engineering, 13(1), pp 139 - 150.

Hansen, K. and Roehm, L., 1979. 'The response of Concrete Dams to Earthquakes', Water Power and Dam Construction, pp 27-31.

Haroun, M. and Abdel-Hafez, E., 1991. 'Dynamic Interaction of Dam-Reservoir Systems', International Journal of Earthquake Engineering, Vol.1, No. 1, pp 41-51.

Humar, J. and Jablonski, A., 1987. ' Boundary Element Analysis of the Hydrodynamic Forces in a 2D Reservoir', Proceedings of the 5th Canadian Conference on Earthquake Engineering, Ottawa, Ontario.

Humar, J. and Jablonski, A., 1988. ' Boundary Element Reservoir Model for Seismic Analysis of Gravity Dams', Earthquake Engineering and Structural Dynamics, Vol. 16, No. 6, pp. 1129-1156.

Jansen, R., 1988. 'Advanced Dam Engineering for Design, Construction and Rehabilitation', Van Nostrand Reinhold, New York.

Kotsov, M.D. and Newman, J.B., 1977.'Behavior of Concrete Under Multiaxial Stress', ACI Journal, V. 74, No. 9, pp 443-446.

Lamb, M. A., 1932. 'Hydrodynamics', Dover Publications, New York.

Leger, P. and Katsouli, M., 1989.'Seismic Stability of Concrete Gravity Dams', Earthquake Engineering and Structural Dynamics, Vol. 18, pp 889-902.

Liu, W.K. and Chang, H.G., 1985. ' A Method for Computation for Fluid Structure Interaction', Computers and Structures, Vol. (20), No. (1-3), pp 311-320.

Loli, M. and Fenves, G., 1988.'Nonlinear Response of Concrete Gravity Dams', Proceeding of the Ninth World Conference on Earthquake Engineering, Tokyo, pp.343-348.

Mlakar, P.F., 1987.'Nonlinear Analysis of Concrete Gravity Dam to Strong Earthquake-Induced Ground Motion', Computers and Structures, Vol. 26, No. 1/2, pp. 165-173.

Murry, D.W., Chitnuyanondh, L. and Wong, C., 1979.'Concrete Plasticity Theory For Biaxial Stress Analysis', Journal of the Engineering Mechanics Division, ASCE, Vol.

105, No. EM6, pp 989-1004.

Naumoski, N., Tso, W.K. and Heidebrecht, A., 1988.'A Selection of Represntative Strong Motion Earthquake Records Having Different A/V Ratios', EERG Report 88-01, Earthquake Engineering Research Group, McMaster University.

Newton,R. E., 1981. 'Effects of Cavitation on Underwater Shock Loading - Part I', Report NPS -69-78-013, Naval Postgraduate School, Monterey, California.

Niwa, A. and Clough, R. W., 1980.'Shaking Table research on Concrete Dam Models', Report No. UCB/EERC- 80/05. Earthquake Engineering Research Center, University of California, Berkely, CA.

Okamoto, S., 1984.'Introduction to Earthquake Engineering', University of Tokyo press.

Olson, L. G., and Bathe, K., 1983.'A Study of Displacement Based Fluid Finite Elements for Calculating Frequencies of Fluid and Fluid Structure Systems', Nuclear Engearing Design, 76(2), pp 137 - 151.

Olson, L. G., and Bathe, K., 1985.' Analysis of Fluid Structure Interactions ; A Direct Symmetric Coupled Formulation Based on Fluid Velocity Potential', Computers and Structures, 21(1/2), pp 21 - 32.

Pal, N., 1976. 'Seismic Cracking of Concrete Gravity Dams ', Journal of Structural Division, Proceedings of the American Society of Civil Engineering, Vol. 102, No. ST9, pp 1827-1843.

Park, R. and Paulay, T., 1975. 'Reinforced Concrete Structures', John Wiley and Sons, Toronto.

Paz, M., 1980.'Structural Dynamics, Theory and Computation', Van Nostrand Reinhold Company, New York.

Rashed, A. and Iwan, W., 1984.'Earthquake Response of Short length Gravity Dams', Proceeding of Seventh World Conference on Earthquake Engineering, Vol. II, pp 343-350.

Saini, S. S., Bettess, P., and Zienkiewicz, O. C., 1978.' Coupled Hydrodynamic Response of Concrete Dams Using Finite and Infinite Elements', Earthquake Engineering and Structure Dynamics 6(4), pp 363 - 374.

Skrikerud, P.E. and Bachmann, H., 1986. 'Discrete Crack Modelling for Dynamically Loaded, Unreinforced Concrete Structures ', Earthquake Engineering and Structural

Dynamics, Vol. 14, pp 297-315.

Stevens, J. E., 1988. 'Hoover Dam', University of Oklahoma Press, Norman, Publishing Division of the University.

Stuardi, J.E. and Prato, C.A., 1990. 'The Influence of Valley Shape on Seismic Response: Piedra del Aguila Dam', Dam Engineering, Vol I, No.3, pp 177-199.

Tasuji, M.E., Slate, F.O. and Nilson, A.H., 1978.'Stress-strain Response and Fracture of Concrete in Biaxial Loading', ACI Journal, Vol. 75, No. 7, pp. 306-312.

Taylor, R. L., and Zienkiewicz, O. C., 1984.' Mixed Finite Element Solution of Fluid Flow Problems', Finite Elements in Fluids, Vol. 4, John Wiley and Sons, Chichester, U.K., pp 1 - 20.

Thomas, H., 1976,I and II. 'The Engineering of Large Dams', John Wiley & Sons, New York.

Tsai, C. and Lee, G., 1990. 'Method For Transient Analysis of Three Dimensional Dam-Reservoir Interactions', Journal of Engineering Mechanics, ASCE, Vol. 116, No. 10, pp 2151-2172.

U.S. Bureau of Reclamation, 1976. ' Design of Gravity Dams', Denver, Colorado.

U.S. Bureau of Reclamation, 1987. ' Design of Small Dams', Denver, Colorado.

Vaish, A.K., and Chopra, A.K., 1974.'Earthquake Finite Element Analysis of Structural Foundation Systems', Journal of the Engineering Mechanics Division, ASCE, Vol. 100, No. EM6, pp 1101- 1116.

Weaver, W. and Jonhston, P.R., 1987. 'Structural Dynamics by Finite Elements', Prentice-Hall, New Jersy.

Westergaad, H.M., 1933.'Water Pressures on Dams During Earthquakes', Transactions, ASCE, Vol. 98, pp 418-472.

Wilson, E. and Bayo, E., 1986. 'Use of Special Ritz Vectors in Dynamic Substructure Analysis'. Journal of Structural Engineering, Vol. 112, No. 8, pp 1944-1953.

Wilson, E. L., and Khalvati, M., 1983.' Finite Elements for The Dynamic Analysis of Fluid -Solid Systems', International Journal of Numerical Methods in Engineering, 19(11), pp 1657 - 1668.

Zienkiewicz, O. C., Paul, D. K., and Hinton, E., 1983.'Cavitation in Fluid Structure Response', Earthquake Engineering and Structure Dynamics, 11(4), pp 463 - 481.

Zhu, W., Luo, X., Liu, S. and Liu, D., 1984. 'Prototype Dynamic Test and Theoretical Analysis of a Concrete Gravity Dams', Proceeding of Seventh World Conference on Earthquake Engineering, pp 359-366.